January 2014

Investigation Into The Binding Interactions Of Klenow Fragment To Dna Modified With Carcinogens Af And Aaf Using Surface Plasmon Resonance

Ashley M. Floyd
Wayne State University, afloyd785@gmail.com

INVESTIGATION INTO THE BINDING INTERACTIONS OF KLENOW FRAGMENT TO DNA MODIFIED WITH CARCINOGENS AF AND AAF USING SURFACE PLASMON RESONANCE

by

ASHLEY M. FLOYD

DISSERTATION

Submitted to the Graduate School

of Wayne State University,

Detroit, Michigan

in partial fulfillment of the requirements

for the degree of

DOCTOR OF PHILOSOPHY

2014

MAJOR: CHEMISTRY (Biochemistry)

Approved by:

_____

Advisor Date

_____

_____

_____

DEDICATION

I dedicate this thesis to those who fueled my inquisitive mind, my parents. Happy 65th birthday dad and Happy (belated) Mother's Day mom.

ACKNOWLEDGEMENTS

In my time here as a graduate student at Wayne State, I have learned more than just biochemistry. The school, the city, and everyone I have interacted with have taught me to be a better scientist and a better person. First and foremost, I am grateful to Dr. Romano for allowing me to join his lab, and thankful for his guidance and encouragement throughout my graduate career. I would also like to thank my committee members, Dr. John SantaLucia, Dr. Sarah Trimpin, and Dr. David Njus, for providing feedback on my research and their support in writing my thesis.

I would like to thank the previous Romano lab members, Dr. Asad Ullah, Dr. Venkataramana Vooradi, Dr. Thomas Christian, Dr. Richard Federley for being so welcoming when I joined the lab and making my first few years at Wayne State enjoyable. Their patience in instructing me various laboratory techniques helped me easily acclimate into life in the Romano Lab. Specifically, thank you to Dr. Thomas Christian for sharing with me his knowledge on fluorescence. I am grateful to Richard Federley for teaching me the ins and outs of surface plasmon resonance, and also for all the valuable conversations we shared, scientific and otherwise. Thank you to Radoslaw Markiewiecz for always inquiring about how my work was coming along. Those discussions always helped me look at my work from a different direction, always resulting in forward progress. Thank you Dr. Kyle Vrtis for always being there to help with anything I had going on within the lab or otherwise. Thank you to the few, but still significant current Romano Lab members, Dr. Alfonso Brenlla and Pramodha Liyange, for their insightful discussions. I would also like to

thank the current and previous undergraduate researchers that have studied in the Romano Lab. It was a pleasure teaching you, and I have learned so much more about the protocols and the science through the experience.

I would also like to acknowledge my family for their immense support, love, and encouragement not only through these past few years of my graduate career, but throughout my life. My mother has always been my role model and my number one cheerleader, supporting me in all that I do. I love that I have inherited the inquisitive nature of my father, who is always looking to learn a little bit more and has never hesitated to ask another question. Trevor, thank you for always reminding me to get out and do something fun from time to time. Without all of you, I would not be where I am today and I am forever grateful, thank you.

TABLE OF CONTENTS

LIST OF TABLES

LIST OF FIGURES

LIST OF ABBREVIATIONS

3-HPA	3-hydroxypicolinic acid
AAF	N-acetyl-2-aminofluorene
AF	N-2-aminofluorene
B[a]P	Benzo[a]pyrene
BF	Truncated DNA polymerase one from *Bacillus stearothermophilus*
ddNTP	2'3'-dideoxyribonucleoside 5'-triphosphate
dG-C8-AAF	N-(2'-deoxyguanosin-8-yl)- N-acetyl-2-aminofluorene
dG-C8-AF	N-(2'-deoxyguanosin-8-yl)-2-aminofluorene
DNA	deoxyribonucleic acid
DNA Pol I	E. coli DNA polymerase I
dNTP	2'-deoxyribonucleoside 5'-triphosphate
E. coli	Escherichia coli
FRET	Förster resonance energy transfer
HPLC	High performance liquid chromatography
k_{off}	Dissociation off rate
K_D	Equilibrium dissociation constant
KF	Truncated *E. coli* DNA polymerase I
KF(exo-)	Exonuclease free *E. coli* DNA polymerase I
MALDI-TOF	Matrix assisted laser desorption time of flight mass spectrometry
NTP	Either a ribo- or 2'- deoxy-nucleoside 5'-triphosphate
PAGE	Polyacrylamide gel electrophoresis
PIFE	Protein induced fluorescence enhancement
PAH	Polycyclic aromatic hydrocarbon
PCR	Polymerase chain reaction
ROS	Reactive oxygen species

R_{max}	Maximum response
rNTP	Ribonucleoside 5'-triphosphate
SPR	Surface plasmon resonance
TdT	Terminal dideoxy Transferase
TLS	Trans lesion synthesis
Tris-HCl	Tris-hydroxymethyl aminomethane hydrochloride
UV-Vis	Ultraviolet visible spectroscopy

Chapter 1: Introduction

Cancer is a disease recognized by the uncontrollable proliferation of cells and the eventual spreading of these cells throughout the body. Cell division is a tightly regulated process that includes numerous checkpoints to ensure the formation of viable new cells. In cancer cells, some of these important checkpoints are disrupted and the resulting daughter cells are unable to cease dividing, creating tumors or lesions within the affected organ. As the tumor grows, the cancer cells can fracture off and move throughout the body, creating tumors away from the original affected organ. Any part of the body can be affected by cancer and more than 100 types of cancer have been identified. Currently in the United States cancer is the second leading cause of death, accounting for 1 in every 4 deaths(*1*). Between 2001 and 2010, deaths rates have declined 1.5% for all types of cancer in both men and women. The decline is attributed to earlier detection and better diagnostic methods for cancers such as breast(*2*), colorectal(*1*), and prostate(*3*), wider range of treatment therapies, and the decrease in tobacco use(*4*).

Studying all aspects of cancer, from the causes and the treatments, has been a major goal of countless researchers for decades. Discoveries such as smoking cigarettes leads to cancer and more recently the discovery that viruses such as the human papillomavirus (HPV) cause cancer have been greatly beneficial in preventing and improving cancer treatment(*5, 6*). The more information that can be acquired about carcinogenic compounds and how these substances affect the human body will further benefit cancer research. The work discussed here focuses on

determining how cells become cancerous by monitoring DNA replication on templates modified with chemical carcinogens known to alter DNA.

I. DNA Damage

Deoxyribonucleic acid, or DNA, is the molecule responsible for information storage in the cell. Faithful transmission of the information stored in these cells to daughter cells is key for cell survival. The genetic code, stored within the DNA, is read as a list of bases. The DNA molecule is a dynamic molecule that is constantly subject to stress, creating breaks in the DNA sugar-phosphate backbone or damage to the nucleotides. Alteration of nucleotides in DNA can be caused by both endogenous and exogenous sources(*7, 8*). Damage leading to the modification of base chemistry can result in distortions in the DNA structure interrupting processes like replication and transcription. Mutations in the nucleotide sequence can occur during normal cell processes such as replication, repair, or recombination(*9*).

A. Endogenous DNA Damaging Agents

DNA itself has some inherent instability from spontaneous hydrolysis of the DNA sugar-phosphate-base structure. Hydrolysis of the glycosidic bond between the deoxyribose sugar and the base creates apurinic/apyrimidinic sites. These abasic sites result in a loss of coding and make the sugar-phosphate backbone susceptible to double strand breaks. DNA base residues that contain exocyclic amines (NH_2) are also susceptible to hydrolysis. The NH_2 groups on cytosine and 5-methylcytosine are the main targets of hydrolysis, but the amines on adenine and guanine can also be hydrolyzed. The deamination of cytosine to uracil can result in

C:G -> T:A transition mutations, but since this is a common occurrence the enzyme uracil-DNA glycosylase readily removes the uracil base which gets corrected through a repair mechanism. The deamination of 5-methylcytosine to thymine produces G:T mismatches, which are slower to be repaired and likely to result in G to A transitions(*10*).

There are a number of chemical compounds produced during metabolic processes within the cell that react with DNA to modify bases(*7, 8*). Reactive oxygen species (ROS) are produced during normal cellular processes such as the reduction of oxygen to water radicals during cellular respiration creating superoxide (O_2^-), hydrogen peroxide (H_2O_2), and hydroxyl radicals (OH^-). These radicals promote DNA strand breaks and oxidative damage to bases within the double helix as well as the free deoxynucleotide triphosphate (dNTP) pools. 8-oxo-guanine (8-oxoG) is produced when a hydroxyl radical is added to the C8 position on guanine within the DNA or free dGTP. 8-oxoG within the DNA results in guanine mispairing with adenine through a Hoogsteen base pair leading to G -> T transversions(*11*).

B. Exogenous DNA Damaging Agents

i. Physical DNA modifying agents

Unavoidable physical agents in the environment such as ionizing radiation and ultraviolet light can induce DNA damage. Ionizing radiation from natural and man-made sources can create lesions on the DNA and other cellular components. DNA lesions created by ionizing radiation include 8-hydroxyguanine and 8,5'-cyclo-deoxyguanosine. Ultraviolet (UV) radiation from sunlight has been shown to be one

of the main causes of human skin cancer(*12, 13*). Exposure to UV light creates covalent linkages between adjacent pyrimidine bases producing 4 membered ring structures such as cyclobutane pyrimidine dimers (CPD) and pyrimidine(6-4)pyrimidine photoproducts (64PPs). CPDs are formed when the 5,6 double bond of two adjacent thymine residues become saturated(*14*). 6,4 photoproducts result from a direct linkage between the C4 of cytosine and the C6 of an adjacent thymine. Both of these photoproducts create major distortions in the DNA structure obstructing replication machinery. UV light also induces oxidative stress in cells by producing ROS leading to oxidative damage as mentioned above(*15*).

ii. Chemical DNA modifying agents

There are a large number of natural and synthetic chemical agents present in the environment that cause damage to DNA that have been shown to impede DNA replication or to be mutagenic. Alkylating agents are a family of reactive chemicals with a high affinity for nucleophilic compounds like DNA. They occur naturally in food and water, but can also be found in air pollutants such as fossil fuel combustion products and tobacco smoke(*16, 17*). Alkylating agents are used in industrial processes as methyl and ethyl donors in the production of chemicals and pesticides. The mutagenic properties of these chemicals depend on their site of DNA modification, and can block essential processes such as DNA replication and transcription. Alkylating agents act nonspecifically on exocyclic oxygen and ring nitrogen atoms in DNA bases as well as oxygen atoms in the DNA phosphate backbone. Alkylation of the O^6 of guanine and the O^4 of thymine are highly mutagenic, resulting in G -> A and T -> C transitions, respectively(*18*). The N^3

position of adenine and N^7 of guanine are highly reactive to alkylating agents, but are not as mutagenic(*19*).

The high reactivity of alkylating agents with DNA made them a popular candidate for chemotherapeutic agents. Bifunctional alkylating agents contain two reactive groups and have the ability to bond with separate DNA bases creating both intrastrand and interstrand crosslinks. Nitrogen mustard, or mechloroethamine, was the first chemotherapeutic drug given to cancer patients and a number of derivatives have been used to treat a variety of cancers(*20*). Another well known bifunctional chemotherapeutic alkylating agent used today is cis-platinum(*21*). The introduction of crosslinks obstructs important DNA related processes that the cancer cell needs to survive.

There are also a number of chemically unreactive compounds that on their own are not carcinogenic, but once ingested in to the body are activated by the metabolic process put in place to remove them from the body. These procarcinogens tend to be hydrophobic in nature and are altered by the enzyme cytochrome P450 to make the compound more hydrophilic for excretion from the body via urine. Making the compound more water soluble also makes the compound more electrophilic, increasing their ability to react with and modify DNA bases(*22*).

Compounds that are metabolically activated by the cytochrome P450 family of enzymes include polycyclic aromatic hydrocarbons (PAH), aromatic amines, and aflatoxins. A PAH of interest to this lab is benzo[a]pyrene (B[a]P). B[a]P is formed

from incomplete combustion of carbon based sources such as the burning of fossil fuels, forest fires, cigarette smoke, and even the cooking of food. After metabolic activation, four major benzo[a]pyrene diol epoxide isomers are produced, which are very electrophilic. The electrophilic epoxides are attacked by the electron rich N^2 of guanine and the N^6 of adenine. A common reaction of the B[a]P diol epoxides is the reaction of (+)-trans with the exocyclic N^2 of guanine, which promotes G -> T transversions(*23*). Aflatoxins are toxins produced by species of fungi that, like B[a]P, are converted to epoxides by the body to increase hydrophilicity for excretion from the body. Activated aflatoxin reacts with the N^7 of guanine, causing G -> T transversions(*24*). Aromatic amines are the primary focus of the work presented here and will be discussed in more detail below.

C. Aromatic Amines

Aromatic amines represent an important class of environmental and industrial chemicals, many of which have been reported to be carcinogens and mutagens. This class of compounds is used in the production of chemicals such as pesticides, medicines, polymers, surfactants, antioxidants, and dyestuffs. Aromatic amines can also be found as a byproduct of cigarette smoke and cooked meats. In the late 1800s, Dr. Ludwig Rehn noted the prevalence of bladder tumors in dye factory workers as well as workers using aniline in chemical factories(*25*). In the 1930's and 40's researchers showed that the commercially available form of β-naphthylamine as well as the partially purified compound caused tumors to form in the bladder of dogs. Ongoing work showed common industrial compounds aniline and benzidine also caused bladder tumors in dogs and rodents(*26*).

In 1967 Sugimura questioned the compounds found in the fumes emitted from cooked meat, knowing that cigarette smoke condensates had shown mutagenic activity. He also analyzed the brown part on the surface of cooked meat and found both the fumes and the browned meat contained mutagenic properties(*27*). The properties were different than those seen with PAHs. The compounds with the mutagenic activity were found to be heterocyclic aromatic amines (HCA). One type of heterocyclic aromatic amines from cooked meat is produced when a mixture of creatinine, amino acids, and sugars are heated together, while another type is formed from the pyrolysis of proteins and amino acids. The prevalent type of HCA produced is temperature dependent(*28*). Cytochrome P450s convert these HCAs into hydroxylamino derivatives, which are further metabolized by sulfotransferases, acetyltransferases and esterification enzymes. The activated forms react mainly with the C8 position on guanine causing misreading of the template during DNA replication. Activated heterocyclic amines have been shown to cause cancers in numerous organs including breast, colon, prostate, and liver(*29*).

D. Aminofluorene

i. History of AF and AAF

Two of the most thoroughly studied heterocyclic aromatic amines are compounds 2-aminofluorene (AF) and N-acetyl-2-aminofluorene (AAF). In 1940, AF was patented by the US Department of Agriculture as an insecticide for mosquito larva and tobacco hornworm(*30*). Toxicity tests showed that AF and AAF, which was also being tested as a pesticide, were carcinogenic and mutagenic in both

prokaryotes and eukaryotes, leading to a ban in the use of AF and AAF as pesticides. Since this discovery, AF and AAF have served as model carcinogens in both metabolic activation of chemical carcinogens and the mechanism of DNA replication and repair leading to mutagenesis(*31-34*).

ii. Metabolic Activation of AF and AAF and DNA adduction

Similar to polycyclic aromatic hydrocarbons, AF and AAF are indirect damaging agents that must be activated within the body to become carcinogenic. Figure 1 shows a schematic of the metabolic activation of AF and AAF. As a mechanism to remove these compounds from the body, hydroxyl groups are added to the relatively hydrophobic AF and AAF molecules by cytochrome P450 monooxygenase. The N-hydroxyl form of AF has the ability to directly react with DNA, yet both AF and AAF undergo further modification to become increasingly electrophilic. Sulfotransferase, O-acetylase, and N,O-acyltransferase react with AF and AAF to create highly reactive ester forms of N-hydroxy-AF and N-hydroxy-AAF. The ester forms of these compounds react with C8 position of guanine to form N-(deoxyguanosin-8-yl)-2-aminofluorene (dG-C8-AF) and N-(deoxyguanosin-8-yl)-2-acetylaminofluorene (dG-C8-AAF)(*35*). The enzymes used in the metabolic activation of AF and AAF are found at the higher concentrations in the liver. The amount of liver tumors induced by AF and AAF can be correlated with the amount of enzymatic activity of cytochrome P450 type enzymes in the liver. For example, guinea pigs which have low levels of enzymes that perform N-oxidation in the liver making them less sensitive to the carcinogenic properties of arylamines (*30*).

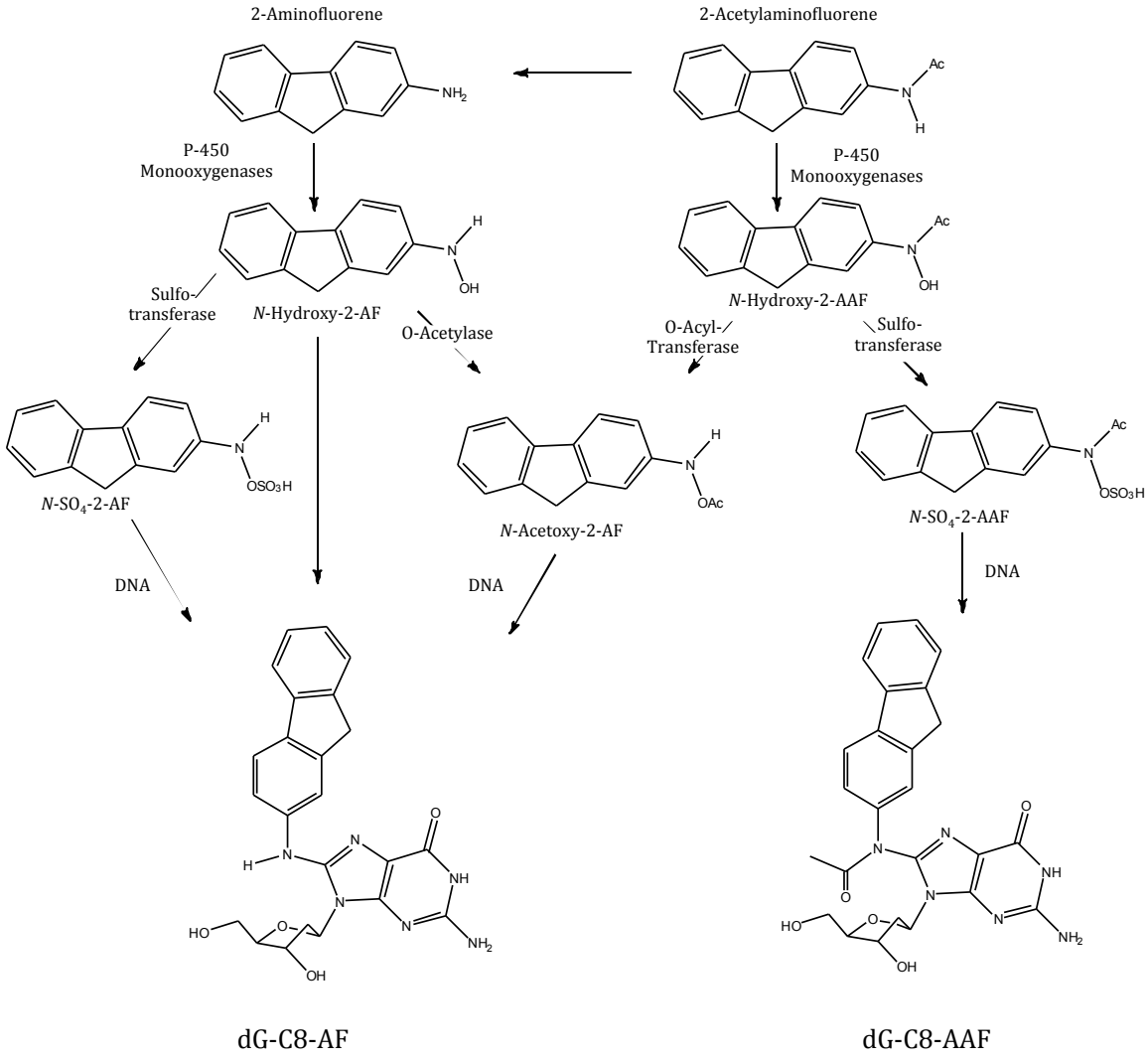

Figure 1. Metabolic activation of N-acetyl-2-aminofluorene and 2-aminofluorene to DNA in the cell (adapted from (35)). Only the major DNA adducts shown here are used in this work.

iii. Structure of AF and AAF in DNA duplex

The overall structures of dG-C8-AAF and dG-C8-AF (from here on dG-AF and dG-AAF will refer to the C8 modified bases) differ by only a single acetyl group (Figure 2). Yet, this acetyl group alters how the dG-AAF modified base sits within the DNA. NMR studies of modified duplex DNA show the AAF modified guanine base is rotated from the natural *anti* to *syn* conformation around the glycosidic bond due to a steric clash between the sugar and the acetyl group. This *syn* to *anti* rotation inserts the fluorene moiety into the double helix, displacing the guanine base into the major groove. This structure of AAF DNA is known as the base displacement or insertion denaturation model (Figure 3) (*36*). The AAF base modification disrupts normal Watson Crick base pairing between modified guanine and opposing cytosine, and also causes helical distortion for the nucleotides surrounding the lesion. In contrast, the absence of the acetyl group allows dG-AF to adopt two interchangeable conformations. The major conformation places the AF moiety outside of the helix and in the major groove, without disrupting normal Watson Crick base pairing. In the minor conformation, the fluorene ring of AF stacks within the helix, similar to the base displacement model seen with AAF (Figure 4) (*37, 38*). The observation of the different conformations that AF and AAF adopt in the DNA double helix is thought to be related to the observed mutagenic properties of each adduct. The disruption of Watson Crick base paring by the insertion of AAF into the helix provides an explanation for AAF being a strong block to replication. The structure of AF is far less distorting when in the major conformation, possibly explaining why

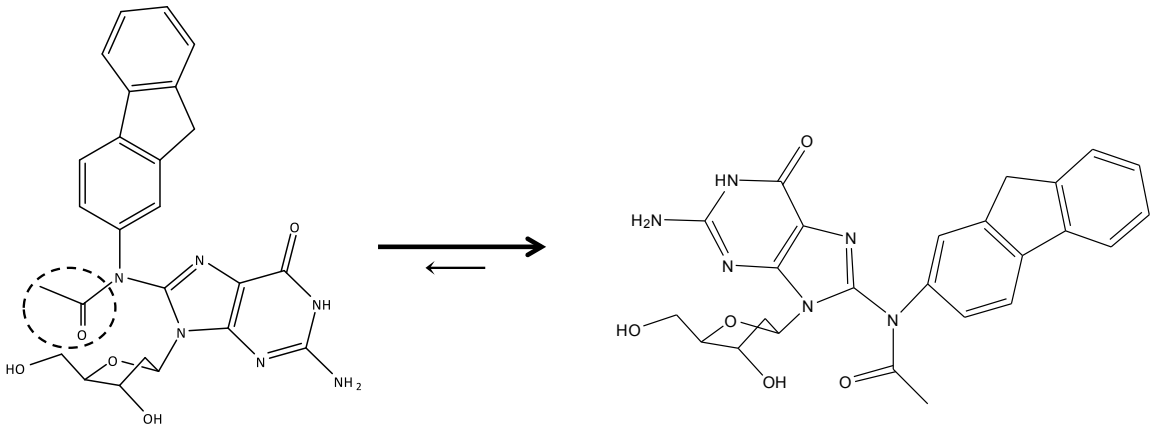

Anti dG-AAF

Syn dG-AAF

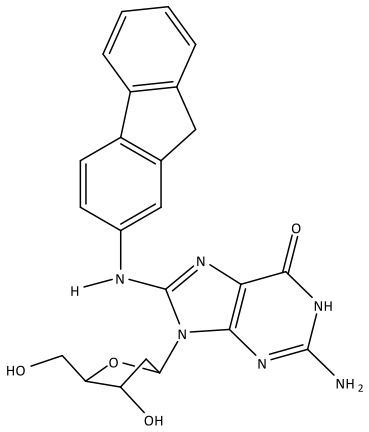

Anti dG-AF

Figure 2. The conformations of dG-C8-AAF and dG-C8-AF. A) Unlike native DNA that favors an *anti* conformation, dG-AAF modified base favors the *syn* conformation due to a steric clash between the acetyl group (in circle) and the deoxyribose sugar. B) dG-AF does not contain an acetyl group, avoiding a steric clash and allowing for both *syn* and *anti* conformations to occur.

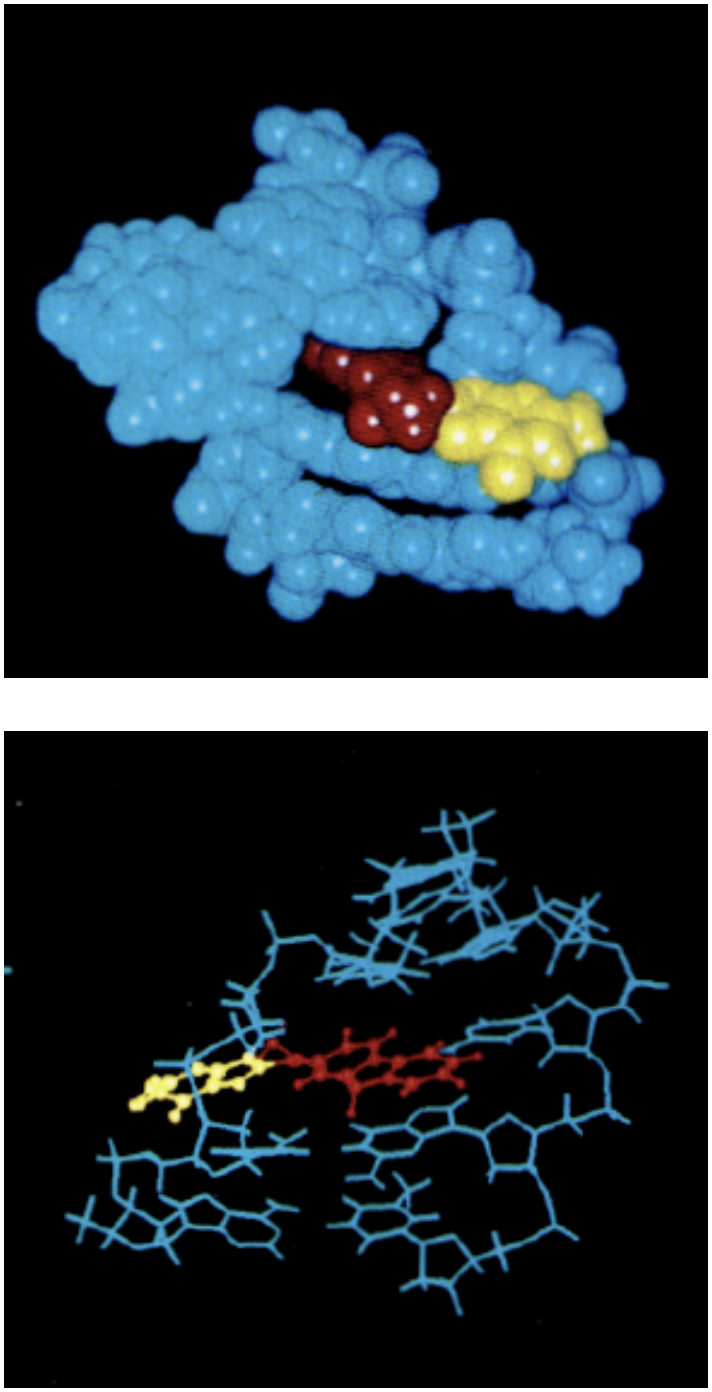

Figure 3. NMR solution structure of AAF modified base intercalated into duplex DNA. Top, space fill and bottom, ball and stick. The deoxyguanosine base is in yellow and the fluorene moiety is in red. (Adapted from (88))

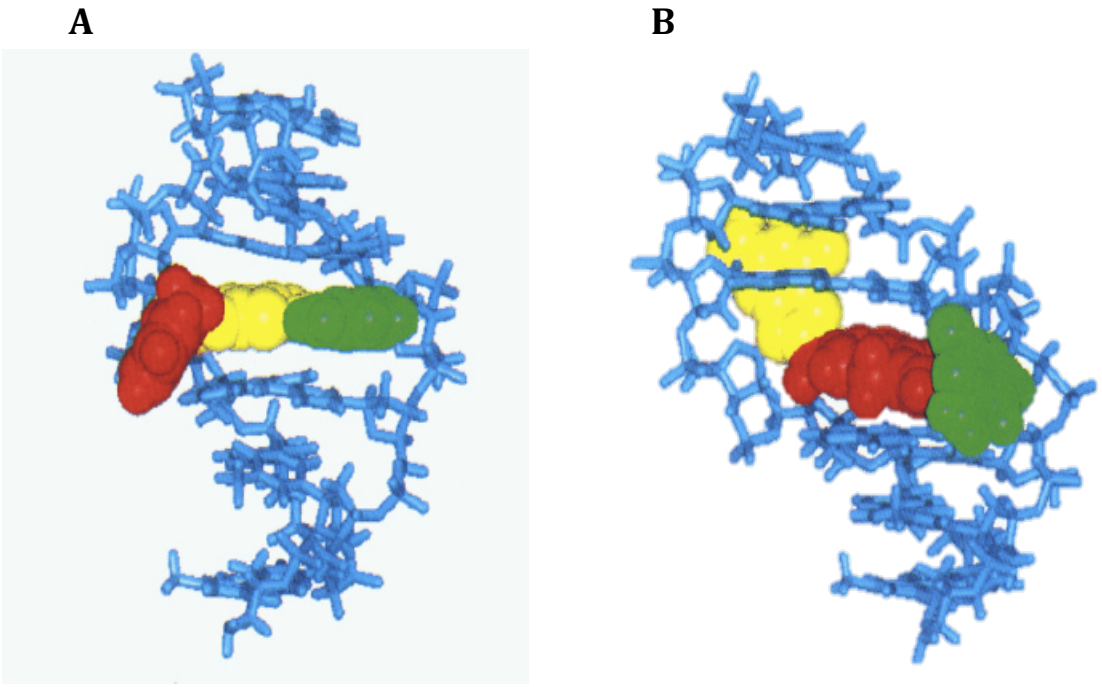

Figure 4. NMR solution structures of the two interchangeable conformations of 2-aminofluorene modified base in duplex DNA (Adapted from Eckel). DNA is blue, AF moiety is red, guanosine base is yellow, and cytosine is green. A) dG-AF adduct is in the external conformation. B) dG-AF adduct is in the internal conformation.

dG-AF is bypassed more easily(*39*). However, these structures alone do not explain the mutational patterns generated during replication.

Before continuing on with the discussion of how AF and AAF alter DNA replication, it is important to take a moment to discuss DNA replication and the enzyme involved in this process. After that, more will be discussed on the topic of the mutagenic properties of AF and AAF.

II. DNA Polymerase

A. Structure and function

Before a cell can divide, the information stored in the DNA must be faithfully replicated to ensure both daughter cells contain identical genetic material. The enzyme performing the accurate synthesis of the DNA is known as DNA polymerase. The replication fidelity of enzymatic DNA synthesis is quite remarkable. Under normal conditions, a replicative polymerase makes one mistake in approximately 10^5 bases incorporated(*40*). Several different types of polymerases exist in the cell, with different roles for DNA replication including chromosomal DNA synthesis, proofreading and lesion bypass. The first type of DNA polymerase discovered was a high fidelity polymerase from *E. coli*, fittingly named DNA polymerase I (Pol I)(*41*). The discovery of this enzyme earned Arthur Kornberg the Nobel Prize in physiology or medicine in 1959. Although it was the first polymerase discovered, it was found that Pol I was not the main DNA replication enzyme in the cell. The role of DNA Pol I is to process Okazaki fragments produced during lagging strand synthesis and assist in repair of damaged duplex DNA(*42*). To accomplish these roles, DNA pol I is

comprised of domains that contain a 5' – 3' polymerase activity for DNA replication as well as 5' – 3' and 3' – 5' exonuclease activities. The 5' – 3' exonuclease activity is needed to process Okazaki fragments, removing RNA primers that are part of the fragment. The 3' – 5' exonuclease activity aids in increasing the fidelity of the polymerase. This proofreading activity removes any nucleotide that was incorrectly incorporated by the polymerase.

A derivative of *E. coli* DNA pol I, Klenow fragment has been used as a model enzyme in countless DNA replication studies. Klenow fragment (KF) was produced through proteolytic cleavage of DNA Pol I separating the protein into two fragments: the C-terminal fragment contained both the 5' – 3' polymerase activity and the 3' – 5' exonuclease (proofreading) activity, and the smaller N-terminal fragment contained the 5' – 3' exonuclease activity. The large C-terminal fragment was known as the Klenow fragment, which was name after the researcher Hans Klenow(*43, 44*). To characterize just the polymerase activity of Klenow fragment for biological studies, a single D424A point mutation in the 3' – 5' exonuclease domain abolished the exonuclease activity(*45*).

The first crystal structure of a DNA polymerase was determined for KF in 1985 by Ollis *et al.(46).* The structure revealed that KF folded into two domains, the large domain with a distinct cleft containing the polymerization domain and a smaller domain containing the 3' – 5' exonuclease domain. After seeing the structure, the authors noted the polymerase resembled the shape of a human right hand, containing three subdomains, fingers, palm, and thumb. As the crystal

structures of other polymerases were determined, this shape was found to be almost universal with DNA polymerases. The crystal structure of *Thermus aquaticus* DNA polymerase I, a homolog of Klenow fragment, mimicked this same structure (Figure 5)(*47*).

B. Polymerase-DNA binary complex

The co-crystal structure of Klenow fragment bound to the primer template terminus of DNA revealed the orientation of DNA within the enzyme(*48*). This structure showed the polymerase held the DNA at right angles to the cleft of the palm domain that contained the active site residues. The 3' end of the primer strand was melted away from the template and placed in the exonuclease domain. The authors used the information they had and modeled the primer strand within the polymerase active site. They found that for the primer strand to bind in the polymerase active site, distortions in the protein are needed for proper DNA binding, and that these changes aid the protein in distinguishing a proper base pair from an incorrect base pair. This change was the first suggestion that conformational changes were taking place within the enzyme and also that the primer strand of the DNA could be shuttled between the polymerase active site and the exonuclease site without the enzyme dissociating first(*48*). These observations were later confirmed with the crystal structure of Klentaq1, the KF homolog from thermophilic *Thermus aquaticus* DNA polymerase I (*49*). Unlike the co-crystal structure obtained by Beese *et al.* the co-crystal structure of Klentaq had the primer template terminus situated in the polymerase active site (Figure 6). The structures of KF and Klentaq revealed widespread non-specific contacts were formed between

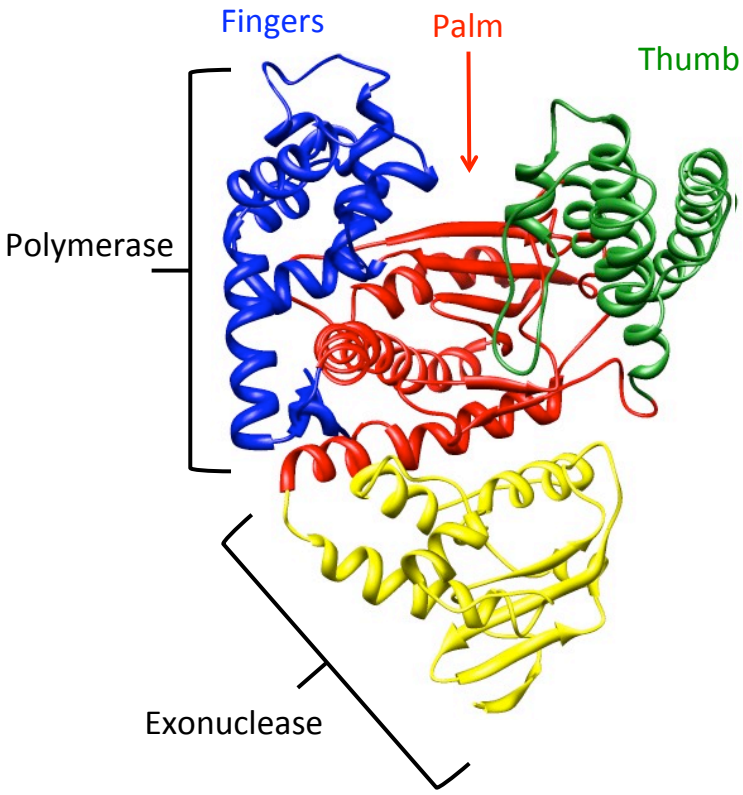

Figure 5. Klentaq1 crystal structure in the absence of DNA. (PDB 1KTQ) The top section contains the polymerase domain, consisting of three subdomains that resemble a human right hand; the palm (red), thumb (green), and fingers (blue) domains. The palm subdomain contains the catalytic active site for 5' to 3' polymerase activity. The exonuclease domain (yellow) contains the active site for 3' to 5' exonuclease activity.

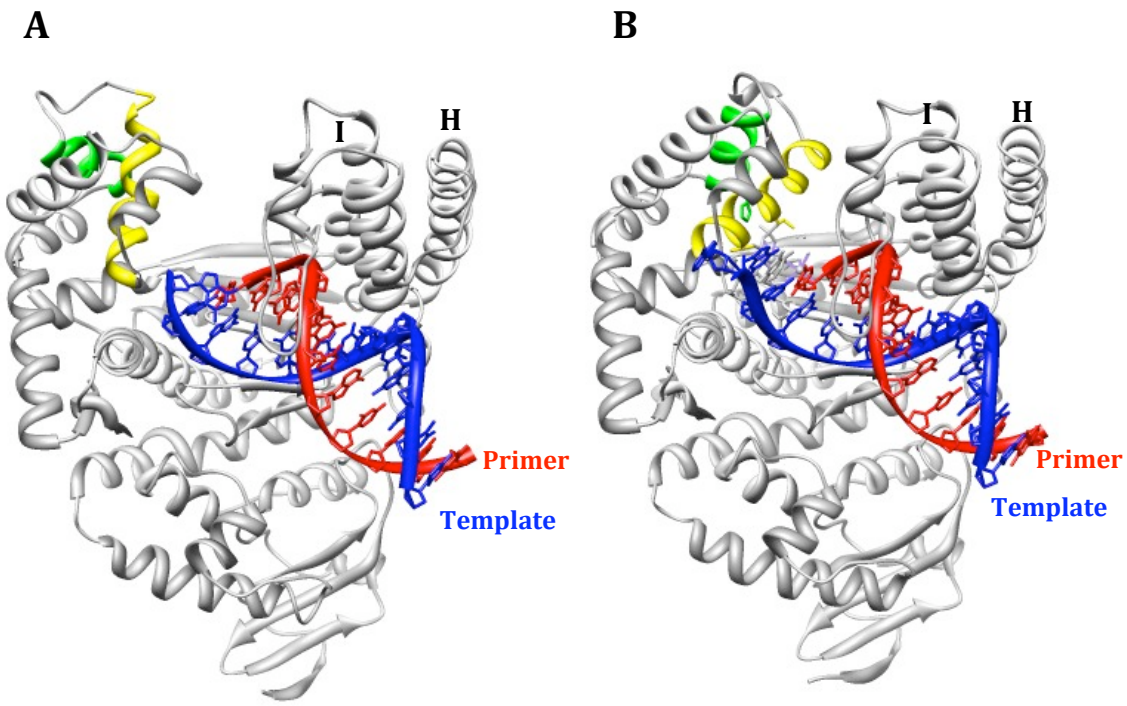

Figure 6. Crystal structures of the open ternary and closed ternary forms of Klentaq1. A) In the open ternary complex (PDB 4KTQ), the primer template terminus is situated in the cleft formed by the thumb, fingers, and palm domains. The thumb domain makes numerous nonspecific interactions with the DNA via the H and I helices. B) In the closed ternary complex (PDB 3KTQ), ddCTP is correctly base paired in the active site and the O helix (yellow) and N helix (green) of the fingers region undergo a large conformational change. In both structures the primer strand is in red and the template strand is in blue.

the enzyme and the phosphate backbone of the DNA, including interactions between the enzyme and hydrogen bond donor and acceptors in the minor groove. These universal interactions are important for polymerase to bind DNA in a sequence independent manner. The Klentaq-DNA binary complex structure showed that once DNA bound, the thumb region of the polymerase shifted, rotating helices H1 and H2 12° towards the DNA, to make a direct contact with a well conserved lysine residue (Lys540 in Klentaq). The closing of the thumb around the DNA is there to ensure the polymerase stays bound to the DNA during the dNTP selection process, increasing processivity. This movement of the thumb region to increase contact with the DNA is an example of one of the conformational changes DNA polymerases undergo during replication. The second conformational change of the polymerase occurs upon correct dNTP binding and is specific to the formation of the catalytically active ternary complex.

C. Polymerase-DNA-dNTP ternary complex

A catalytically competent ternary complex must be formed in order for DNA polymerase to successfully replicate DNA. Proper geometric alignment of the primer template terminus of the DNA, catalytic residues of the polymerase, the correct dNTP, and metal ions must occur in the active site for a successful dNTP incorporation to take place. The first ternary complexes of replicative DNA polymerase crystalized revealed a large amount of information about catalytically active residues in the active site, the location of incoming dNTP binding, importance of metal ions, and a large conformational change of the protein(*49-51*). The replicative polymerases crystalized were from a wide variety of organisms including

rat, bacteria, and bacteriophage, and yet all shared the right handed architecture seen in *E. coli* derived Klenow fragment as well as active site geometry.

Within the active site of the ternary complex, oxygens of the triphosphate group interact with positively charged residues near the O helix, positioning the triphosphate almost parallel to the O helix. It is hypothesized that the interaction of the phosphates on the incoming nucleotide are a primary recognition portion of the incoming dNTP(*49*). Crystal structures of Klentaq1 with each of the four dNTPs showed the phosphate groups in analogous positions, but the base and sugar of the four dNTPs were not in the same orientations. The most obvious difference between the crystals with the four dNTPs was the large conformation change the polymerase undergoes once the correct dNTP is based paired across from the templating base (Figure 6). A Klentaq1 crystal with a dideoxy form of dNTP (ddNTP) resulted in two forms of the polymerase ternary complex, an open and a closed form. The open form was similar to the binary complex (polymerase-DNA) in that the space between the palm, thumb, and fingers domain was open even though there was a ddNTP bound. In the closed ternary complex, the finger domain closed this crevice, decreasing the solvent exposure of the polymerase active site and forcing proper alignment of the catalytic residues for nucleotide addition. The movement of the fingers domain consists of two rotations affecting different helices in the finger domain. The first involved a rotation of the N, O, O1, and O2 helices partially closing the crevice. A second movement rotated the N and O helices 40° toward the primer template terminus, further closing off the crevice. This movement also has a specific effect on nucleotide selection. Tyrosine 671 of

Klentaq1 (Tyr766 in KF) on the O helix is stacked with the template base in the open conformation, allowing for incoming dNTP to be tested against the templating base, but keeping it from entering the active site. The location of the templating base during this preview is known as the pre-insertion site. Once the correct dNTP is selected and the conformational change occurs, Tyr671 rotates away from the nucleotide binding site allowing the templating base to move from the pre-insertion site to position itself across from the incoming ddNTP in the active site, or insertion site. This tyrosine residue is thought of as a gate, allowing for the preview but not incorporation of incorrect dNTPs.

Biochemical studies with Klenow fragment further explored the formation of the closed complex(*52*). It was shown that the lysine and arginine residues involved in dNTP binding in the KF active site were cleaved by trypsin when KF was bound to duplex DNA in an open conformation. With the addition of nucleotide, the same tryptic digestion pattern did not occur. It was believed the cleavage was inhibited by the formation of the closed complex, protecting the residues of the active site from cleavage since this cleavage pattern was not observed when an incorrect nucleotide was added. The same experiment was performed in the presence of ribonucleic acids with a correct base, but the inhibited cleavage pattern was not seen, further proving that the conformational change could only occur if correct dNTP was bound in the polymerase active site. This, along with the crystal structure of the securely aligned geometry within the active site of the closed ternary complex, showed that formation of a tight pocket around the templating base and incoming

nucleotide explains the low misincorporation rate observed for replicative DNA polymerases.

D. Reaction mechanism of nucleotide addition

The first mechanism for DNA replication was hypothesized by Watson and Crick when they said that one strand on DNA could be used as template to synthesize a new strand(*53*). Since then, the mechanism has expanded to numerous steps including the conformational change discussed above (Figure 7). In the initial step, as Watson and Crick hypothesized, the polymerase binds the DNA to be replicated and forms the binary complex. For DNA polymerases that contain an exonuclease domain in addition to the polymerase, the enzyme can bind at either the polymerase (E_p) domain or the exonuclease (E_x) domain. Correctly paired DNA tends to bind the polymerase domain, while DNA with mismatches near the primer template terminus have been shown to increase binding to the exonuclease domain(*54*). With the DNA bound to the polymerase active site, dNTP can bind to form a ternary complex that first forms in an open conformation(*49*). If the dNTP in the open ternary complex can form Watson Crick base pairing with the templating base, a conformational change occurs to the closed ternary complex(*49-52*). The ternary structure aligns the alpha-phosphate of incoming dNTP for nucleophilic attack by the 3'OH of the primer resulting in phosphodiester bond formation. After the nucleotide is incorporated another conformational change occurs, returning the polymerase to an open conformation, releasing pyrophosphate, and the polymerase continues down the DNA to the next templating base where the process starts all over again.

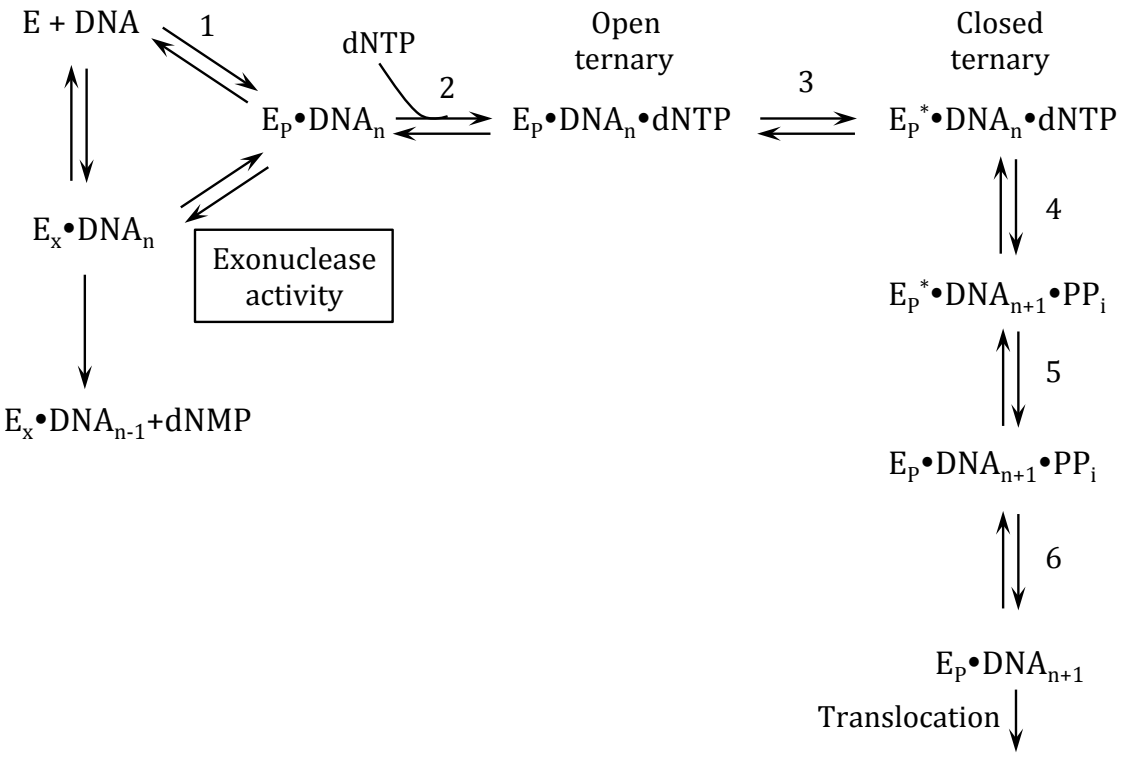

Figure 7. Reaction mechanism of DNA synthesis by a replicative DNA polymerase. Each number above the arrows corresponds to each step. E_p represents the DNA bound to the polymerase active site, and E_x represents DNA bound to the exonuclease active site. In step 1 the enzyme forms a binary complex in either the polymerase or exonuclease active site. Step 2 shows the binding of dNTP to form the open ternary complex. If the nucleotide chosen is the next correct nucleotide, the polymerase undergoes a conformational change in step 3 to form a closed ternary complex. Catalysis occurs in step 4 and steps 5 and 6 represent the polymerase re-opening and releasing pyrophosphate (PP_i). Once this occurs, the enzyme translocates and the process is started all over again.

As noted in the first section of this introduction, the incorporation of correct nucleotides is important for proper cellular function in daughter cells. The process of nucleotide selection by DNA polymerases not only involves choosing a base complementary to the templating base, but also involves the recognition of a deoxyribose sugar over a ribose sugar. For KF, the selection process against mispaired rNTPs and dNTPs occurs when the polymerase is in an open conformation(*55, 56*). Complementary rNTPs on the other hand are thought to be selected against as the fingers domain moves during the conformational change. In KF, the 2'OH of the ribose sugar interacts with Glu-710 in the active site, hindering the fingers closing movement(*57*). This again adds to the importance of the conformational change in successful DNA synthesis.

III. Interactions of AF and AAF with polymerase

A change in DNA sequence at a confined site within a gene is known as gene mutation or point mutation. Two types of point mutations are single base pair substitutions and frameshift mutations. A base pair substitution occurs when one DNA base pair (e.g. C:G) is replaced by another (e.g. T:A) and yet the number of base pairs does not change. Frameshift mutations on the other hand do cause a change in the number of base pairs, a gain or a loss, in the original sequence. Commonly, frameshifts cause a gain or loss of one or two base pairs, enough to alter the genetic code reading frame(*58*). Biochemical studies revealed that dG-AF and dG-AAF have distinct mutagenic profiles in *Escherichia coli*. In the studies where the *E. coli* genome was modified with AF, the dG-AF adduct predominately produced base substitution mutations that were randomly distributed throughout the genome(*59,*

60). dG-AAF on the other hand produced frameshift mutations that were found most frequently in specific repetitive sequences(*61, 62*). *In vivo* mutagenic studies using rats found AAF formed DNA adducts and produced both frameshift mutations and G to T transversions in a number of cell types, with the highest concentration in the liver(*63, 64*). *In vitro* primer extension studies revealed that nucleotide incorporation across from a dG-AAF adduct by the Klenow fragment of *E. coli* DNA pol I was strongly blocked(*33*), similar to the dNTP incorporation by T7 DNA polymerase and T4 DNA polymerase(*34, 65*). The dG-AF adduct slowed or stalled nucleotide incorporation, but the DNA polymerase was able to eventually bypass the lesion(*33*).

Further biochemical studies revealed that even though polymerase was unable to incorporate a nucleotide across from dG-AAF, polymerase binding affinity increased at this position. Gel shift binding studies with Klenow fragment (KF) showed that dG-AAF as the templating base increased KF binding affinity 5-10 fold over both unmodified DNA and DNA modified with an AF templating base. Also, the addition of dCTP, the nucleotide able to form a correct Watson Crick base pair with dG-AAF did not enhance polymerase binding affinity(*33*). To explain this observation, Dzantiev and Romano hypothesized that the AAF ring structure was interacting with a number of hydrophobic amino acids, close to the polymerase active site. Positive interactions like this would stabilize the binary complex of DNA and KF. These interactions were also thought to be responsible for the lack of binding enhancement seen with the addition of the next correct nucleotide, which is seen after a conformational change of the polymerase (discussed above). It was in a

subsequent paper that the same authors explored the KF conformational change when binding to DNA modified with AF or AAF. Using tryptic digestion, which for KF cleaves near the polymerase domain active site only when the polymerase is in the open conformation, they saw that when KF was bound to DNA modified with dG-AAF in the presence of dCTP the KF was cleaved by the trypsin(*66*). This implied that when KF bound to DNA with dG-AAF as the templating base, the polymerase was unable to undergo the conformational change and bound to dG-AAF modified templating base in an open conformation. When a different primer was used, placing dG-AAF at position +1 (single stranded region of the template strand), tryptic digestion showed a conformational change was occurring and dG-AAF did not alter binding. KF binding to dG-AF as the templating base showed reduced levels of KF in the closed complex. The difference between dG-AF and dG-AAF was attributed to the different conformations each adduct adopts when in a DNA helix.

To further investigate the type of interactions between the AAF moiety and the polymerase, Lone and Romano performed experiments using an Y766S KF mutant. In wild type KF, tyrosine 766 stacks on top of the template base when KF is in an open conformation, and then swings away during the transition from the open to the closed complex allowing for the incoming nucleotide to bind. Tyrosine 766 has been shown to be an important residue for correct active site geometry, and a mutation in Y766 leads to an increase in the rate of incorrect nucleotide insertions and reduced ability of the polymerase to extend after these misincorporations(*67*). An incorporation assay with wild type KF showed the polymerase mainly stalled one nucleotide before the dG-AAF adduct, yet was able to incorporate

approximately 20% across from the adduct, and 6% full primer extension. In contrast, the Y766S mutant Klenow fragment showed 40% incorporation across from dG-AAF, but only gave 1% extension beyond the adduct. On top of the higher incorporation percentage, the Y766S mutant also showed a higher V_{max}/K_m for incorporation of the next correct nucleotide, dC, across from dG-AAF. This study showed that polymerases with larger active sites would be able to more easily incorporate across from modified DNA bases, and it also showed the importance tyrosine 766 has on polymerase fidelity.

A. AF and AAF Binary Crystal Structures

The slight difference in structure between dG-AF and dG-AAF accounts for the different conformations for each of the modified bases within duplex DNA. However there was no direct evidence for the biological effects, such as polymerase stalling at dG-AAF or increased polymerase binding affinity at dG-AAF, until the determination of the crystal structures of dG-AAF and dG-AF in the active site. Dutta *et al*. obtained crystal structures of bacteriophage T7 DNA polymerase bound to duplexed modified DNA containing either dG-AF or dG-AAF as the templating base(*68*). Figure 8 shows the crystal structure of T7 pol bound to dG-AAF modified DNA. The most notable part of the crystal structure was the location of the modified base, which was flipped out of the polymerase active site. The modified base was in the *syn* conformation, as it had been in duplex DNA, which allowed the fluorene moiety to insert itself into a hydrophobic pocket behind the O helix in the fingers domain. The AAF ring structure was stabilized by interacting with a number of leucine side chains in the pocket and stacks against phenylalanine 528. The acetyl

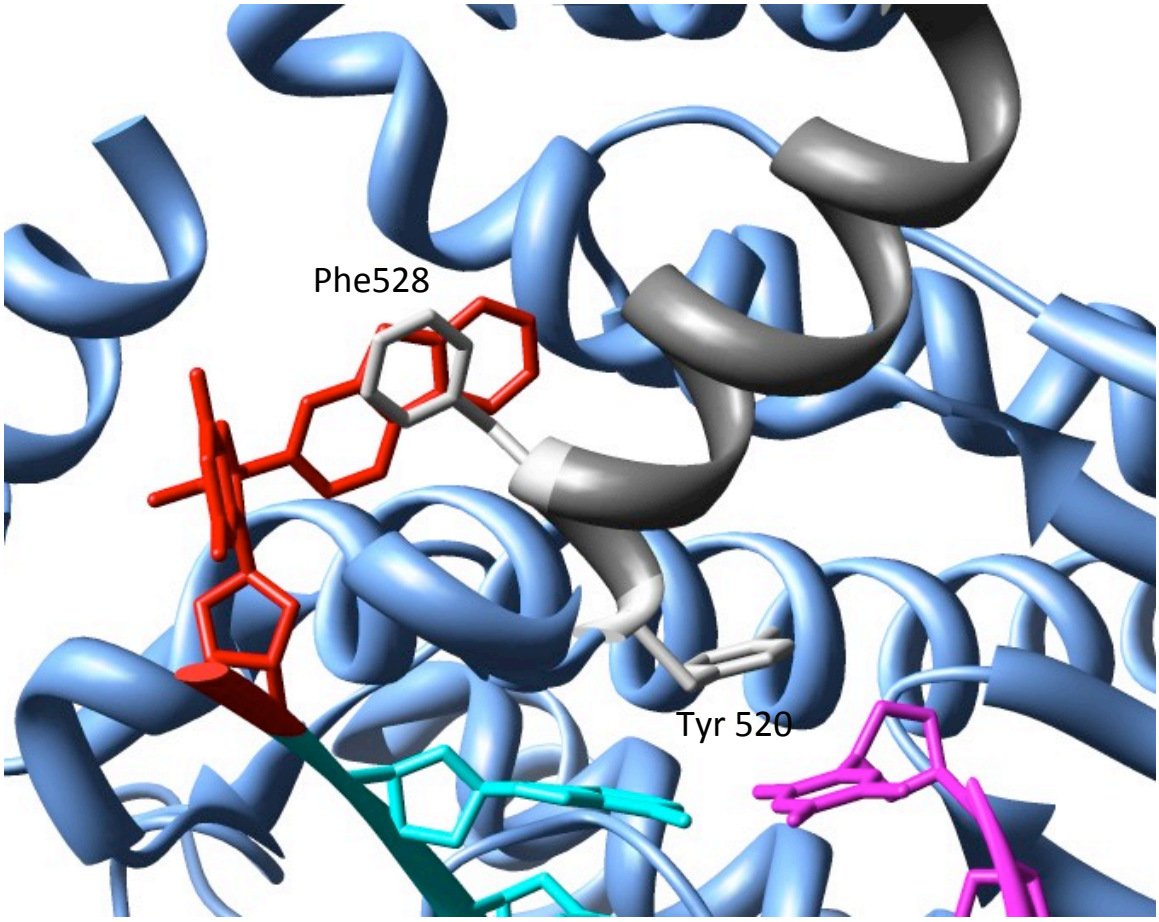

Figure 8. Crystal Structure of T7 DNA pol I bound DNA containing an AAF modified guanine as a templating base. (PDB 1X9M) The dG-AAF base (red) is rotated out of the active site, where the fluorene ring intercalates into a hydrophobic pocket behind the O helix (dark grey). Phe528 (light grey) from the O helix stacks with the AAF moiety, and disrupting the position of the O helix. The disruption of the O helix pushes Tyr520 into the nucleotide binding pocket where it stacks with the last formed base pair (Template cyan, primer pink).

group of AAF did not make contact with the polymerase and is directed away from hydrophobic pocket, facing the solvent. The modified base was further stabilized by hydrogen bonds between asparagine 534 and arginine 566 with the N^2 and N^7 functional groups of guanine, respectively. The fluorene ring caused the hydrophobic residues with which it interacts to repack, distorting the C terminus of the O helix. This pushed the O helix into the polymerase active site, partially blocking the nucleotide binding site. In addition, the crystal was grown in the presence of dCTP, but there was no evidence of a nucleotide bound to the nucleotide binding site(*68*). This crystal structure of T7 DNA polymerase with dG-AAF modified DNA verifies that the increased binding affinity seen in biochemical studies was not due to a conformational change from an open to a closed complex, but rather to the stabilization of the fluorene moiety on the modified base within the protein.

The crystal structure of T7 DNA polymerase with DNA containing a dG-AF modified templating base is similar to the crystal structure with the dG-AFF DNA (Figure 9). The main difference between the two is the lack of electron density corresponding to the dG-AF nucleotide. Although the AF moiety location is of poor quality and it was difficult to determine the precise positioning of the dG-AF nucleoside, the authors made a point to state where dG-AF was not located. The structure of the polymerase clearly showed the nonpolar side chains in a native conformation, filling in the hydrophobic pocket, showing that the AF moiety was not bound in the hydrophobic pocket behind the O helix like AAF. The dG-AF nucleoside was also not located in the polymerase active site, as the tyrosine 530 side chain occupied the space of the templating base in a ternary complex. The structure of the

polymerase was well defined and the fingers region of the polymerase clearly sat in an open conformation. The lack of a clear electron density was indicative of the ability of dG-AF to fluctuate between *syn* and *anti* conformations(*69*). To gather more information about how polymerase binds to dG-AF modified DNA, the authors modeled the dG-AF in the *anti* conformation into a closed polymerase crystal structure. The model showed that there was little to no steric or electrostatic clashes between *anti* dG-AF and the polymerase active site(*68*). This explains why in the biochemical studies, KF had a weaker binding affinity to dG-AF modified template than dG-AAF modified template.

B. AF ternary complex

The interactions between AF modified DNA and the polymerase active site were of interest to other labs as well. The Beese lab produced crystal structures of thermophilic *Bacillus* DNA polymerase I fragment (BF), a homolog of KF, bound to DNA with an AF modified base as the templating base and in the DNA duplex terminus (post insertion site). Unlike the T7 crystal structure, the dG-AF modified base was fully visible in the crystal. Similar to unmodified DNA, the AF modified templating base was located in the pre-insertion site, where the fluorene moiety forms a number of van der Waals interactions with residues on the pre-insertion site surface and was protected from solvent exposure. The guanosine base stacked with the sugar residue of the +1 nucleoside on the template strand. The increased size of the modified base lead to a disordered O1 helix, yet did not disrupt the O helix, which remained in an open conformation with the nucleotide binding site free to accept an incoming nucleotide(*70*). In addition to the polymerase active site being

relatively unperturbed, both the primer and template strands kept normal Watson Crick base pairing and the 3'-hydroxyl of the primer strand is positioned for attack on an incoming dNTP. This crystal structure showed that when dG-AF was the templating base, it occupied the pre-insertion site in a similar manner as an unmodified base. The primer strand and polymerase active site were unaffected and ready for nucleotide addition(*70*). To expand their study on the interactions between the dG-AF base and the polymerase, BF-DNA co-crystals were added to a solution containing dCTP and recrystallized. The new crystals showed BF was able to incorporate dCTP across from dG-AF.

Unlike dG-AF as the templating base, the adduct in the primer template terminus adopts an *anti* conformation. In this *anti* conformation, the guanosine of dG-AF formed Watson Crick hydrogen bonds with cytosine and the AF moiety moves into the major groove, resembling the major conformation of dG-AF in duplex DNA (above). The AF moiety stacked with the templating base, keeping the base from entering the pre-insertion site. The C:G-AF terminal base pair caused distortions in a number of regions near the polymerase active site including the post-insertion site, insertion site, and template pre-insertion site(*70*). Together, these distortions imposed by dG-AF in the newly formed base pair explain why polymerase is able to incorporate across from dG-AF but has difficulty continuing synthesis beyond that point(*33*). Overall, the structures obtained by the Beese lab (*70*) and Dutta *et al.* (*68*) correlate well with previous biochemical data and further explain how mutational effects by AF and AAF are related to the conformations each adduct adopts within the active site of the polymerase.

C. Effects of sequence context on AF and AAF mutagenesis

Spontaneous base slipping was shown to occur at sites with repetitive bases, which leaves some bases unpaired or bulged out of the DNA helix(*58*). During DNA replication, if a bulge occurred in the template strand one or two bases would be deleted from the newly synthesized strand, while a bulge in a primer strand would lead to an insertion of an extra base. Slipping models proposed by Streisinger and Owen were relevant to the mutations induced in the presence of DNA adducts (Figure 9 a and b) (*58*). Sequence hotspots like repeating guanine residues (GGGG) as well as guanine-cytosine repeats (GGCGCC) were shown to cause slipping intermediates leading to mutations. These same sequences modified with AAF resulted in -1 and -2 frameshift mutations for the single nucleotide run (GGGG) and GC repeats (GGCGCC), respectively(*71, 72*). One of the most well studied repetitive sequences is the recognition sequence of the restriction enzyme *Nar*I, $G_1G_2CG_3CC$. A -2 frameshift occurs at this site at a very low frequency, but is increased when modified with an AAF adduct, specifically if the third guanine (G_3) is mutated, producing G_1G_2CC(*73*). This sequence modified with AF does not lead to the same frameshift mutations(*74*). A slipped structure mechanism within the DNA was thought to create this dinucleotide deletion, one where the primer misaligns with the template strand within the active site of the polymerase. The misalignment would be stabilized by the formation of Watson Crick base pairs with adjacent base pairs, causing the polymerase to skip nucleotides near the adduct. Gill and Romano used primer extension studies to explore the slipping mechanism on the *Nar*I recognition site(*32*). A number of different primers were duplexed with AAF

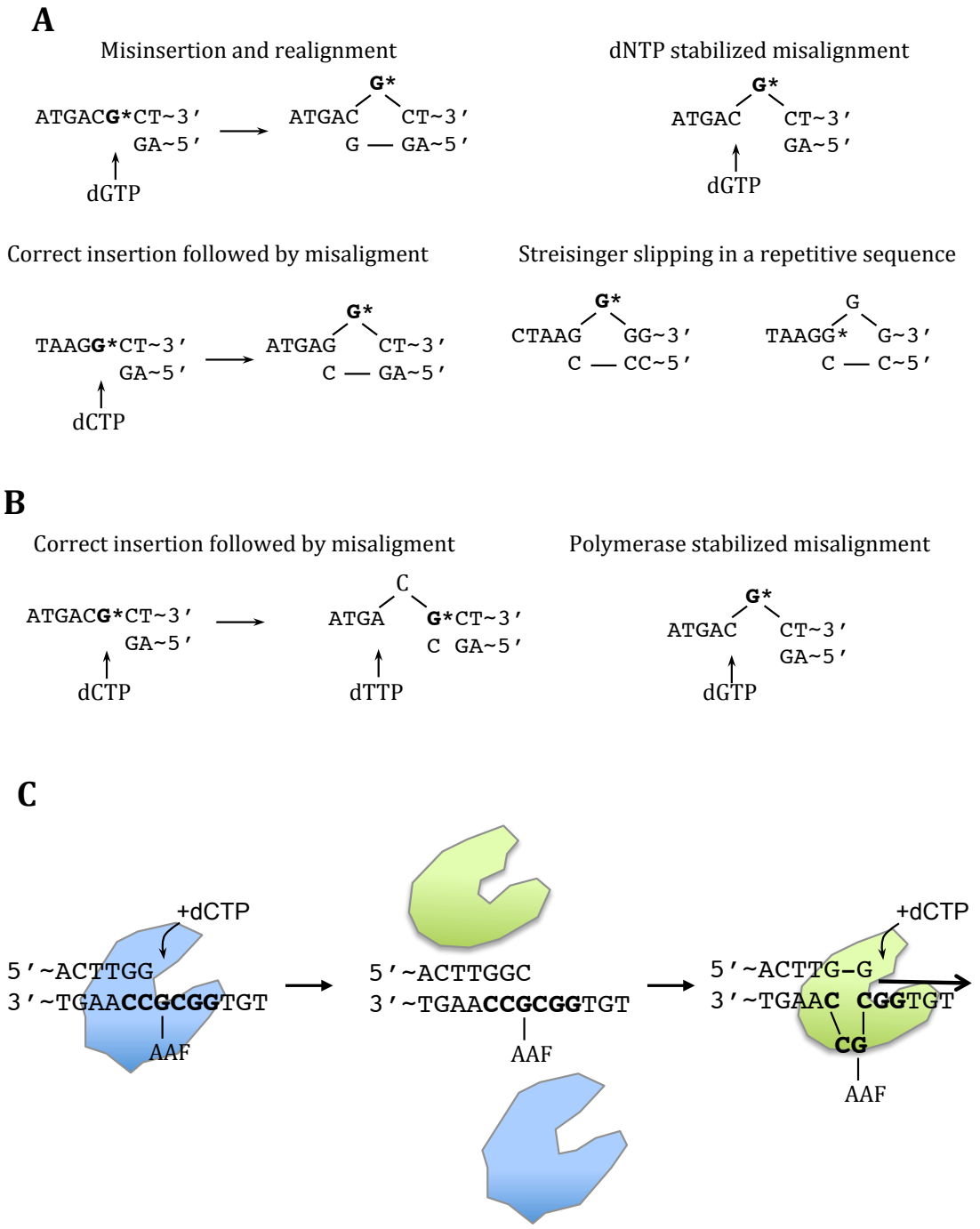

Figure 9. Bypass mechanism used in the presence of DNA lesions. A) Base pair stabilized misalignment during DNA synthesis of DNA with lesions B) Polymerase stabilized misalignment during DNA synthesis of DNA with lesions C) Two step mechanism for bypass of dG-AAF in the NarI sequence. A polymerase suited for incorporations across from bulky lesions incorporates dCTP across from the modified G and dissociates. A rearrangement in the DNA occurs and a second polymerase continues on with extension of the primer, creating a -2 frameshift deletion.

modified *Nar*I template, and the polymerase binding affinity with correct and incorrect nucleotides was monitored to determine which nucleotides lead to complementary binding. The results showed that *Nar*I with a G_3 AAF modification created a GC bulge across from the adduct leading to -2 frameshift mutation. In addition, the AAF modified *Nar*I sequence (AAF at G_3) did not induce the same increase in KF binding affinity as it had for the non-*Nar*I sequences, suggesting that the dG-AAF base does not occupy the same location in the polymerase when part of this sequence. A two step mechanism for the formation of the GC deletion has been postulated and is shown in figure 9c (*75*). First, dCTP is incorporated across from dG-AAF. Once C is incorporated, a structural rearrangement occurs causing dG-AAF and the 3'C to bulge out and the primer to bind upstream of the dG-AAF modified base. A second polymerase, one with a more open active site that could accommodate the bulky lesion, could bind the new primer template terminus and continue replication(*75*).

D. DNA lesions and bypass polymerases

DNA lesions exist as strong blocks to replicative DNA polymerases, yet cells have developed a pathway to replicate past these lesions. Specialized polymerases known as translesion synthesis (TSL) polymerases are able to perform replication in the presence of bulky adducts like AAF and AF. These TLS polymerases can replicate DNA in an error-free or error-prone manner depending on the type of adduct, the sequence context, and the polymerase performing the replication. The characteristic feature that separates TLS from replicative polymerase is their larger/more open active site, which accommodates bulky DNA lesions. Yeast

polymerase eta (Polη) and Dpo4 are examples of Y-family polymerases. Besides having a larger active site, Y-family polymerases are also characterized by stubby fingers and thumb domains as well as a polymerase associated domain (PAD) or little finger domain(*76*). Although there are some structural differences between replicative and Y family polymerases, the process of undergoing a conformational change as part of the mechanism is shared by both. Polη, from both yeast and humans, can efficiently incorporate across from and synthesize past UV induced 6-4 thymine-thymine dimers. Also, Polη can incorporate across from bulky adducts like dG-AAF, but cannot efficiently extend beyond them. Extension assays using yeast Polη showed full bypass of dG-AF, but not with dG-AAF(*77*). When dG-AAF acted as the templating base, the binding affinity of yeast Polη increased in the presence of dCTP, which indicated the formation of a closed ternary complex. Yet, after dCTP was incorporated across from dG-AAF, the next correct nucleotide was unable to enhance the binding affinity of Polη. This lack of enhancement is consistent with the inability of the polymerase to fully extend beyond the adduct.

Crystal structures of the archaeal Y-family polymerase Dpo4 with AF modified DNA give insight into how a translesion polymerase accommodates and extends from a bulky C:G-AF base pair. From a single asymmetrical unit of the crystal, two molecular structures were distinguished. The first showed correct base pairing between the G modified with AF and the opposing C. dG-AF was in the *anti* conformation and the AF moiety is placed in the major groove. The incoming dGTP base paired with the templating dC, but was not aligned properly in the active site. The C:dGTP base pair was shifted so the dGTP stacked above the center of the

modified C:G-AF base pair, and the templating C was slightly above the AF moiety. Side chains on the little finger domain of the polymerase kept the AF moiety from being exposed to the solvent(*78*). The second crystal obtained showed a polymerase active site where the single stranded region of template strand, downstream of the AF lesion, and the incoming dNTP were both misaligned. The C that should be acting as the templating base was looped out of the DNA into the major groove where it stacked with the surface of the little finger domain. The next nucleotide of the templating strand stacked above the C:G-AF terminal base pair, but did not pair with the incoming dGTP. The incoming dGTP did not pair with any templating base, but sat between the DNA double helix and the polymerase. The dG-AF base was in the *anti* conformation, fully base paired with dC, placing the AF moiety in the major groove, which was bent toward the 3' end of the template strand but still interacting with the little finger of the polymerase(*78*). These structures both showed the importance of the larger active site for adduct bypass, but also the importance of the little finger domain that is a feature of Y-family polymerase enzymes. The increased stability from the little finger domain allows the polymerase to manage primer-template misalignments, even if the misalignment results in a mutagenic outcome.

IV. Surface Plasmon Resonance

A very useful technique for investigating interactions of various biomolecules is surface plasmon resonance (SPR). SPR is a label free technique that measures analyte binding to a ligand in real time. Even thought the physical principles of SPR were discovered in 1902, the use of SPR for the investigation of biomolecules did

not take off until the 1980's. While creating an experiment to teach undergraduate students about surface plasmons, Leidberg *et al*. utilized SPR to study immunoglobulins(*79*). This teaching lab turned into one of the most advanced and established label-free techniques for the study of biomolecular interactions and kinetic properties that is used today.

A. Physical description

A surface plasmon wave is an electromagnetic wave that exists along the boundary of a metal and a dielectric medium. The existence of these waves is dictated by the conduction electrons found in the metal (charge density wave). These waves have a rippling nature that permits the formation of surface plasmons upon excitation. Excitation by a photon results in a transfer of energy from the photon to the charge density wave on the surface of the metal producing an evanescent wave. The evanescent wave produced varies with the energy and momentum of the photon. Only photons that hit the metal at angles that cause an evanescent wave to match with the charge density wave will produce resonance to occur(*80-82*). The resonance ability of the charge density wave is influenced by the mass near the metal. Figure 10 shows a typical SPR setup with a prism, gold surface, and dielectric medium. Incident light shines through the prism on to the gold surface at three different angles, two of which are reflected off the gold surface and do not create an evanescent wave or resonance. One of the angles coincides with the charge density wave and is reflected at decreased intensity because the energy of the photon is transferred to the metal surface. Plotting the reflected light intensity as a function of the angle of light reveals a sharp decrease in light intensity

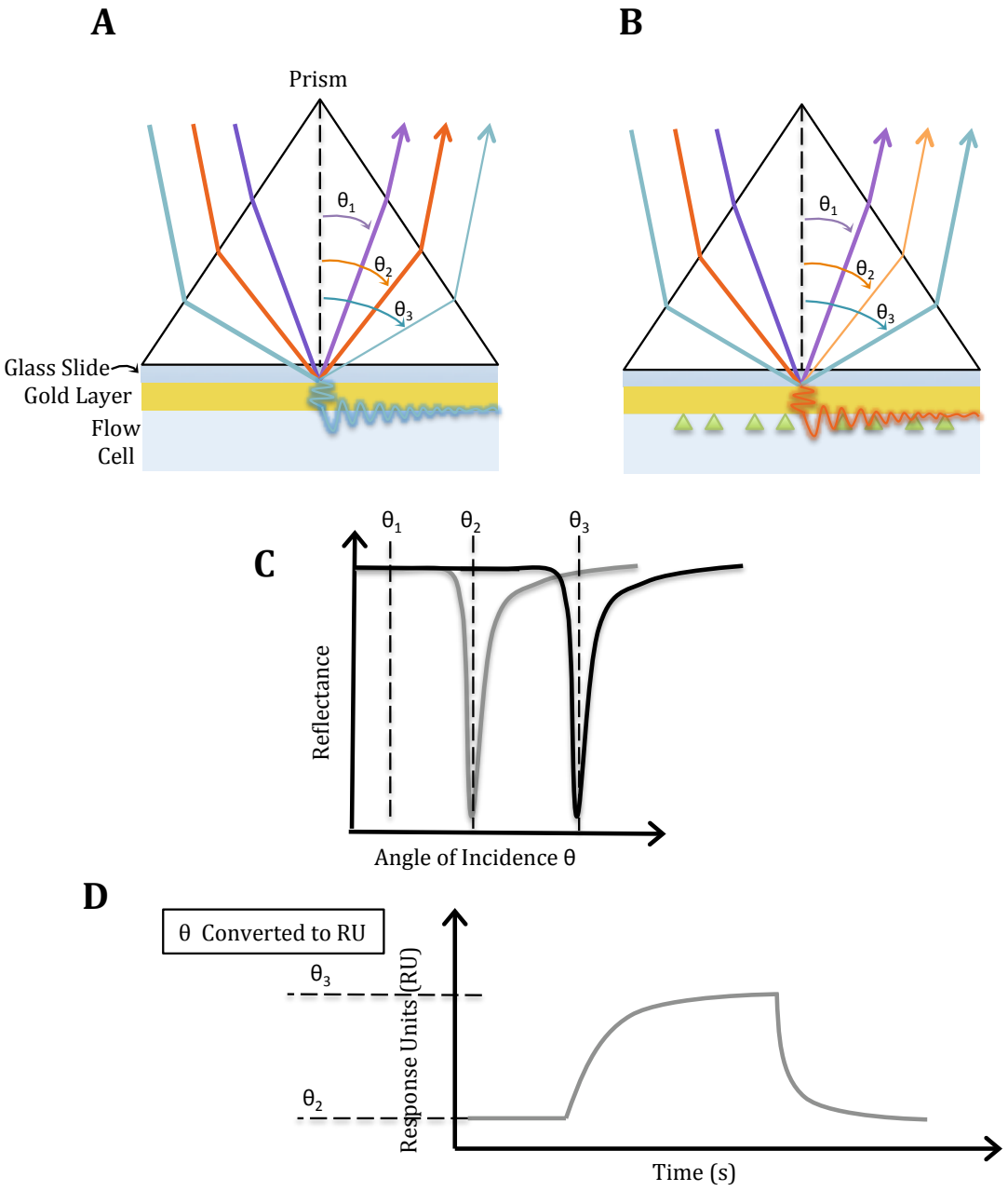

Figure 10. Surface plasmon resonance setup and principles of SPR. A) Light of various angles is shined through a prism onto a gold surface. The energy of light from angle θ_2 is transferred to the plasmons, producing an evanescent wave, and the intensity of the reflected light is decreased. B) After immobilization of ligand to the gold surface, the change in mass causes the reflected light from θ_3 to be of the lowest intensity. C) Plot of reflected light intensity vs. the angle of light. The grey line represents the reflected light from figure A and the black line is the reflected light from figure B. D) The angle of minimum reflectance is converted into response units through mathematical transformation. Plotting response units over time is called a sensorgram.

at one angle (Figure 10c). The angle that corresponds to the lowest reflected intensity is the angle that gave the largest amount of resonance.

The angle of light able to produce resonance is influenced by the amount of mass associated with the metal surface. As the mass on or near the surface of the metal changes, the angle of light to create an evanescent wave to create resonance also changes (10a vs 10b). Sensorgrams are produced by monitoring the change in the reflected angles, specifically the angle giving the lowest reflected intensity, over time (figure 10d). The shift in the lowest reflected intensity is mathematically transformed into response units (RU). The signal of 1000 response units corresponds to a change in mass of approximately 1 ng/mm^2 on the sensor surface.

B. SPR for Biological Systems

The SPR system takes advantage of the principle that the angle of light creating surface plasmons is very sensitive to the amount of mass close to the sensor surface. It allows for ligand to be bound to the metal surface, and the binding of analyte to this ligand to be quantified in real time. The ligand bound to the surface can be reused, allowing for direct comparisons to be made between binding properties of different analytes. This also is helpful if there are limited quantities of the ligand sample. The instrument sets up multiple flow cells on the metal surface permitting up to three experiments to be run in tandem using the same analyte, again allowing for direct comparison of numerous ligands with numerous analytes.

V. Fluorescence

Light emitted from any molecule is known as luminescence. Depending on the properties of the excited state, luminescence can be separated into two categories, fluorescence and phosphorescence. Fluorescence occurs when a molecule emits light from the singlet-excited state to ground state. Phosphorescence occurs from the emission of light from the triplet-excited state. Fluorescence lifetimes are short, typically in the low nanosecond range, and the release of fluorescence by a molecule can be plotted as fluorescence intensity (arbitrary units) versus wavelength (nanometers) resulting in a fluorescence spectrum. A Jablonski diagram (Figure 12) shows the absorption of light initiates the excitation of molecules to the singlet-excited state (S_1 or S_2) from the ground state (S_0). Each excited state has a number of vibrational states, and at room temperature, the majority of molecules populate the lowest vibrational state. Upon light excitation, molecules can initially populate high vibrational states within the electronic excited states. Internal relaxation towards the lower vibrational level occurs very fast, in the low picosecond time scale, and before the molecules can emit fluorescence. Therefore, there is a net loss of energy, which results in the emitted photon to have less energy (higher wavelength) than the initially absorbed one. In addition, emission can occur to high vibrational levels of the electronic ground state, resulting in a further loss of energy for the emitted photon(*83*).

A. Fluorescent molecules

A fluorophore is a chemical compound that can emit fluorescent light upon light excitation. Some biomolecules such as aromatic amino acids, flavins, NADH,

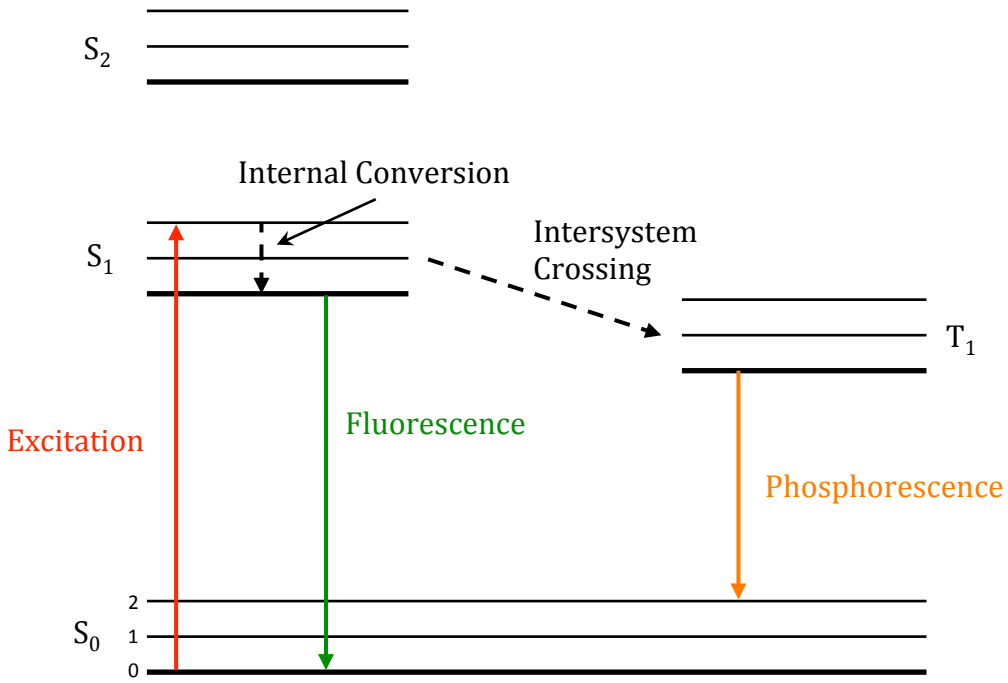

Figure 11. Characteristic Jablonski energy diagram. Black lines represent levels of the ground state (S_0) and excited singlet (S_1 and S_2) and triplet (T_1) states. Each state has a number of vibrational levels (thinner black lines).

and chlorophyll are intrinsically fluorescent. Molecules that contain aromatic functional groups are typically fluorescent. The amount of molecules that emit fluorescence compared to the amount of molecules excited is known as the quantum yield of the molecule. The quantum yield of an aromatic hydrocarbon increases with the number of rings. The rigidity of a molecule and the local environment of the molecule have been shown to affect fluorescence. An increase in temperature or decrease in solvent viscosity increases the frequency of collision between molecules, decreasing fluorescence efficiency. Polarity of a solvent also has an effect on fluorescence emission. In general, polar fluorophores are more sensitive to solvent polarity than nonpolar molecules, such as un-substituted aromatic hydrocarbons(*84*). Protein-induced fluorescence enhancement is the increase of fluorescence due to a nearby protein altering the local environment(*85*). Recently Vrtis *el al.* found that when unlabeled KF bound to DNA labeled with Cy3 fluorophore, there was a sudden increase in fluorescence intensity. They attributed this increase in intensity to a change in the local environment caused by the presence of the polymerase(*85, 86*).

Chapter 2: Experimental Procedures

VI. Materials

A. DNA Oligonucleotides

All unmodified DNA and biotinylated DNA used in the following experiments were purchased from Midland Certified Inc (Midland, Texas). Fluorescently labeled DNA was purchased from Eurofins MWG Operon (Huntsville, AL) or Integrated DNA Technologies (Coralville, IA). Most purchased DNA was purchased GF (gel filtration) grade desalted and further purified using the HPLC method described below. The fluorescent labeled DNA was purchased RP HPLC purified.

B. Klenow Fragment Protein

The enzyme used in the SPR and fluorescence experiments, DNA polymerase I Klenow fragment of *Escherichia coli,* was purified using FPLC as previously described(*87*). Briefly, the plasmid pXS106 containing the Klenow fragment gene with a D424A mutation was overexpressed in CJ376 *E coli* cells, both a generous gift from Dr. Cathy Joyce (Yale). The D424A mutation almost fully removes the 3'→5' exonuclease activity of KF. Cellular contents were purified using ammonium sulfate precipitations, as well as FPLC (ÄKTApurifier with monitor UV-900, GE Uppsala, Sweden) purifications with anion exchange and hydrophobic interaction columns (GE Health, Uppsala, Sweden). The purification of the protein was performed with the help of undergraduate Meredith Ann Manire.

C. Miscellaneous Materials

The fluorescence PIFE experiments were conducted using an AVIV Model AFT 105 Spectrofluorometer (AVIV Instruments, Lakewood, NJ). Small sample sizes were achieved by using a 10µl quartz cuvette, 10mm path length (Starna Cells, Atascadero, CA). All SPR experiments were performed using the Biacore 2000 instrument (Uppsala, Sweden). Research grade CM5 (carboxymethylated dextran length 5) sensor chips and Amine Coupling kit were purchased from GE. The amine coupling kit contains *N*-Hydroxysuccinimide (NHS), 1-Ethyl-3-(3-dimethylaminopropyl) carbodiimide hydrochloride (EDC), and 1 M Ethanolamine hydrochloride-NaOH pH 8.5. Streptavidin was purchased from Sigma. Dideoxy termination reactions were performed using Terminal deoxynucleotide transferase enzyme (USB) and dideoxynucleotidetriphosphates (ddNTP) (USB).

VII. Methods

A. DNA Purification

Before every experiment all DNA oligonucleotides (Figure 12) were thoroughly purified using reverse phase HPLC. Using a Varian ProStar (Palo Alto, CA), DNA was passed through a Alltima C18 column with 5µm particles and detected with a Varian ProStar photo diode array detector (PDA). Running buffer (buffer A) was 0.1 M triethylamine acetate pH 7.0 (TEAA) and mobile phase buffer (buffer B) was either a 30% acetonitrile or 90% acetonitrile mixed with 70% or 10% 0.1 M TEAA (buffer A), respectively. All buffers were filtered and degased before use on the HPLC. Each HPLC purification was started by equilibrating the column at 4-8%

A	21mer Primer	5’-GGAGAGTGATTGGTAGTGTGA-3' OH
B	22ddT Primer	5’-GGAGAGTGATTGGTAGTGTGAT
C	22ddC Primer	5’-GGAGAGTGATTGGTAGTGTGAC
D	22ddG Primer	5’-GGAGAGTGATTGGTAGTGTGAG
E	22mer Primer	5’-GGAGAGTGATTGGTAGTGTGAT-3' OH
F	23ddC Primer	5’-GGAGAGTGATTGGTAGTGTGATC
G	23ddA Primer	5’-GGAGAGTGATTGGTAGTGTGATA
H	23ddG Primer	5’-GGAGAGTGATTGGTAGTGTGATG
I	23C Cy3	Cy3-5’-GGAGAGTGATTGGTAGTGTGAT-3'
J	23A Cy3	Cy3-5’-GGAGAGTGATTGGTAGTGTGAA-3'
K	28mer Template	5'-CTCAT**G**ATCACACTACCAATCACTCTCC-Biotin

Figure 12. All DNA oligonucleotides used in this study.

acetonitrile. The most commonly used method for adequate separation of unmodified DNA increased the acetonitrile concentration from 8% to 15% over 40 minutes. DNA with hydrophobic modifications such as a carcinogen or fluorescent tag, required a higher acetonitrile percentage for elution. An increase of 8-30% acetonitrile over 45 minutes was sufficient for elution of a single peak.

Once a single peak was acquired from the HPLC, the correct product was confirmed by matrix assisted laser desorption ionization time of flight mass spectrometry (MALDI-TOF). This was done following the method previously described (*88*) using a Bruker Ultraflex or Shimadzu MALDI-TOF mass spectrometer. Briefly, a saturated solution of 3-hydroxypicolinic acid (3-HPA) was prepared in 25 mM ammonium citrate with 7.5% (v/v) acetonitrile, vortexed and centrifuged. A 1 µL drop of the solution was spotted on a MTP 384 ground steel target plate (Bruker) coated with a thin parafilm layer. The hydrophobic parafilm layer is useful in that it causes the liquid matrix to form a smaller bead. As the bead dries, the matrix is concentrated into a smaller spot on the plate. Once the matrix spot dried, 10-50 pmoles of DNA was desalted with a Ziptip as described in the Millipore instructions, and the DNA was eluted with 1-2 µL of 50% acetonitrile (in water) directly onto the crystalized 3-HPA matrix. The plate was loosely covered until the sample spot was dry. The oligonucleotide spots were shot in reflectron positive mode to give better mass resolution. Bruker's Flex Analysis software was used to analyze and process the collected spectral data.

B. DNA Modification

i. Dideoxyterminated Primers

Primers used in Klenow fragment binding studies were made non-extendable by the addition of dideoxyterminated nucleotides to the 3' end. 5 nmoles of either 21mer or 22mer primer were mixed with 100nM of a single ddNTP in buffer for the terminal deoxytransferase, 5 mM $CoCl_2$, 125 mM sodium cacodylate pH 7.2 and 0.5 mM DTT. 40-50 units of terminal deoxytransferase (USB Affymetrix) were added to start the reaction, which was carried out at 37° C for 4 hours. The reaction was stopped by heating to 75° C for 5 minutes. Each dideoxynucleotide addition reaction was HPLC purified to separate any unextended primer, and purity was verified using MALDI-TOF. Both 22mer and 23mer dideoxyterminated primers were produced (Figure 13).

C. SPR Methods for Unmodified DNA

i. Chip assembly

CM5 chips from Biacore were the platform for all SPR experiments using the Biacore 2000. All experiments were performed at 25° C. Before binding DNA, the carboxydextran layer must be conditioned. In a HBS-EP running buffer (0.01M HEPES pH 7.4, 0.15M NaCl, 3mM EDTA, 0.005% P20) 10 µL of 10 mM NaOH was injected over the chip surface at 100 µL/min in triplicate, followed by 10 µL injection of 500 mM NaCl, also done in triplicate. Conditioning hydrates and opens up the carboxydextran matrix. Once conditioned, the chip was activated for streptavidin immobilization via amine coupling. This can be accomplished one of two ways. The Biacore control software Application Wizard offers a step-by-step,

automated method where small amounts of streptavidin are injected until the response target is reached, but if the IFC (Integrated Microfluidic Cartridge) is older, a manual method may be required. To start, HBS-EP was run at a flow rate of 5 µL/min in a single flow cell. A 1:1 mixture of 0.05 M EDC and 1 M NHS from the Amine Coupling Kit (see Materials above) was flowed over the surface for 7 minutes (35 µL injection). For best results, the EDC/NHS mixture should be mixed just prior to injection, either manually or the MIX method on the Biacore Control Software may also be used. Once the surface was activated, 35 µg/mL in 10 mM sodium acetate buffer pH 5.0 streptavidin can be added. The streptavidin injections should start off small, 5 µL, and then increase based on how many response units of streptavidin have been bound after each injection. The amount of bound streptavidin is calculated by subtracting the initial baseline response units from the final baseline after the end of the injection. Streptavidin injections are continued until the desired response level is reached. Typically, one 5 µL injection followed by two 10 µL injections of 50 µg/ml streptavidin are enough to reach 1000 RU of bound streptavidin. After the streptavidin is bound, the remaining reactive NHS esters are capped with 1 M ethanolamine. A 30 µL injection is sufficient to cap all unreacted esters. This same method is repeated in all flow cells, starting at 4 and ending at 1.

ii. DNA Immobilization

Template modified with a 3' Biotin was annealed to primer in a HMS buffer (10 mM HEPES pH 7.4, 150 mM NaCl, 10 mM $MgCl_2$, 0.05% P20). The primer concentration is in 5-fold excess to be sure all biotinylated template is duplexed when bound to the SPR chip. 40 nM biotinylated template and 200 nM primer was

combined, vortexed, centrifuged and placed in a boiling water bath. The water bath was promptly removed from the heat source and set aside to cool down back to room temperature. The duplexes were further diluted to 40:8 nM and 10:2 nM primer-template mixtures. Using the SPR, HMS buffer was flowed over a single flow cell at 5 µl/min. 20 µL of the 40:8 nM concentrated duplex was injected first. A 3-4 minute contact time was sufficient enough for the 3' biotin on the duplexed DNA to interact with and be received by streptavidin on the surface, immobilizing the DNA to the surface. Following the initial injection, smaller injections using the more dilute 10:2 nM primer template mixture were used to increase the amount of bound DNA to the desired response level, usually 100 RU of bound DNA. DNA was added to flow cells 2-4, leaving flow cell 1 and a reference flow cell. The reference flow cell is subtracted to remove the bulk refractive index change and any nonspecific binding between polymerase and streptavidin during the injection.

iii. Klenow fragment preparation for binding experiments

All Klenow fragment binding experiments were performed in a Tris running buffer (50 mM Tris base, pH 7.4, 150 mM NaCl, 10 mM $MgCl_2$). Due to the sensitivity of the SPR instrument, it is important for the samples being injected to be as close to the running buffer composition as possible. To minimize large refractive index changes at the start and end of each injection, KF is dialyzed into the Tris running buffer to remove the KF storage buffer. The KF was dialyzed using a 10 kDa MW cutoff membrane Pierce Slide-a-lyzer mini Eppendorf dialysis tube (Rockford, Il). The tube was first placed in 1 L of filtered water for 20-30 minutes to remove any residual glycerol. The dialysis tube was then transferred to 1 L of Tris running

buffer, cooled to 4° C and equilibrated for 5-10 minutes. A small amount of buffer (10-20 µL) was added to the dialysis tube followed by the addition of Klenow fragment. The enzyme was dialyzed for 4-6 hours, while slowly stirring to keep a fresh stream of buffer moving past the dialysis tube. When it was needed for use, the KF was removed and concentration of the enzyme was calculated by UV-Vis. The absorbance at 280 was measured using the NanoDrop ND 1000 spectrophotometer (GE Healthcare) and concentration was calculated using Beer's Law and the extinction coefficient of 58,800 M^{-1} cm^{-1}.

iv. KF binding experiments

From the dialyzed Klenow fragment, solutions of KF ranging from 0-200nM were made using TRIS buffer. To these KF solutions that required it, 0.4 mM dATP, dCTP, dGTP or dTTP was added. Using an automated method made on the Biacore software, the flow rate was set to 35 µL/min and 35-60 µL of KF samples was injected. Each injection was followed immediately by an injection of Tris buffer or buffer with dNTP, corresponding with the KF-dNTP injection, for 30-600s (depending on the nature of the experiment). After this injection, buffer flow resumed until the response returned to baseline. All KF binding experiments were run at 25° C. All data sensorgrams for these injections were taken in real time at a rate of 60Hz.

v. SPR Data Analysis

The SPR sensorgrams were analyzed using both an equilibrium method and a direct kinetic method. The equilibrium method plotted equilibrium binding levels of

the sensorgrams against Klenow fragment concentrations to determine an apparent equilibrium binding constant. In the direct method, the dissociation phase of the sensorgram was directly fit to equations to determine a kinetic off rate.

Raw sensorgrams from flow cells 2-4 were subtracted from the reference flow cell, which contained only bound streptavidin. An average response unit level at equilibrium was taken from the reference-subtracted sensorgrams as a function of the Klenow fragment concentration, [KF]. These points were then fit to a 1:1 Langmuir binding equation.

$$RU = \frac{R_{max}}{1+\frac{K_D}{[KF]}} \qquad \text{Equation 1}$$

RU is response units, K_D is the dissociation constant, and R_{max} is the theoretical maximum binding level of the DNA bound to the chip. The line for this equation was fit by varying K_D and R_{max} to minimize the residual differences between the actual equilibrium data points and the theoretical data points (RU in Equation 1) using Scrubber 2 (Cores, Utah) or Solver, an add-on to Microsoft Excel. The theoretical R_{max} is calculated from the levels of DNA bound in each flow cell (see DNA immobilization). This theoretical level can be used as a verification tool; to confirm the R_{max} calculated in Equation 1 is the result of only one polymerase binding to each DNA strand. To compare the three flow cells, the amount of DNA bound was taken into account. Response units were converted to percent bound by dividing RU data points by the calculated R_{max}. The dissociation constants reported here were

determined from an average of three fits, and all errors are standard errors from the non-linear regression fit to the data.

Dissociation rates of Klenow fragment from the various DNA constructs, the sensorgram data was fit to both a single and double exponential decay equation. Like with the equilibrium data analysis, both Scrubber 2 and Solver were used to fit Equations 2 and 3 to the data. The data was fit to each equation by minimizing residual differences between the sensorgram data and the calculated data points. Richard Federley, a former PhD student in this lab, modified Equations 2 and 3 to include an accurate starting point of the equation at the end of equilibrium.

$$RU = \text{If}(t \geq 0, R_o * e^{-(k_d * t)} + R_\infty, R_{eql}) \qquad \text{Equation 2}$$

$$RU = \text{If}(t \geq 0, R_{o1} * e^{-(k_{d1} * t)} + R_{o2} * e^{-(k_{d2} * t)} + R_\infty, R_{eql} \qquad \text{Equation 3}$$

Where R_{o1} is the response level that will decrease as a function of the first off rate, k_{d1}, and R_{o2} is the response level that will decrease as a function of the second off rate, R_{o2}. R_{eq} is the response before the start of dissociation, and R_∞ is the response level at infinity. If time t is before the start of the dissociation, no slope is fit and it is set to the equilibrium level. After the start of the dissociation, time 0, the slope of the line is fit to either equation 2 or 3.

D. AAF and AF modified studies

i. AF and AAF Modified Template:

A 28-nucleotide template with a single guanosine was modified with N-acetoxy-acetylaminofluorene. 50 nmoles of 28mer DNA was dissolved in 2 mM sodium citrate, pH 6.9 and was purged with argon or nitrogen for 10-15 minutes to remove any oxygen. In a separate vial, 0.5 µmoles of N-acetoxy-acetylaminofluorene (AAAF) was dissolved in 100% ethanol and purged with argon or nitrogen for 5 minutes. Septum caps were placed on both vials to keep atmospheric oxygen out of the reaction, as the correct reaction for the product of interest will only proceed under anaerobic conditions. The AAAF/ethanol mixture was added to the vial containing the 28mer DNA, vortexed, and purged with argon or nitrogen for another 5-10 minutes. The DNA-AAAF mixture was then incubated at 37° C under dark, anaerobic condition for 3 hours. Once the reaction mixture turned light brown in color, the reaction was removed from the water bath and the excess AAAF was removed through ether extraction. The resulting mixture was dried down and re-suspended in 0.1 M TEAA pH 7.0 (HPLC running buffer). The N-acetyl-2-aminofluorene (AAF) 28mer was HPLC purified, and mass of the product was confirmed using MALDI-TOF. Presence of the AAF was also verified by measuring the increased absorbance at 310 nm by UV-Vis.

Aminofluorene modified 28mer was produced by deacetylating the purified AAF 28mer. To do so, dry AAF 28mer was re-dissolved in 1 M NaOH and 0.25 M 2-mercaptoethanol and vortexed thoroughly. A septum cap was placed on the vial containing the DNA mixture and purged with argon or nitrogen for 10 minutes. The mixture was left at room temperature for three hours to react under dark, anaerobic conditions, and was re- vortexed every hour. The reaction mixture was neutralized

with 1M HCl. The AF modified 28mer was HPLC purified using the same method as the AAF 28mer. Again, the AF modified product was verified with MALDI and UV-Vis, with an added absorbance increase at 335 nm.

ii. Ensemble PIFE Assay

A fluorescence assay similar to one previously described was developed(*89*). Primer-template (8-6.66 μM) was annealed in KF reaction buffer (50 mM TRIS pH 7.5, 10mM $MgCl_2$, 1 mM DTT). Each template contained either an AF or AAF modification on the single G at position 23. An initial DNA-only fluorescence scan was obtained. 5 μL of highly concentrated KF was added to the duplex DNA (now 6.5-5 μM) to ensure all DNA was bound, resulting in KF concentration 5-15x that of the DNA. The DNA-KF mixture was incubated for 30 minutes prior to scanning. Next, 100 μM dNTP was added to the DNA-KF mixture and a final fluorescence measurement was taken. For the AAF modified DNA, samples were excited at 310nm, while AF modified samples were excited at 315nm. Emission was recorded from 360-580nm for all samples. Results for the three scans, DNA only, DNA-KF and DNA-KF-dCTP, were corrected for DNA concentration, normalized, and processed using Excel.

iii. Single Nucleotide Incorporation Assay and Gel

The effect of an aminofluorene adduct on Klenow fragment activity was assessed through a single nucleotide incorporation assay. A 23mer extendable primer, labeled with a 5' Cy3 modification, was annealed to a 28mer template, unmodified or containing an AF modification. 100 pmoles of KF was incubated with

15 nM primer-template and 100 μM of a single dNTP in reaction buffer (10 mM $MgCl_2$, 50 mM TRIS pH 7.5, 1mM DTT, 50 μg/mL BSA). Reactions were carried out for 10-60 minutes, depending on the construct, and the reactions were stopped by adding an equal volume of loading buffer (10 mM EDTA, 1 mg/mL bromophenol blue in 10 mL formamide) to each reaction and heating to 75° C for 5 minutes. 5 μl of each sample was run on a 20% denaturing polyacrylamide gel at 1000 V for 16-18 hours. Gels were scanned for Cy3 using a Typhoon 9210 Variable Mode Imager (GE Healthcare). Variations of this method are noted in the text.

iv. DNA and SPR chip preparations

DNA duplexes similar to those used for the unmodified experiments, but with the single G template modified with AAF or AF, were annealed by mixing 200 nM unmodified primer with 40 nM modified template. Duplexing the modified template with a 22mer primer situates the modified G as the templating base, while duplexing with the 23mer primer places the modified G in the last formed base pair. The primer-template mixture was placed in a 95° C water bath for one minute, and then placed in a dark drawer to cool back to room temperature slowly, for at least one hour. Both AAF and AF are light sensitive, it is important to cover the modified duplexes whenever possible. Once cool, the duplexes are diluted and ~100 RU of DNA are added to a new CM5 chip covered with ~1000 RU of bound streptavidin, as stated in the DNA immobilization section above.

v. KF binding studies of AF and AAF modified DNA

KF was dialyzed into Tris running buffer as in the unmodified SPR section. KF injections were made using one of two methods. The first was based off the co-injection method noted in the unmodified section above, injecting 50 µL of KF, with or without dATP, dCTP, dGTP or dTTP, followed by a 100 µL injection of buffer with the corresponding nucleotide. The second method consisted of one single, long 315 µL injection of KF with and without nucleotide followed by a 540 s dissociation phase of buffer flow only to bring the response back to baseline. All data sensorgrams for these injections were taken in real time at a rate of 60Hz.

vi. Data Analysis for modified templates

Both the equilibrium binding and dissociation rate data analysis was conducted as described above. Kinetic association rate constants (k_{on}) were calculated for low concentrations of KF binding to templating base AAF or AF modified DNA by fitting the date to a non-linear curve, Equation 4.

$$RU = \frac{k_{on}[KF]R_{max}}{k_{on}[KF]+k_{off}}\left(1 - e^{-(k_{on}[KF]k_{off})t}\right) \qquad \text{Equation 4}$$

Where RU is the response level at time (t), k_{off} is the rate of KF dissociation rate constant, and R_{max} is the theoretical maximum binding level for the amount of DNA bound to the flow cell. The data was globally fit using Excel and Solver from time 0 to the time it reached the equilibrium level, which varied based on KF concentration. Error rates were the standard deviation from triplicate measures.

Chapter 3: Results

I. DNA Modifications

Studying the effects that aromatic amine DNA adducts have on polymerization required a single nucleotide to be modified. N-acetoxy-acetylaminofluorene reacts predominately with the C8 of guanine, therefore, site specificity is gained by having the 28-nucleotide template contain a single guanine at position 23. The aromatic addition to the DNA makes for easy HPLC separation of the AAF modified product from the unmodified starting material. The AAF oligonucleotide was further characterized by UV-Vis spectroscopy, displaying a distinct increase in absorbance at 310 nm. Removal of the acetyl group from AAF to form AF changes both the HPLC retention time as well as the absorbance spectrum. To further verify the correct DNA modifications and purity of the products, MALDI-TOF was performed (Figure 13).

II. Surface Plasmon Resonance

Surface plasmon resonance is a very useful tool for the study of biomolecular interactions. The advantages of this instrument were utilized for the DNA-polymerase binding experiments performed and discussed here. The SPR chip contains four connected flow cells, three of which contain different immobilized primer-templates, allowing for three binding experiments to be run in parallel. Having the same analyte injected over each flow cell reduces the amount of sample needed for each experiment. DNA immobilized onto the flow cell is viable for numerous rounds of KF binding experiments conducted with each nucleotide

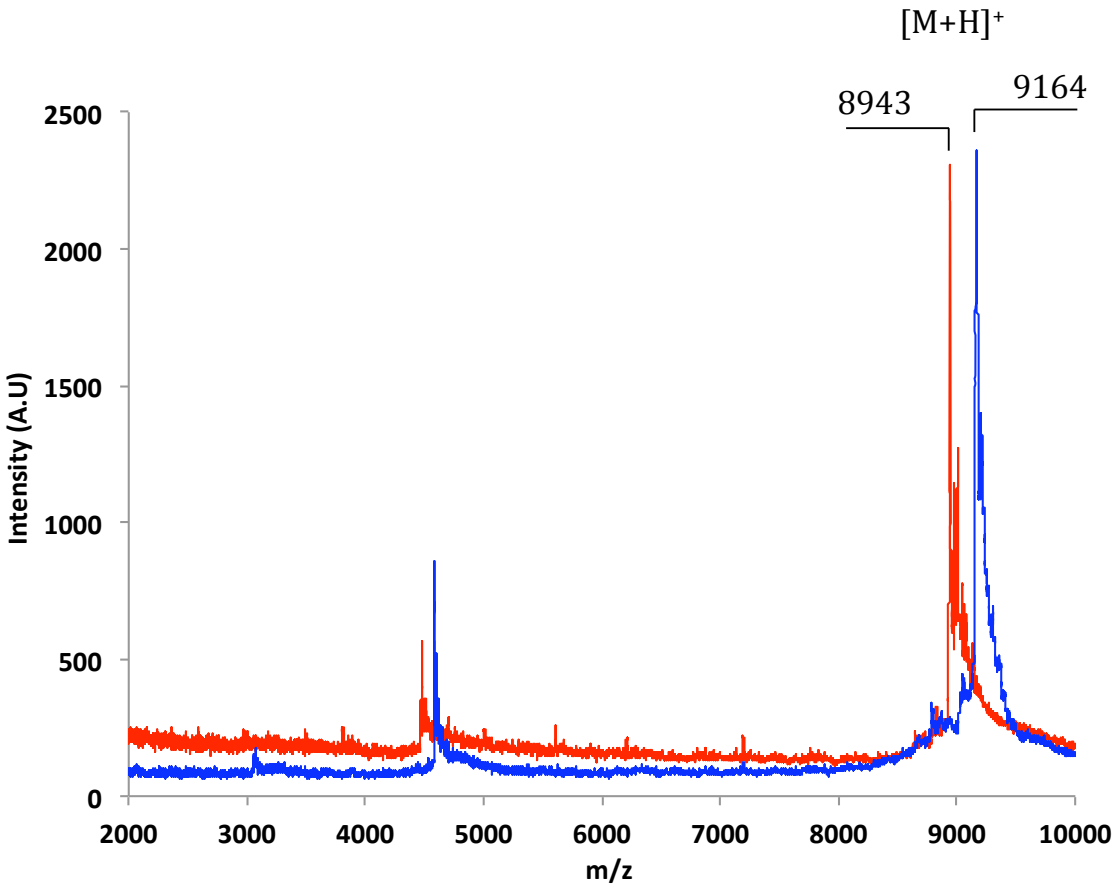

Figure 13. Overlapped MALDI-TOF mass spectra of unmodified and AAF modified 28-nucleotide template DNA. The spectra for the unmodified 28mer template is shown in red, and the AAF modified 28mer template is shown in blue.

on the same DNA, even though run separately. Together this reduces variability between the KF and nucleotide binding experiments. KF binding and dissociation are monitored in real time and a characteristic sensorgram is shown in Figure 14. Both equilibrium and kinetic data are interpreted from one set of results. The unmodified DNA-KF binding trials were completed not only as a control for the modified studies, but also to optimize the SPR system for use with modified substrates. The experiments tested the effect dNTPs have on Klenow fragment binding to unmodified DNA, and also the effect a mismatch as part of the primer-template terminus has on the stability of the protein DNA complex.

A. Streptavidin Binding and DNA Immobilization

The strong biotin-streptavidin interaction was utilized to immobilize the DNA to the sensor surface. Approximately 1000 response units (RU) of streptavidin were covalently attached to the carboxydextran surface through amine coupling (Figure 15). A solution of EDC and NHS activates the carboxydextran surface, and this activated surface reacts with free amines on streptavidin. A 35 µg/ml streptavidin solution in sodium acetate pH 5.0 is suitable for the Application Wizard to immobilize the 1000 RUs of streptavidin. It is important for the streptavidin to be dissolved in the pH 5.0 sodium acetate buffer. A buffer pH below the isoelectric point (pI) of the protein being immobilized leads to an electrostatic attraction between the protein being immobilized and the sensor surface, allowing for a low streptavidin concentration to be used for covalent attachment. The streptavidin immobilization process is completed by capping any unbound NHS esters with ethanolamine.

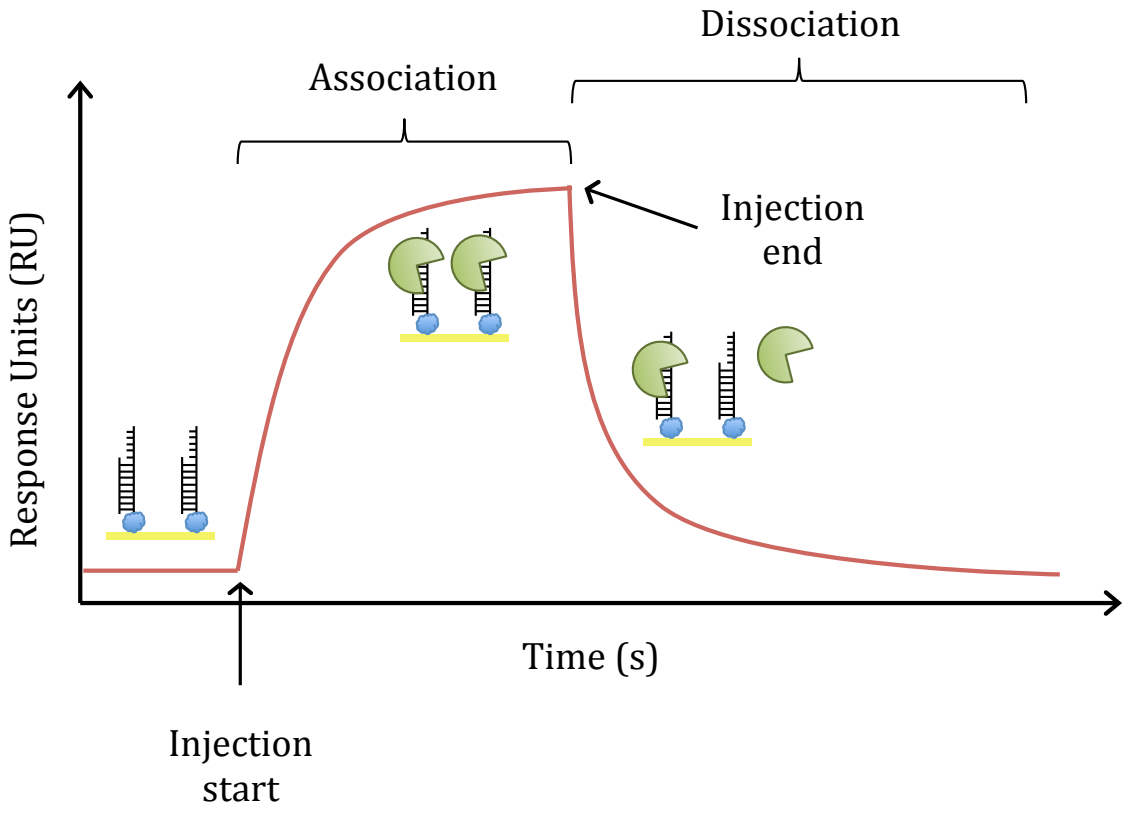

Figure 14. Schematic representation of a typical sensorgram showing KF binding to and dissociating from DNA immobilized on the SPR chip surface. Before the injection start, baseline level corresponds to buffer flowing over DNA bound to the chip. After the start of the injection, KF binds to the surface immobilized DNA, which leads to an increase in response units. The association phase includes initial KF binding and equilibrium binding. At the end of the injection, KF dissociates from the DNA, leading to a decrease in the response units. The dissociation phase is complete when all KF has dissociated from the DNA and the response units return to baseline levels.

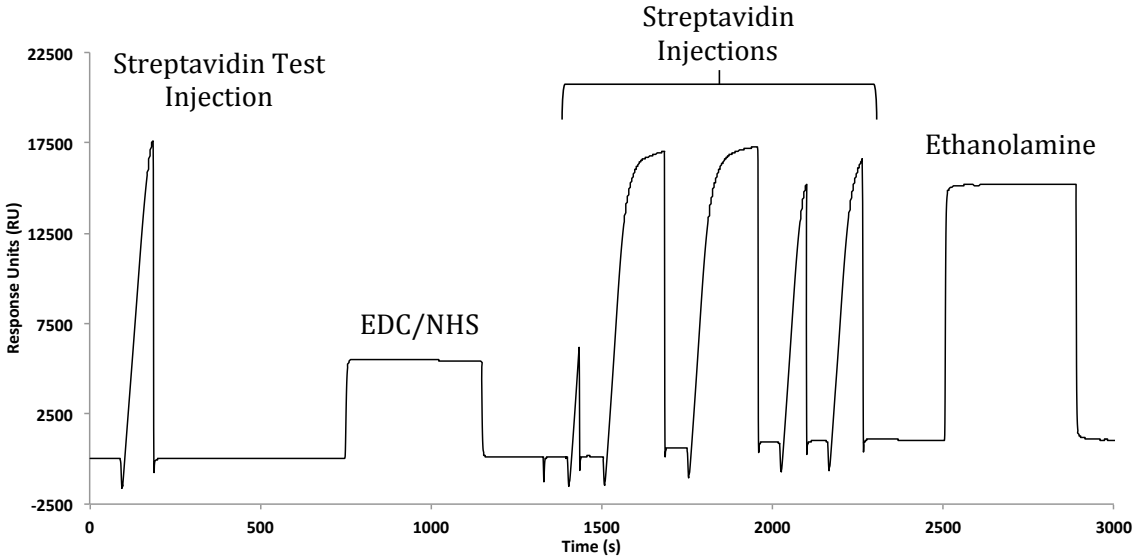

Figure 15. Streptavidin immobilization to carboxydextran matrix. First, the surface is tested with an injection of streptavidin to check for correct binding rate. Next, the surface is activated with a mixture of EDC and NHS. Once activated, a series of streptavidin injections are flowed over the surface until the baseline response level reaches ~1000 RU. Ethanolamine is injected at the end to cap any remaining unreacted esters.

With the streptavidin bound and the free esters capped, three different types of DNA duplex were added to flow cells 2, 3, and 4. Flow cell 1 was used a reference flow cell, and the response from this flow cell was subtracted from the other flow cells to remove any bulk refractive index change from the buffer and any non-specific interactions between the analyte and the sensor surface. The template strand of the duplex was modified with a 3' biotin. When duplexing the DNA constructs, a five-fold excess of primer strand was used to assure all template strands bound to the SPR chip were in the duplex form. Limiting the amount of template strand was very helpful for the modified complexes, where lower amounts of the modified template are available. With a main focus of the experiments being the collection of kinetic binding data, a low level of about 100 RU of DNA duplex was immobilized to reduce possible mass transfer effect (Figure 16)(*90*). The use of low flow rates and varying duplex DNA concentrations during DNA immobilization to the streptavidin both assist in attaining consistent bound DNA amounts between flow cells. The 22P:28T DNA constructs immobilized on to the unmodified flow cell are shown in Figure 17. SPR chips made for the modified experiments use similar DNA constructs, but with an AF or AAF modification on the single G on the template.

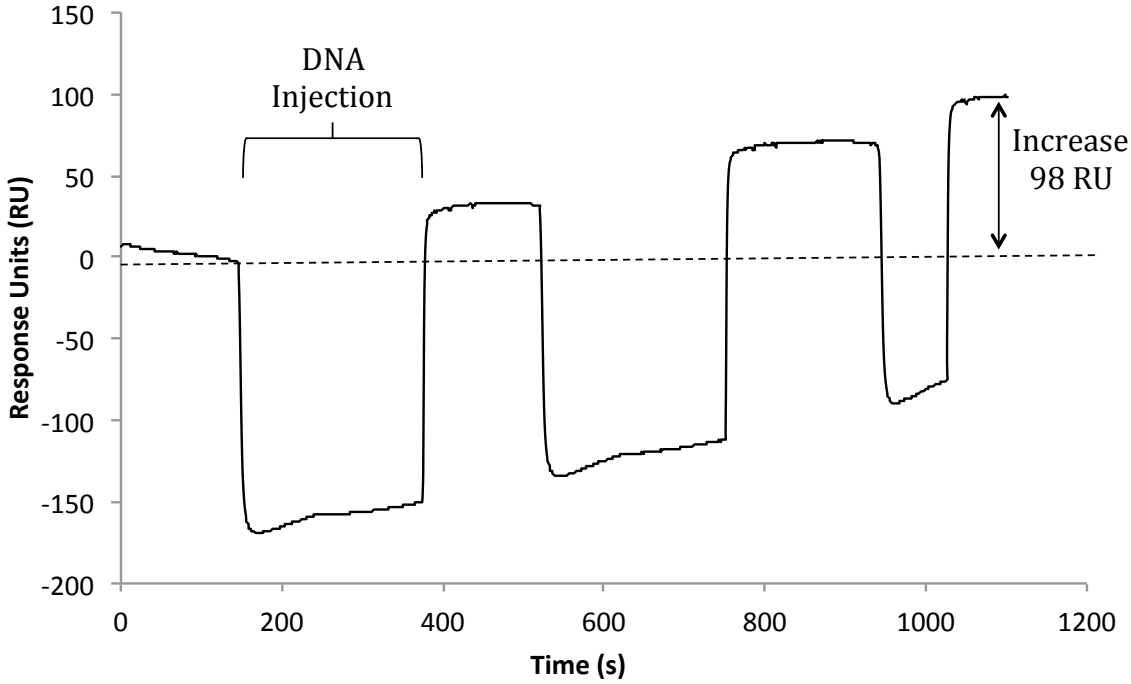

Figure 16. DNA immobilization on a single SPR flow cell. Duplex DNA containing a template modified with a 3'-biotin is flowed over the streptavidin through a series of injections and is captured by the streptavidin. Injections are repeated until the correct amount of DNA is bound.

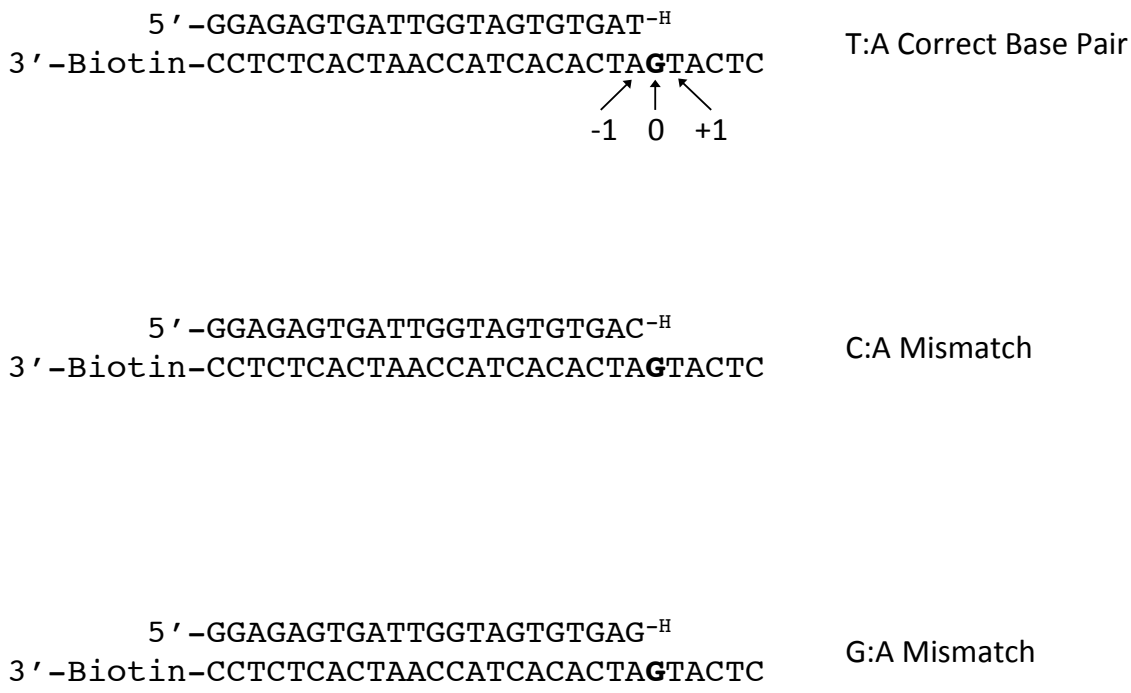

Figure 17. DNA constructs with a 22mer primer and a 28mer template. The single G on the 28mer template acts as the templating base. The top construct is fully complementary, while the other two contain a single mismatch at the primer template terminus, or the -1 position. The bold G marks the position where AAF and AF modifications were added to the template.

B. Unmodified Results

i. KF Binding curves

Sensorgrams for Klenow fragment binding experiments show the Klenow fragment binding to and dissociating from the DNA in real time (Figure 18a). Using the Biacore software, an automated method was created to monitor KF interactions with the different DNA constructs. First, running buffer (50mM TRIS pH 7.4, 10mM $MgCl_2$, 150mM NaCl, 0.05% surfactant P20) was flowed over the chip giving a baseline RU level, 0-24 seconds in Figure 18. Next, an injection of KF was flowed on to the sensor surface, 25 – 95 s. During this step, KF binds to the surface-immobilized DNA, causing an increase in mass at the sensor surface and resulting in an increase in RU, reaching a plateau, or equilibrium binding level. The association phase of the sensorgram for the high concentrations of KF was fast, close to the rate of diffusion, allowing for the use of short sample injections, which decreased the amount of polymerase required for each injection. Increasing KF concentrations showed faster association times and higher equilibrium binding levels, converging on a maximum binding level. The actual maximum binding level, or the theoretical R_{max}, is determined using equilibrium binding levels and equation 1. The theoretical R_{max} matches the calculated R_{max}, which is determined based on the amount of DNA immobilized in the flow cell ($R_{max} = R_L (MW_A/MW_L) S_m$). High concentrations of KF bound to correctly paired C:G DNA reached an equilibrium level within 10-12% of the R_{max}. The process used for immobilizing biotinylated DNA to the chip may leave some DNA inaccessible for KF binding, even at high concentrations. During the dissociation step (96 – 200 seconds) running buffer with no KF is flowed over the

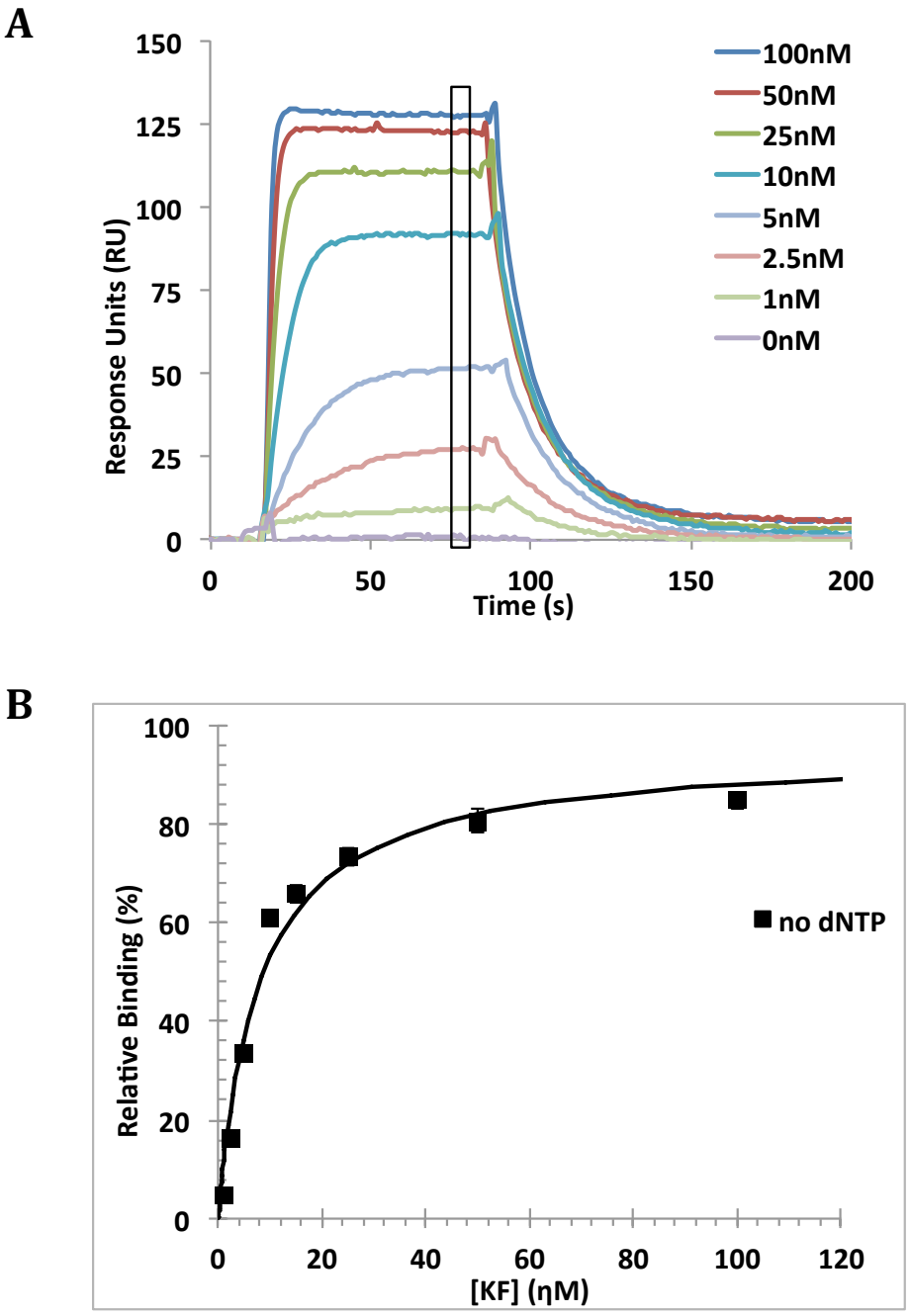

Figure 18. KF binding to unmodified DNA monitored by SPR. A) Overlapping sensorgrams of 0-200 nM KF binding to correctly paired DNA. The sensorgram starts off with buffer flow only from 0-24 seconds. KF was injected for 70 seconds (25 – 95 s). Buffer flow continues after the KF injection until the response units have reached baseline. B) Binding curves for KF and obtained from the SPR equilibrium data shown in (a). Equilibrium values (from box in A) were converted to % bound by using the R_{max} calculated for that flow cell.

chip and DNA-bound KF begins to dissociate, reflected as a decrease of RU, which eventually returns to baseline. The dissociation portion of the curve is slower than the association, and was used to fit apparent kinetic off rates for KF. An average RU level from the equilibrium binding region (85 – 90 s) was obtained from each sensorgram, plotted against the KF concentration, and fit to a 1:1 Langmuir binding isotherm (equation 1) (Figure 18b). Apparent equilibrium dissociation constants (K_D) were calculated for the unmodified DNA construct without nucleotide (Table 1)

ii. Influence of nucleotide on KF binding

The effects of a correct or incorrect nucleotide on KF binding have been comprehensively studied. The data presented here follows the same trends of previous experiments. A similar method was used for KF binding in the presence of nucleotides. For the KF + dNTP method, the KF injection (25-95 s Figure 19a) included a single nucleotide. A second injection was added as part of the dissociation step, a mixture of running buffer and the same nucleotide (96 – 215 seconds). The arrow in Figure 19a denotes the end of the dNTP-buffer injection. Since KF binding is being monitored in real time, basic information on KF binding can be visually gleaned from sensorgrams. Figure 19a shows overlapping sensorgrams of 200nM KF without or with each nucleotide. Similar to KF binding in the absence of nucleotide, the association phase of KF in the presence of any nucleotide is fast. KF binding in the presence of any incorrect nucleotide shows decreased equilibrium KF binding. The dissociation phase of KF binding in the presence of incorrect nucleotide is faster, and varies with nucleotide identity.

Table 1. Equilibrium Dissociation Constants (K_D) for Klenow Fragment Binding to Duplex DNA with Various Primer Templates[a]

DNA Construct	Dissociation Constants, K_D (nM)[b]				
	KF Only	dCTP[c]	dATP	dGTP	dTTP
TA Correct Base Pair	8 ± 0.6	1.7 ± 0.2	66 ± 2	102 ± 4	33 ± 4
CA Mismatch	797 ± 8	252 ± 2	3100 ± 100	3200 ± 100	2290 ± 80
GA Mismatch	513 ± 5	1100 ± 20	2890 ± 90	3000 ± 100	1800 ± 20

[a]Primer length 22 nucleotides.
[b]Values shown are an averages of triplicate measurements ± standard deviation
[c]Next Correct Nucleotide

5′-GGAGAGTGATTGGTAGTGTGAT-H
3′-Biotin-CCTCTCACTAACCATCACACTAGTACTC

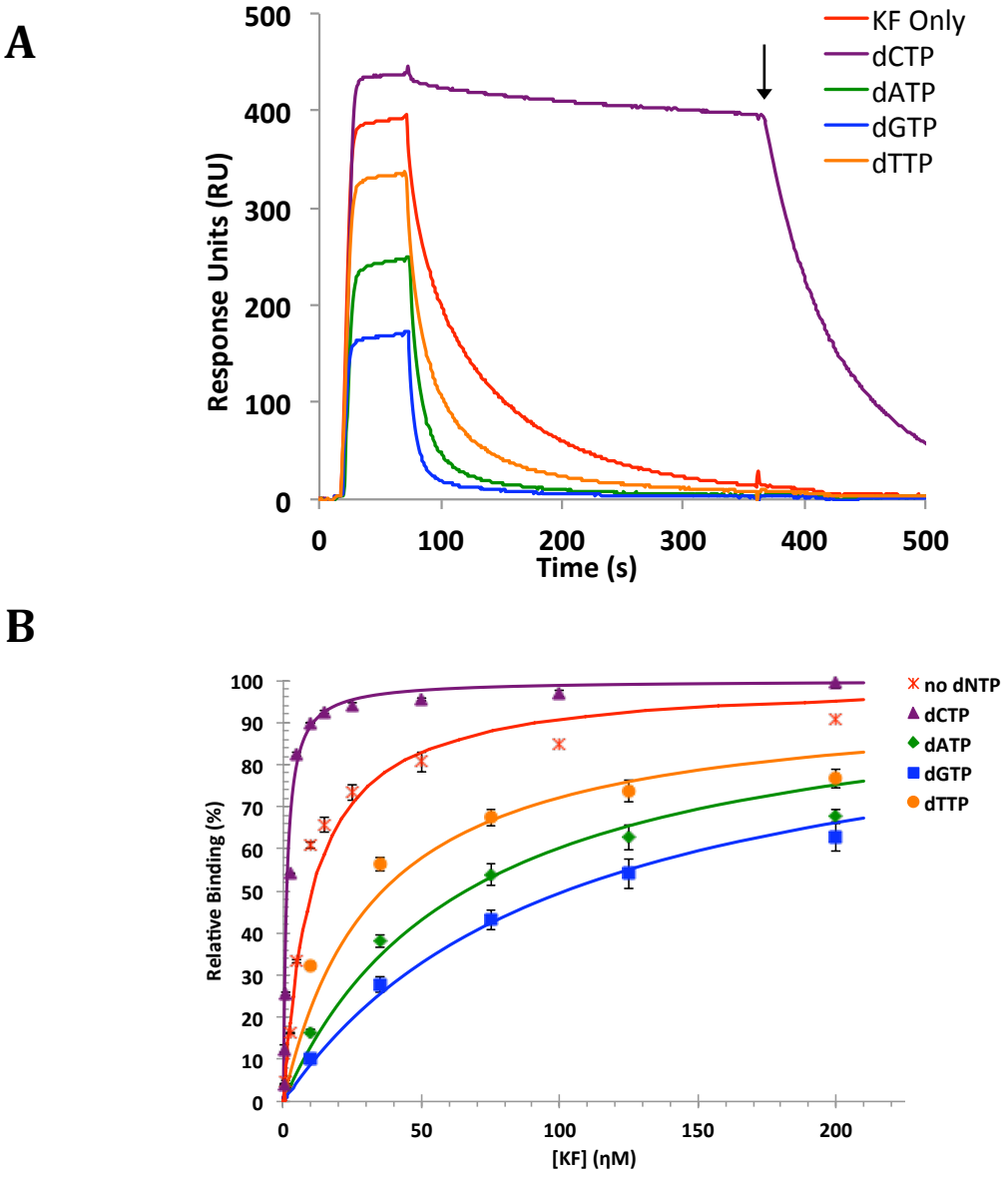

Figure 19. DNA-polymerase complex is stabilized in the presence of the next correct nucleotide and destabilized by incorrect dNTPs. a) Sensorgrams for 200 nM Klenow fragment binding to unmodified DNA in the presence and absence of dNTPs. Experimental procedure is same as in Figure 18, except dNTP is added to the KF injection and is followed by a dNTP + buffer injection (ends at black arrow). Buffer flow only continues until baseline is reached. b) KF-DNA binding curves based on the SPR equilibrium data for each nucleotide.

Conversely, the addition of the next correct nucleotide increases KF binding at equilibrium and drastically slows the dissociation phase, up until the point where dCTP is removed from solution (black arrow in figure 19a).

KF binding curves were constructed for KF binding in the presence of each nucleotide. Figure 19b and Table 1 show the binding curves and K_Ds calculated from the curves for the correctly paired constructs with and without nucleotide. Addition of the next correct nucleotide increases binding nearly 5 fold, while the addition of incorrect nucleotides diminished KF binding 4 to 12 fold. This increase in KF stabilization with the addition of only the next correct nucleotide is indicative of the polymerase undergoing a conformational change from an open to a closed complex(*52*). The formation of the closed complex is also apparent in the dissociation phase. Kinetic off rates for KF were calculated by fitting the dissociation portion of the curves to the double exponential equation, equation 3. The two rates calculated from the fit were described as "fast" and "slow" dissociation rates, and each have a percentage that relates to the population of KF dissociating at that rate (Table 2). KF binding in the absence of nucleotide represents KF being bound in the binary complex, while KF + dCTP represents KF bound in a ternary complex. For KF bound as the binary complex, the slow rate, 0.031 s^{-1}, dominates over the fast rate, 32 vs. 68%. When the next correct nucleotide is added, not only does the slow rate decrease by two orders of magnitude, 0.0002 s^{-1}, but also the amount of polymerase dissociating at the slow rate increases to 93%. On the other hand, KF binding with an incorrect nucleotide does not significantly change the fast and slow dissociation rates, the percentage of

Table 2.
Dissociation Rates (k_{off}) of KF from Unmodified DNA

Nucleotide	k_{off} (s^{-1})[a]	
	fast	slow
KF only	0.212 (32)	0.031 (68)
dATP	0.145 (65)	0.033 (36)
dCTP[b]	0.086 (7)	0.0002 (93)
dGTP	0.227 (81)	0.023 (19)
dTTP	0.157 (39)	0.028 (61)

[a]Values shown are an average of triplicate measurements
[b]Next correct nucleotide
Values in parentheses are the percentage of polymerses dissociating at each rate

KF dissociating at the fast rate is increased. Overall, the purines lead to greater destabilization of KF than the smaller, incorrect pyrimidine, dTTP (Table 2).

iii. Influence of terminal mismatch on KF binding

DNA constructs with a terminal mismatch are shown in Figure 17. Each contains either a pyrimidine-purine C:A or a purine-purine G:A mismatch located at the primer-template terminus, or the post-insertion site with respect to the polymerase. KF was injected over the mismatched DNA constructs and compared to binding to the correctly paired DNA. Typical binding curves for an injection of 200 nM KF to the three constructs are represented in Figure 20. Since the three flow cells each contain a different amount of bound DNA, response units could not be compared directly, therefore response units were converted to percent bound using the R_{max} for each flow cell. Similar to the correctly base paired construct, the association phase for the mismatches was fast, reaching equilibrium quickly. However, the equilibrium binding levels of the mismatched constructs decreased 80-90% from the binding levels for a correctly paired DNA. The large change seen in the sensorgrams is also apparent in the equilibrium binding K_Ds (Table 1). The mismatched constructs resulted in 60-100 fold weaker binding than the correctly paired construct of the same length. Any mismatch in the primer-template terminus also resulted in faster dissociation of the polymerase. Table 3 shows the apparent off rates (k_{off}) of KF for each of the DNA constructs. For both the mismatched constructs, KF predominately dissociates at the fast rate, while a larger fraction of KF tends to dissociate from the correctly paired construct at the slow rate than the fast.

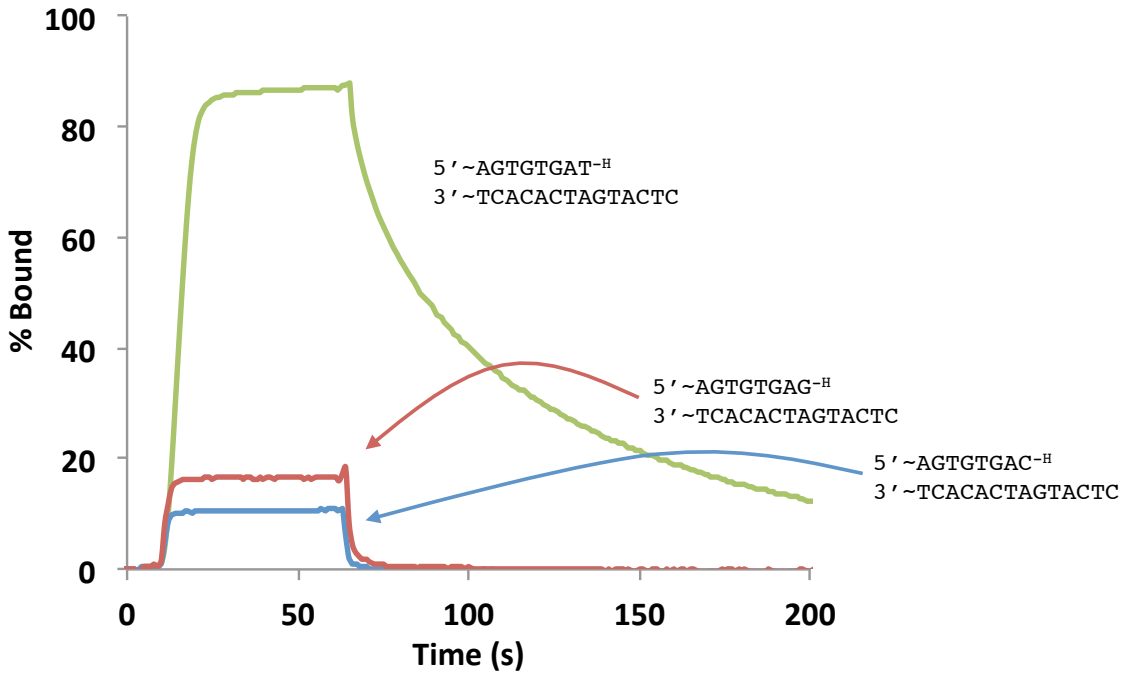

Figure 20. Sensorgrams of 200 nM KF binding to different types of DNA to show the effect of terminal mismatches on KF binding affinity for DNA. Correctly paired DNA (green line) shows the highest equilibrium binding and longest dissociation phase.

Table 3.

Dissociation Rates (k_{off}) of KF from Mismatched DNA

DNA Construct	k_{off} (s^{-1})[a]	
	fast	slow
TA Correct Base Pair	0.212 (32)	0.031 (68)
CA Mismatch	1.18 (82)	0.147 (18)
GA Mismatch	0.83 (80)	0.117 (20)

[a]Values shown are an average of triplicate measurements

Next, the effect that dNTPs have on KF binding to DNA containing a terminal mismatch was monitored. The C:A mismatch represents a construct where a slipped DNA structure could occur upon KF binding. For example, the mismatched C could re-adjust within the polymerase to pair with the templating G, now making T at position +1 the templating base. If a DNA slipping mechanism were occurring, KF binding in the presence of dATP, and not dCTP, would lead to an increase in KF stabilization. KF binding to DNA with a G:A mismatch, which does not have the ability to misalign and form a slipped structure, was also monitored. KF binding experiments for these constructs were performed at the same time as the unmodified DNA. Binding curves were constructed and equilibrium dissociation constants were calculated for the C:A and G:A mismatched constructs in the presence of correct and incorrect nucleotides (Figure 21). For the C:A mismatch, addition of the next correct nucleotide stabilizes KF binding 3-fold, but is still almost 150 times weaker than KF binding to correctly paired DNA with dCTP. There is no further stabilization with the addition of dATP, which destabilized KF binding almost 4 fold. The addition of the other incorrect nucleotides also destabilized KF binding 2.8-4 fold. The other DNA construct with a terminal mismatch contains a bulkier G:A mismatch that is very unlikely to create a slipped structure. All nucleotides destabilized KF binding to the G:A mismatch construct with rates slightly below the CA mismatch results. Table 1 shows all equilibrium K_Ds calculated for the unmodified DNA constructs.

A

5′-GGAGAGTGATTGGTAGTGTGAC-H
3′-Biotin-CCTCTCACTAACCATCACACTA**G**TACTC

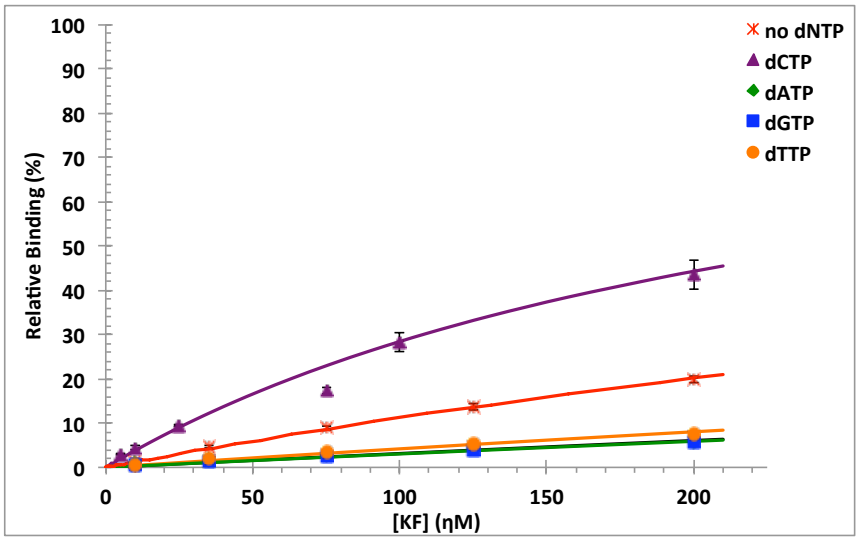

B

5′-GGAGAGTGATTGGTAGTGTGAG-H
3′-Biotin-CCTCTCACTAACCATCACACTA**G**TACTC

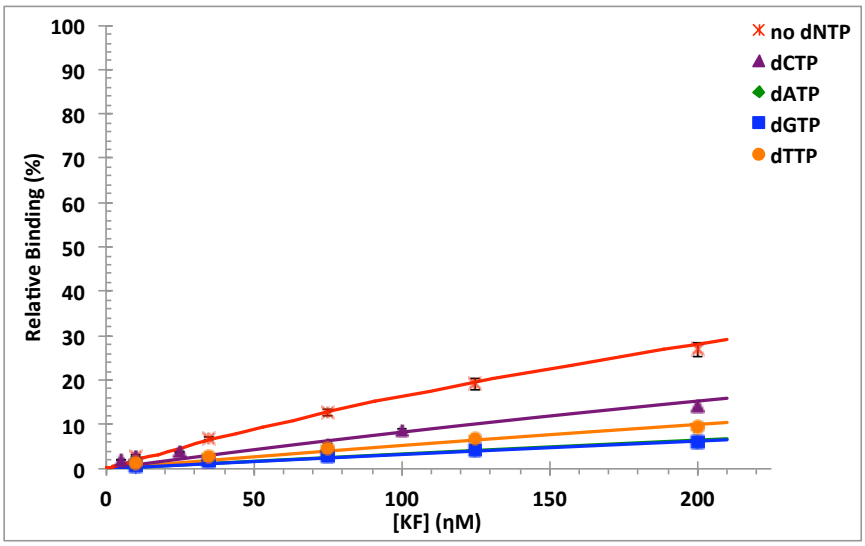

Figure 21. Correct dNTP has little influence on stabilizing KF binding affinity when the DNA contains a terminal mismatch. Binding curves for KF binding to a) CA mismatch and b) GA mismatch DNA constructs in the presence and absence of dNTP based on the SPR equilibrium data.

iv. KF binding results with longer primer

KF binding to a second, unmodified DNA construct was also monitored (Figure 22). Here, the primer strand was extended one nucleotide and duplexed to the same template, placing the single G in the terminal base pair, or the post-insertion site with reference to the KF. Klenow fragment binding to the 23mer primer-unmodified template construct follows the same trend as the construct with the primer of 22 nucleotides (above). The next correct nucleotide dATP stabilizes KF binding nearly 10-fold, while incorrect nucleotides decrease binding 5 to 15 fold (Figure 23, Table 4). KF binding to two constructs where the single G was part of a terminal mismatch was also studied, one that could result in a slipping mechanism (G:A) and one that could not (G:G). Unlike the C:A mismatch discussed above, the A:G mismatch does not show KF stabilization in the presence of the next correct nucleotide. Addition of any nucleotide present destabilizes KF binding to both the A:G and G:G mismatched constructs (Table 4).

C. AAF and AF Modified DNA Results

Surface plasmon resonance was also used to study Klenow fragment binding to DNA modified with either N-acetyl-2-aminofluorene or 2-aminofluorene. The DNA constructs used for the first set of modified experiments contained the shorter primer (22 nucleotides in length) duplexed to a template containing the single modification. Using this primer, the single modified G acts as the templating base. Three sets of DNA duplexes were monitored at the same time on the same SPR chip, one containing a correctly paired primer-template terminus, and two with a single mismatch at the primer-template terminus (Figure 18). Running the experiments

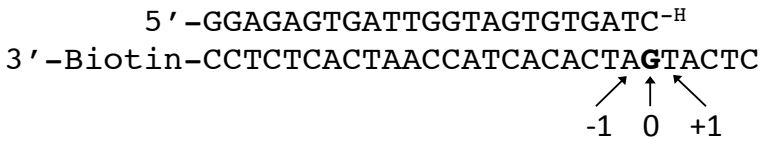

C:G Correct Base Pair

5′-GGAGAGTGATTGGTAGTGTGACA-H
3′-Biotin-CCTCTCACTAACCATCACACTAGTACTC

A:G Mismatch

5′-GGAGAGTGATTGGTAGTGTGAGG-H
3′-Biotin-CCTCTCACTAACCATCACACTAGTACTC

G:G Mismatch

Figure 22. DNA constructs with a 23mer primer and a 28mer template. The single G on the 28mer is in the terminal base pair. The top construct is fully complementary, while the other two contain a single mismatch at the primer template terminus, or the 0 position. The bold G represents where AAF or AF was added to the template.

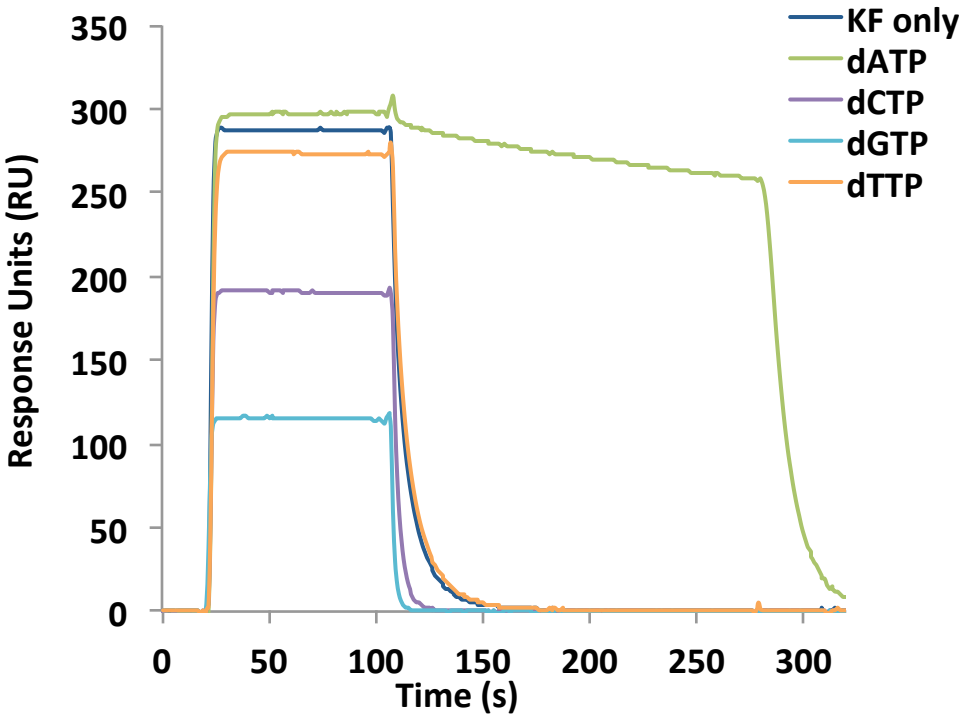

Figure 23. Addition of the next correct nucleotide stabilized KF binding to unmodified DNA. Sensorgrams for KF binding in the presence and absence of dNTP to unmodified DNA duplex containing a 23mer primer.

Table 4. Equilibrium Dissociation Constants (K_D) for Klenow Fragment Binding to Correctly Paired, Unmodified Duplex DNA[a]

K_D (nM)[b]				
KF Only	dATP[c]	dCTP	dGTP	dTTP
22 ± 0.8	3.4 ± 0.3	126 ± 9	340 ± 39	310 ± 30

[a] Primer length 23 nucleotides

[b] Values shown are an averages of triplicate measurements ± standard deviation

[c] Next correct nucleotide

concurrently decreases variability between each experiment. Initially, the AAF modified-KF binding experiments were run using the same method as unmodified experiment, but the 50 µL injection (85 second contact time) was not sufficient enough for the lower KF concentrations to reach equilibrium. Not having the equilibrium binding levels for these lower concentrations lead to distortions in the equilibrium binding curves. To create complete equilibrium binding curves that included low KF concentrations, 140 µL of KF with or without nucleotide was injected followed by 240 s of buffer flow with or without the related nucleotide (Figure 24).

i. Influence of a Modified Template Base on KF Binding

Figure 24 shows 200nM KF binding to AAF modified template in the presence and absence of each nucleotide. The most notable change in KF binding compared to the unmodified data is that KF binds the AAF modified DNA with the same affinity regardless of the type of nucleotide present. The addition of the correct nucleotide did not stabilize KF binding, nor did an incorrect nucleotide lead to a destabilization in KF binding. In addition to these similar binding levels, there is also little variability in the dissociation phase for each. Furthermore, the rate of KF dissociation does not increase when the next correct nucleotide is removed from the system (Figure 24, black arrow). The equilibrium dissociation constants show that in the absence of nucleotide, KF has a higher affinity for the AAF modified templating base than an unmodified templating base (Table 5 and 1, respectively). The dissociation constants verify that there is no further KF stabilization or destabilization to the modified DNA with the addition of nucleotides (Table 5). This

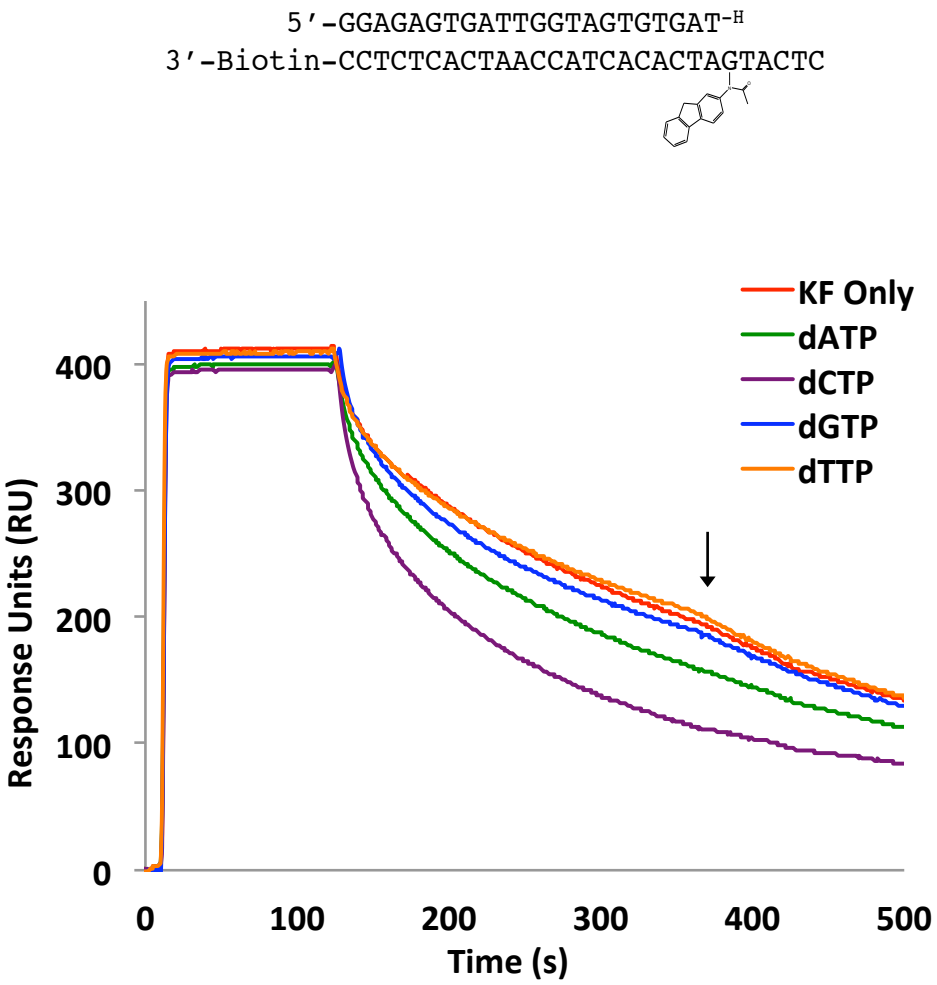

Figure 24. dNTPs have no effect on KF binding to DNA with an AAF modified templating base. Sensorgrams showing 200 nM KF binding to duplex DNA containing an AAF modified G templating base with and without nucleotide. The black arrow represents when dNTP is removed from solution.

Table 5. Equilibrium Dissociation Constants (K_D) for Klenow Fragment Binding to Modified Duplex DNA with Various Primer-Templates[a]

Modification	DNA Construct	K_D (nM)[b]				
		KF Only	dCTP[c]	dATP	dGTP	dTTP
AAF	TA Correct Base Pair	3.4 ± 0.2	4.3 ± 0.2	4.8 ± 0.2	2.9 ± 0.2	2.2 ± 0.1
	CA Mismatch	101 ± 1	221 ± 3	426 ± 7	293 ± 4	235 ± 3
	GA Mismatch	185 ± 2	428 ± 6	650 ± 10	690 ± 10	486 ± 7
AF	TA Correct Base Pair	11.9 ± 0.2	15.6 ± 0.5	10.9 ± 0.3	11.4 ± 0.4	13.1 ± 4
	CA Mismatch	55 ± 2	170 ± 4	142 ± 6	159 ± 4	183 ± 5
	GA Mismatch	114 ± 3	331 ± 6	378 ± 7	268 ± 5	392 ± 8

[a]Primer length 22 nucleotides.
[b]Values shown are an averages of triplicate measurements ± standard deviation
[c]Next Correct Nucleotide

trend of increased KF affinity for DNA with an AAF modified templating base agrees with the work previously reported by this lab(*33*). The crystal structure of T7 bound to AAF modified DNA shows that the KF-DNA binary complex is stabilized by the AAF moiety of the dG-AAF nucleoside binding in a hydrophobic pocket behind the O helix (see section III in introduction). The SPR results shown here, both dissociation constants and dissociation phase, verify that KF does not bind the next correct nucleotide, and therefore does not undergo a conformational change to the closed complex. The T7 crystal structure also showed that having AAF stably bound behind the O helix distorts the fingers region of the polymerase, pushing the O helix towards the active site, blocking the nucleotide-binding pocket and keeping the nucleotides from being tested by the polymerase. It is for this reason that the addition of incorrect nucleotides does not have a destabilizing effect on KF affinity.

KF has comparable affinity for the AF modified construct as it had for the unmodified DNA (Figure 25) (Table 5 and 1). Unlike dG-AAF, dG-AF is able to retain the natural *anti* conformation around the glycosidic bond, leading to little disruption in polymerase binding in the binary complex(*69*). The addition of nucleotide had only a small effect on KF binding affinity for the AF modified DNA and dATP was the only nucleotide to increase KF binding affinity. Also, sensorgrams show that after the removal of dNTP from solution (Figure 25 black arrow), the phase does not stay consistent before and after the arrow as it did for the AAF modified construct. This change in the dissociation phase suggests dNTPs are being tested by the polymerase, unlike KF bound to the AAF modified template (Figure 24).

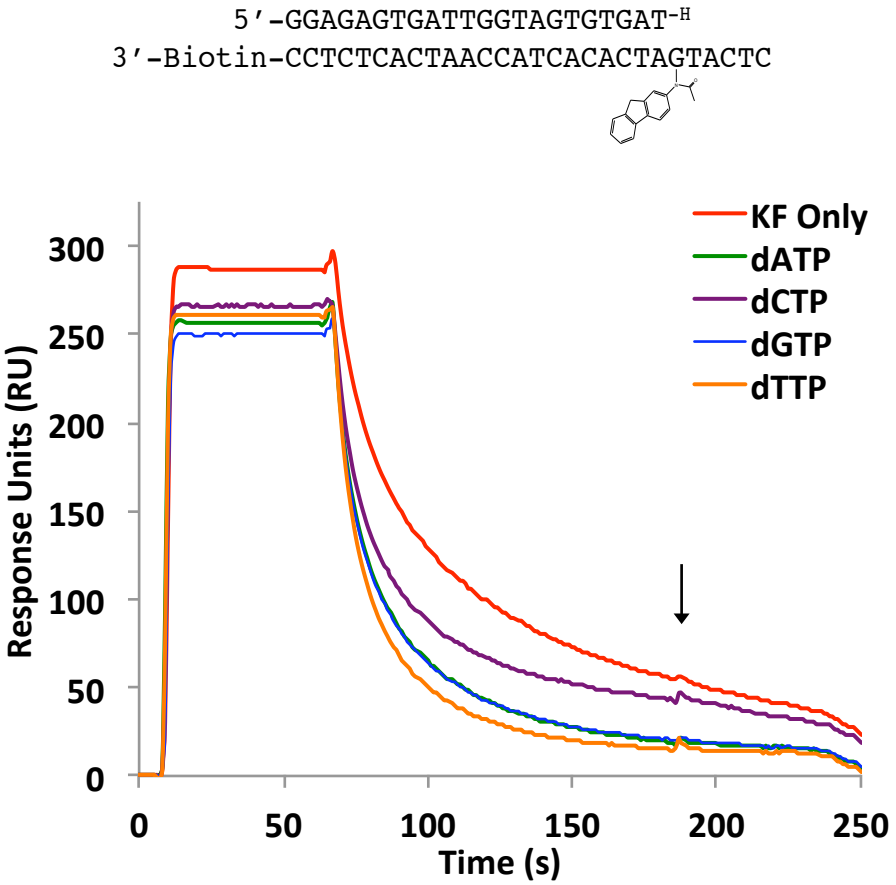

Figure 25. Next correct nucleotide has the same effect on KF binding affinity as an incorrect nucleotide when the templating base is modified with AF. Sensorgrams of 200 nM KF binding to duplex DNA containing an AF modified G templating base with and without nucleotide. The black arrow represents when dNTP is removed from solution.

ii. Effect of AF and AAF on KF dissociation and association rates

Similar to the equilibrium dissociation constants, KF dissociation rates from the AAF and AF modified templating base indicate that binding affinity is independent of dNTP (Table 6). For AAF-modified DNA, the slow rates show almost no variation with dNTP addition while the fast rates vary only slightly. Neither the fast nor the slow rate varied in the amount (percentage) dissociating at each rate. Both fast and slow dissociation rates for AF increased when dNTP was added, and the fraction dissociating from the fast rate increased.

In addition to calculating dissociation rates, the long injections for the low KF concentrations allowed for the association rates to be calculated. KF concentrations below 10 nM were used in equation 4, because the larger KF concentrations bound near the rate of diffusion. Association rates for KF binding in the absence of nucleotide to AAF and AF are shown in Table 7. The rate of KF association for the modified DNA is slower than the association rate to unmodified DNA. The slower rate may result from the rearrangement of the modified base in the DNA structure, such as AAF moving into the hydrophobic pocket behind the O helix. KF may take longer to bind to AF modified DNA because modified base is rotating from *anti* to *syn* conformation.

iii. Influence of AAF and AF on DNA slipping mechanisms

As mentioned above, the SPR chip also contained template modified DNA with a terminal mismatch. The mismatched, modified constructs contain the same mismatches used in the unmodified experiments. The C:A mismatch represents a

Table 6.

Dissociation Rates (s^{-1}) and Percentages for Correctly Paired and Modified DNA

	AAF		AF	
	fast	slow	fast	slow
KF only	0.026 (24)	0.004 (76)	0.137 (34)	0.019 (66)
dATP	0.086 (21)	0.006 (79)	0.199 (45)	0.031 (55)
dCTP*	0.043 (20)	0.003 (80)	0.178 (48)	0.029 (52)
dGTP	0.041 (24)	0.003 (76)	0.186 (46)	0.031 (54)
dTTP	0.079 (20)	0.005 (80)	0.189 (52)	0.036 (48)

*Next Correct Nucelotide

Table 7

Associaiton Rates (k_{on}) for correctly paired DNA

	k_{on} (M^{-1} s^{-1})		
[KF]	Unmodified	AAF	AF
1	n/a[a]	4.02E+05	2.40E+05
2	n/a[a]	6.56E+05	3.73E+05
2.5	4.76E+06	8.98E+05	4.65E+05
5	5.61E+06	1.33E+06	5.88E+05
10	8.29E+06	1.86E+06	7.47E+05

[a]Not enough equilibrium binding to calculate

stand of DNA that could form a slipped DNA structure, while the bulky purine-purine G:A mismatch is not prone to slippage. A slipping mechanism where the mismatched C misaligns with the AF or AAF modified G would account for the prevalence of -1 frameshift mutations that occur near AAF modified DNA(*71*). Table 5 shows the apparent equilibrium dissociation constants for all the AF and AAF template modified constructs. The presence of a terminal mismatch before the modified base destabilizes KF binding, similar to the unmodified constructs, but not to the same extent. This suggests the fluorene moiety is still enhancing KF stabilization, but by a different mechanism. Unlike the unmodified results, the addition of dCTP (next correct) and dATP (next correct in a slipping mechanism) both further destabilize KF binding. dATP leads to the largest amount of KF destabilization with any nucleotide to the AAF modified DNA confirming that for this experiment there is no slipping mechanism occurring. For the AF modified DNA, although dATP destabilized KF the least of all the nucleotides, it still does not stabilize the KF binding complex as it would if a slipping mechanism were occurring.

iv. Influence of AAF and AF in terminal base pair

In vivo and in vitro studies show replication can occur past these adducts, therefore KF binding experiments were also conducted on DNA that contained a modified G in the terminal base pair (Figure 22). These DNA constructs represent a scenario where a nucleotide had been incorporated across from the modified G. Sensorgrams for 200 nM KF binding to correctly paired DNA containing a terminal AAF or AF modification show that the addition of any nucleotide disrupts KF binding to the modified DNA (Figure 26). The next correct nucleotide, dATP leads to the

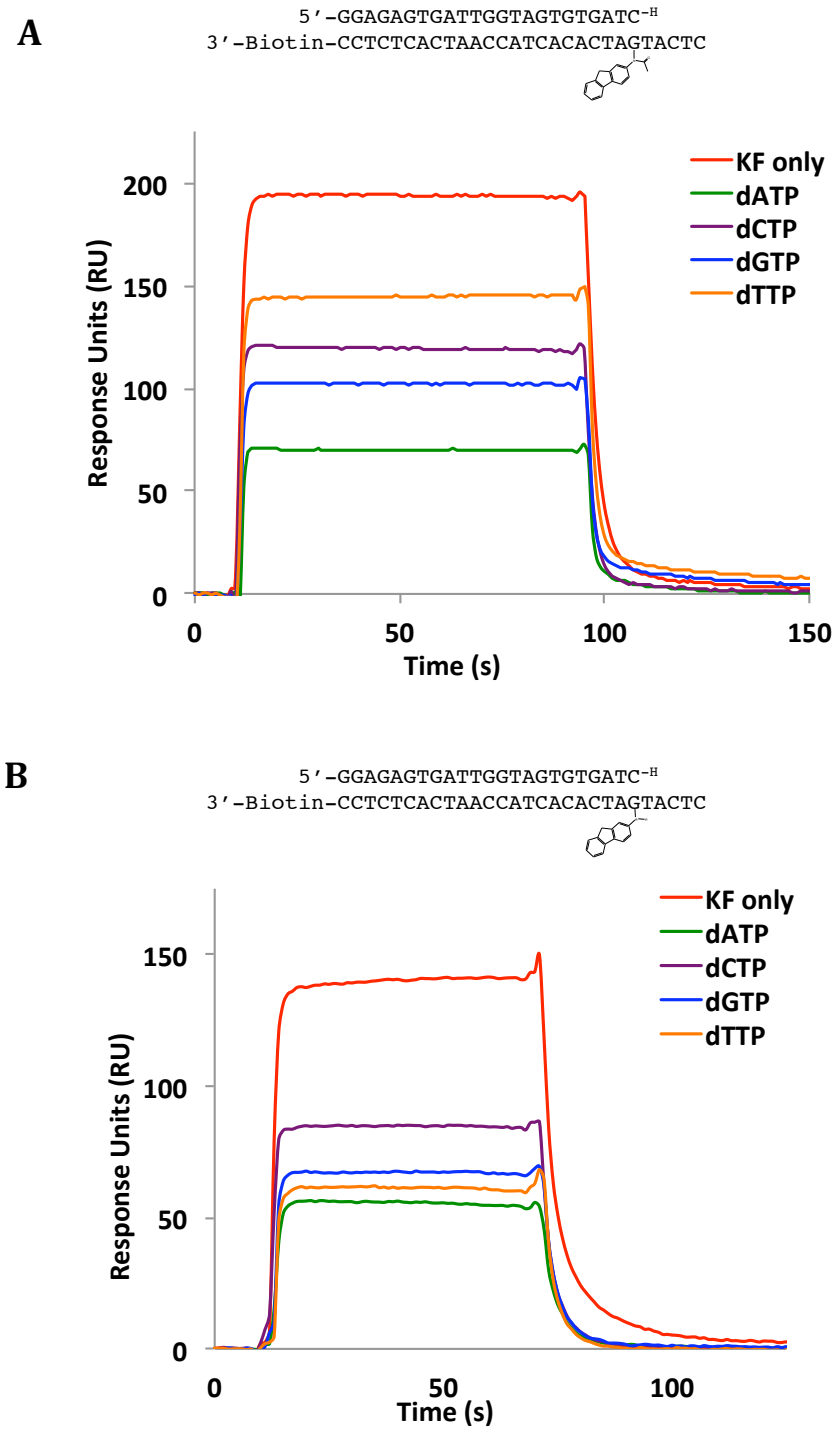

Figure 26. AF or AAF in the terminal base pair decreases KF binding affinity with or without nucleotide. Sensorgrams of KF binding to DNA with an a) AAF or b) AF in the terminal base pair in the presence and absence of dNTPs.

largest decrease in KF equilibrium binding levels for both AF and AAF modified constructs. For AAF modified DNA, the smaller pyrimidines show the least amount of KF destabilization. Equilibrium dissociation constants show a 5 fold decrease in KF stabilization when the terminal base pair contains an AF or AAF modified G (Table 8).

The next set of AF and AAF modified experiments monitored KF binding to DNA constructs that would result from a mis-incorporation across from an AF or AAF modified base (Figure 22). Altering the AAF modified terminal base pair with a mismatch decreased KF binding affinity less than two fold. Therefore, whether correctly paired or mis-paired, dG-AAF causes distortions in the DNA structure that lead to poor KF binding affinity. Addition of nucleotides to the mismatched dG-AAF decreased KF binding affinity even further, with dCTP causing the least amount of destabilization.

KF binding to the DNA constructs with a terminal dG-AF does not follow the same trend as the AAF modified DNA. Altering the modified terminal base pair with a mismatch actually stabilized KF binding (Table 8, bottom). Also, compared to unmodified AG mismatched DNA of the same length, the addition of the AF modification increased KF binding almost 10 fold (K_D 800 nM for unmodified, 90 nM for AF modified). This suggests the AF moiety is stabilizing KF binding to the DNA. Furthermore, addition of nucleotide did not induce the same amount of decrease in KF binding affinity as it had for the correctly paired construct, yet each still destabilized KF binding compared to having no nucleotide present. The next correct

Table 8
Equilibrium Dissociation Constants (K_D) for Klenow Fragment Binding to Duplex DNA with Various Primer-Templates[a]

Modification	DNA Construct	K_D (nM)				
		KF Only	dATP[c]	dCTP	dGTP	dTTP
UnMod	CG Correct Base Pair	22 ± 0.8	3.4 ± 0.3	126 ± 9	340 ± 39	310 ± 30
	AG Mismatch	800 ± 20	3500 ± 800	2000 ± 500	4000 ± 900	1900 ± 200
	GG Mismatch	460 ± 90	2100 ± 400	1300 ± 200	2700 ± 500	1200 ± 200
AAF	CG Correct Base Pair	131 ± 7	680 ± 30	250 ± 10	350 ± 20	260 ± 10
	AG Mismatch	200 ± 10	1560 ± 70	430 ± 20	1140 ± 50	690 ± 30
	GG Mismatch	260 ± 20	2300 ± 200	580 ± 40	1340 ± 90	790 ± 50
AF	CG Correct Base Pair	124 ± 7	430 ± 20	330 ± 20	420 ± 20	500 ± 20
	AG Mismatch	90 ± 6	390 ± 30	220 ± 20	310 ± 20	390 ± 30
	GG Mismatch	89 ± 7	430 ± 20	240 ± 20	320 ± 20	390 ± 20

[a]Primer length 23 nucleotides.

[b]Values shown are an averages of triplicate measurements ± standard deviation

[c]Next Correct Nucleotide

nucleotide destabilized KF binding to the mismatched-AF construct the most, while dCTP has the least destabilizing effect.

III. Ensemble PIFE results

The results showing that a terminal mismatch modified with AF leads to a greater KF binding affinity has not been seen before. To further explore these KF binding results, additional studies were carried out using ensemble fluorescence and single nucleotide incorporation assays. In the process of optimizing AF and AAF as FRET donors, it was found that when KF binds to DNA containing AF and AAF, the emission intensity increased. Although the fluorescence emission for AF and AAF was not suitable for FRET studies, this protein induced fluorescence enhancement (PIFE) was seen as a useful tool in expanding upon the SPR results.

A. PIFE from AAF and AF modified template bases

For the KF binding studies with AF/AAF, it was proposed that an increase in fluorescence emission occurred due to AF/AAF stabilization within the protein. For example, when KF binds to DNA containing dG-AAF as a templating base, the AAF fluorene rings are stabilized in a hydrophobic pocket within the protein. The blue line in figure 27a represents the fluorescence emission of AAF as part of a modified primer-template duplex. KF binding to the AAF modified duplex result in an increased emission from AAF (red line). The results are similar when the same DNA duplex is modified with AF; as AF emission is increased after KF binds the DNA. As shown in the SPR results above, the addition of nucleotide does not have any effect on KF binding to the AAF modified DNA, specifically, KF does not undergo a

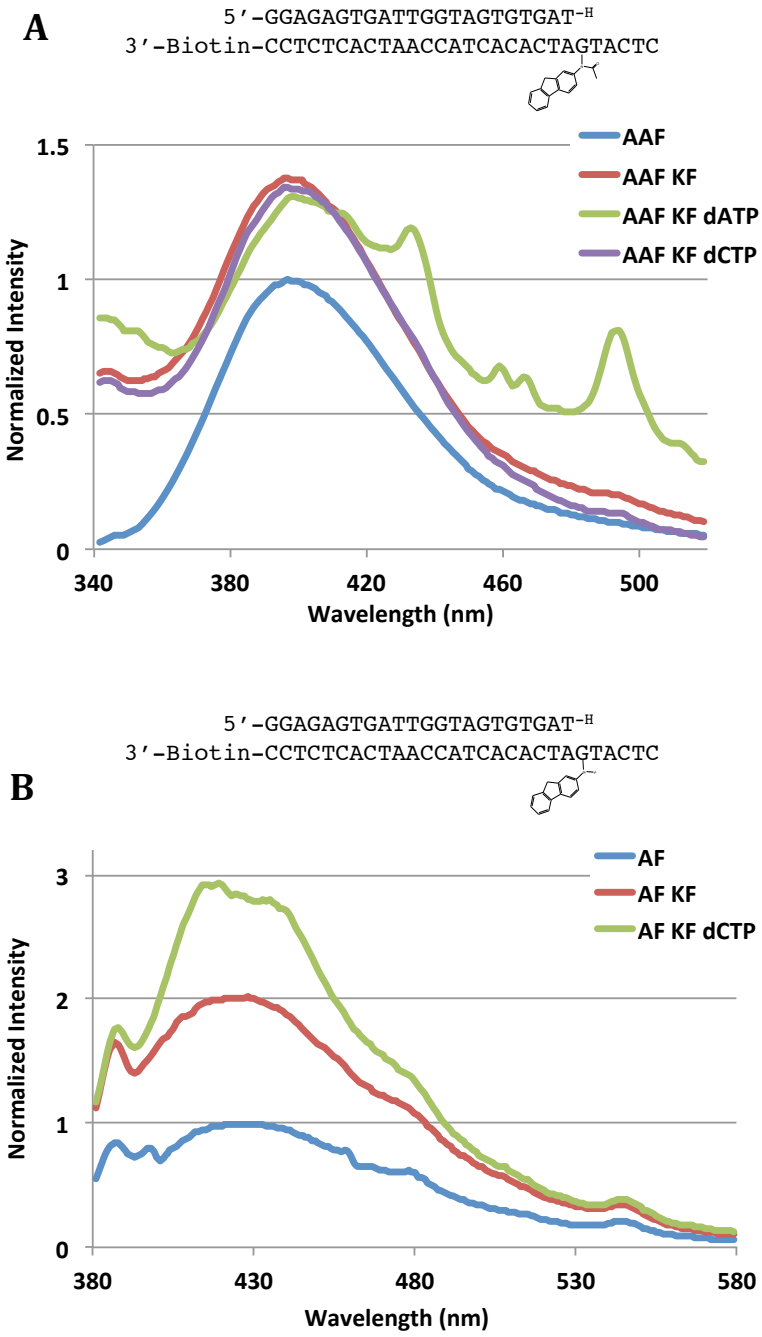

Figure 27. KF binding to DNA with an AF or AAF modified templating base increases fluorescence emission of AF or AAF. Fluorescence emission a) AAF and b) AF in the presence and absence of KF and dNTPs. AAF and AF modified DNA are duplexed to a 22mer primer, making the modified G the templating base. AF emission in (b) increase in the presence of the next correct nucleotide, while AAF in (a) has no change in fluorescence when dNTP is added.

conformational change to a closed complex. As a control, we added dCTP to the AAF modified KF-DNA binary complex as well as the AF modified binary complex (Figure 28b). There was no change in the AAF emission when the next correct nucleotide was added, yet when dCTP was added to the AF DNA-KF binary complex, there was a further increase in AF emission. It was hypothesized the increase in AF emission, but not AAF, with the addition of dCTP results from the protein undergoing a conformational change to the closed complex, further stabilizing AF and increasing fluorescence.

B. PIFE from AF in terminal base

To investigate the mechanism behind higher KF binding affinity for the AF modified mismatched construct but not when AF was part of a correct pair (Table 8), similar PIFE experiments were made with the AF modified terminal base pair DNA. This trend of increased binding affinity for the AF modified mismatched construct was also observed for incorrect nucleotides, but not for the next correct nucleotide. PIFE was used to examine the possibility of KF forming a closed complex around this DNA structure in the presence of incorrect, but not correct, nucleotide. A terminal AF-modified base pair shows a similar increase in emission upon KF binding as it did when the AF was on the templating base, confirming AF DNA-KF binary complex (Figure28a). The addition of nucleotides did not induce a further increase in AF emission like when AF was on the templating base, but the addition of each nucleotide lead to a decrease in AF emission for the AF DNA-KF binary complex. This decrease in PIFE shows the closed complex is not forming, but suggest AF is binding in a less ordered position in the polymerase after dNTP is tested by the

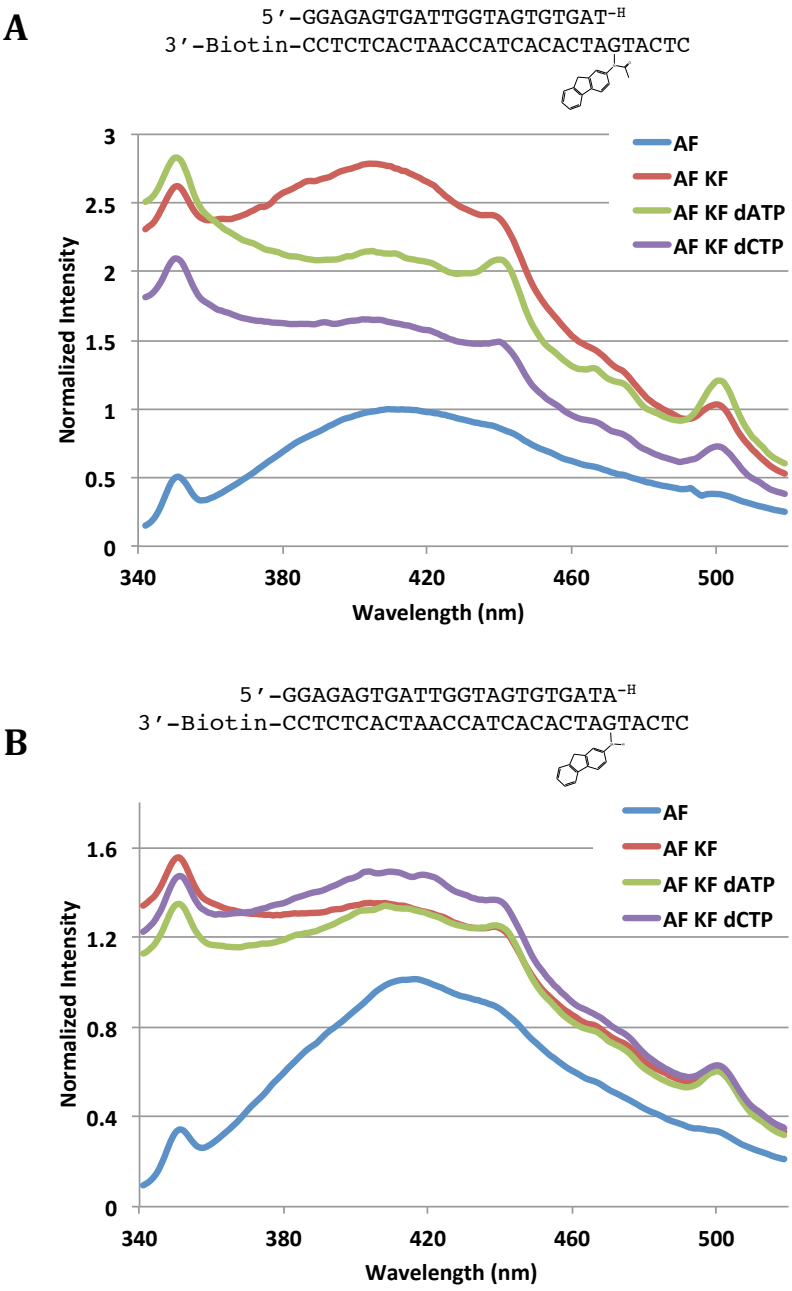

Figure 28. KF binding increases AF fluorescence when binding to correctly paired and mismatched DNA, but the addition of dNTPs have differing effects. Fluorescence emission of AF in a a) correctly paired DNA construct and a b) DNA construct with a terminal A:G mismatch in the presence and absence of KF and dNTPs. AF modified DNA are duplexed to a 23mer primer, placing the modified G in the terminal base pair. AF emission in (a) decreases in the presence of a nucleotide, while AF in (b) shows an increase in fluorescence when an incorrect dNTP is added.

polymerase. AF as part of a terminal mismatch shows the same increase in AF emission from KF binding, but the addition of the correct and incorrect nucleotide to the AF DNA-KF binary complex lead to different PIFE results (Figure 28b). Adding next correct nucleotide to the system does not induce a change in AF emission from AF DNA-KF binary complex. The addition of the incorrect nucleotide however leads to a slight increase in AF emission, suggesting AF has been stabilized. To determine if the AF stabilization could be from the formation of a closed complex, a single nucleotide incorporation assay was performed.

For KF to incorporate a nucleotide, the polymerase must undergo a conformational change to the closed complex. A single nucleotide incorporation assay would determine if the incorrect nucleotide dCTP was added to the growing DNA strand. The next correct nucleotide was preferentially incorporated on the unmodified, correctly paired DNA, as expected (Figure 29a). KF was still able to incorporate dATP onto the AF modified DNA construct. Having a mismatched primer template terminus did not allow for any incorporation, but when the G of the terminal base pair was modified with AF KF incorporated dATP as well as small amounts of incorrect incorporation of dCTP and dTTP. Since both dATP and dCTP were incorporated, the increase in PIFE seen when dCTP is added to the mismatched AF DNA-KF binary complex (Figure 29b) does not correspond to KF transitioning to the closed ternary complex. The stability must arise from an alternate, active ternary structure(*55*).

A

5′Cy3~AGTGTGATC
3′~TCACACTA**G**TACTC

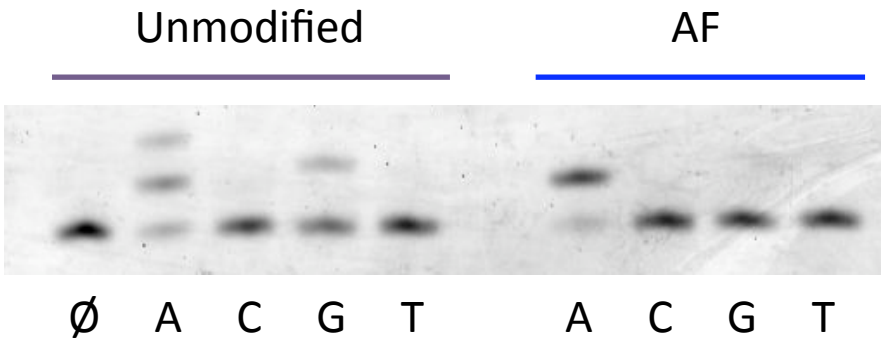

B

5′Cy3~AGTGTGATA
3′~TCACACTA**G**TACTC

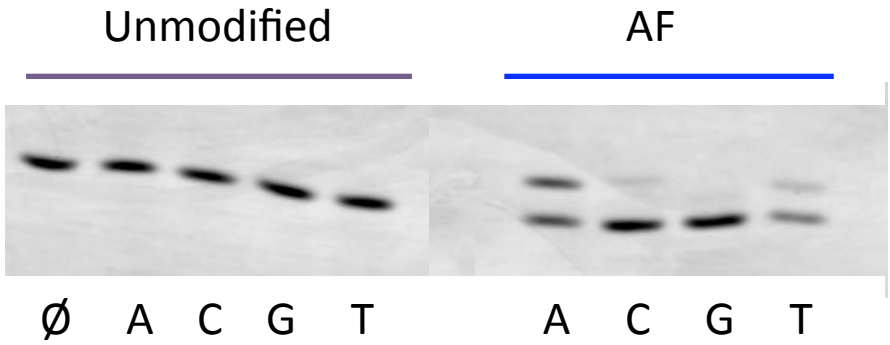

Figure 29. KF can incorporate correct dATP onto DNA with an AF modified terminal base pair. Single nucleotide incorporation assay by KF using an unmodified or AF-modified construct that is either correctly paired (A) or with a A:G terminal mismatch (B) (sequences above gels). The bold **G** in the template marks the position of the AF modification (terminal base pair). Reactions were initiated by the addition of the corresponding dNTPs indicated below the gel. ø means no dNTP was added.

Chapter 4: Discussion

I. Unmodified DNA

DNA replication is an important process in the cell, it is imperative for daughter cell survival that replication occurs with little or no mistakes. The process of incorporating nucleotides by DNA polymerase can be complicated by the presence of DNA adducts such as N-acetyl-2-aminofluorene (AAF) and N-2-aminofluorene (AF) on the template strand. The errors caused by these adducts can lead to numerous problems in the cell, such as the production of cancerous cells. It is important to investigate how the adducts interfere with DNA replication to understand how the mutagenic outcomes occur. The experiments performed here explore the effect DNA adducts have on polymerase binding to DNA. The label free technique of surface plasmon resonance (SPR) was utilized to characterize DNA-Klenow fragment binding interactions in the presence and absence of these adducts. The sensorgrams produced by SPR were used to determine apparent equilibrium dissociation constants (K_Ds) for Klenow fragment binding to a number of DNA constructs. The binding and dissociation portions of the sensorgrams were also used to obtain kinetic association and dissociation rates, respectively.

A. SPR Results

The polymerase-DNA complex is a dynamic molecule, and crystal structure and FRET studies show KF binding in both an open and a closed state(*49, 50*). The movement in the fingers and thumb domains increase fidelity of the polymerase. The equilibrium binding constants (K_D) for KF binding to unmodified DNA support

the previous results stating the stably bound closed state can only be formed with the next correct nucleotide(*52*). The stable structure formed with the next correct nucleotide delivers a 5-fold increase in KF binding that is not seen with incorrect nucleotide, which produces a 4 – 13 fold decrease in KF binding (Table X). Since the AAF and AF modified DNA experiments were run using DNA containing two different primer lengths, the unmodified DNA experiments were essentially run twice, for comparison purposes. Using two different primer lengths, the same unmodified experiments were run for DNA with G or T as the templating base. In the absence of nucleotide, the templating base affected KF binding affinity, as K_D 22 nM for T as the templating base versus 8 nM for G. However, when the next correct nucleotide is added, KF binding affinity for both DNA constructs increased approximately 5-fold. This implies that templating base identity may effect the DNA-KF binary complex stability, but not the closed DNA-KF-dNTP ternary complex with the next correct nucleotide.

i. Dissociation rates relate to KF binding conformation

For DNA replication to proceed with minimal errors, DNA polymerase must select against incorrect nucleotides in an effective manner. The correct dNTP must be selected from a pool that also includes complementary rNTPs and non-complementary dNTPs and rNTPs. KF undergoes a conformational change to a closed ternary complex only in the presence of the next correct nucleotide(*52*). It has been proposed that KF selects against non-complementary dNTPs and rNTPs while the polymerase is in an open conformation(*55*). The complementary rNTP is selected against during the transition of the fingers region from an open to closed

conformation, because the 2'OH on the sugar of the ribonucleotide is sterically hindered by Glu-710 in the KF active site(*57*). The closing of the fingers domain is an important step taken by the polymerase to guarantee only the correct nucleotide is incorporated into the growing DNA strand. The SPR sensorgrams and subsequent apparent equilibrium binding constants presented here show incorrect dNTPs destabilize KF binding to unmodified DNA, while the correct nucleotide increased KF binding affinity, in agreement with previous results(*52, 91, 92*). In addition to the equilibrium binding levels, the presence of nucleotides also had an effect on the dissociation pattern of KF. Kinetic off rates were determined for KF by fitting the dissociation portion of the curve, where KF was no longer in solution, to both a single exponential and double exponential decay equation. Fitting to the double exponential resulted in better fits (residuals) than the single exponential equation. The presence two kinetic off rates suggests that KF bound to DNA can exist in more than one conformation before it dissociates from DNA. The two off rates calculated from the double exponential fit have been designated "fast" and "slow" rates, with the slow representing a polymerase bound in a more stable form. Each rate has a percentage associated with it, describing the amount of KF dissociating from the DNA at that rate. Here, it is proposed that these off rates can be correlated to the conformation that KF adopts prior to dissociation from the DNA.

For example, the SPR binding results for an injection of KF in the absence of dNTP represents the formation and decay of a DNA-KF binary complex (Figure 18 and Table 2). A stable polymerase is bound to DNA at the primer template terminus ready for an incoming dNTP to be tested, but since dNTP is not available, the

polymerase dissociates after a short time. The rate of KF dissociating from this stably bound KF-DNA binary structure is assigned to the slow rate (Table 2, KF only). Also, since the polymerase is a dynamic molecule, the added stability over the polymerase dissociating at the fast rate could arise from the fingers region fluctuating between open and a partially closed state while bound(*85*). The fast rate on the other hand represents KF dissociating from DNA that is unable to stably bind at the primer-template terminus. It is also possible that the fast rate is a mixture of unstable binary DNA-KF bound at the polymerase site and KF bound to DNA with the primer strand at the exonuclease binding site. KF has been crystalized with a correctly paired primer terminus bound in the exonuclease site(*48, 93*). Previous studies have shown that when KF binds to DNA with a terminal mismatch, there is an increase in exonuclease site binding(*54, 94*). The dissociation rates calculated for the DNA constructs containing a terminal mismatch would represent KF dissociating from the exonuclease active site (Table 3). The two dissociation rates for the each of the mismatched constructs (C:A and G:A terminal mismatch) both have slow rates that are comparable to the fast rate of the correctly paired DNA (0.147 s^{-1} and 0.117 s^{-1} vs 0.212 s^{-1}, respectively). These numbers suggest the fast dissociation rate of KF from correctly paired binary complex could include KF dissociating from exonuclease binding site. The small increase in correctly paired binary complex rate suggests the correctly paired fast rate (0.212 s^{-1}) represents a mixture of exonuclease site binding and unstable duplex binding, which would increase the overall average rate.

The addition of dNTP to KF in the SPR injections promotes the formation of DNA-KF-dNTP ternary complex. Both the correct and incorrect nucleotides had a significant effect on KF dissociation compared to KF only, though in opposite manners (Figure 19). The DNA-KF-dCTP ternary structure that is formed is different than the DNA-KF-dNTP structure, where dNTP is dATP, dGTP or dTTP. Only the presence of the next correct nucleotide can induce KF to transition from an open to a closed ternary structure (*52*). The two dissociation rates determined for the DNA-KF-dCTP ternary complex were still labeled as "fast" and "slow", but the fast and slow rates for the DNA-KF-dCTP ternary complex were different by one order of magnitude than the rates for DNA-KF binary complex (Table 2). The ternary complex fast rate is comparable to the slow rate from the binary complex, implying that this rate represents polymerases that are dissociating from a stable binary complex. It is also possible that the few polymerases dissociating at this rate (only 7%) are bound in an unstable, open ternary complex that is unable to transition to the closed complex.

The slow rate determined for DNA-KF-dCTP is two orders of magnitude slower than the slow rate for the DNA-KF binary complex. With the presence of the next correct nucleotide the templating base moves from the pre-insertion to insertion site, KF aligns the correct nucleotide in the active site, and once aligned KF undergoes a conformational change from the open to the closed ternary complex. The substantial change in the slow dissociation is an example of the increase in stability created by the closed complex that has not been noted before. According to the SPR data, 93% of polymerases are able to complete a conformational change to

the closed complex. KF continues to dissociate at this slow rate until nucleotide is no longer in solution (black arrow in Figure 18). If the polymerase happens to transition back to the open conformation and release the dCTP, a new dCTP can bind to the binary complex without the KF dissociating first.

The addition of an incorrect nucleotide disrupted KF binding and did not induce this same effect in KF dissociation rates as the correct dNTP, in agreement with previous experiments(*52, 91, 92*). The two dissociation rates determined for the incorrect nucleotides can also represent KF dissociation from different conformations, but the conformations are harder to discern (Table 2). In the experiments performed here only incorrect nucleotide was present. Under physiological conditions when all nucleotides are present, it has been proposed that incorrect nucleotides are selected against when KF is in an open conformation, and the polymerase stays bound, continuing to test nucleotides until a correct nucleotide is available(*55, 56*). During the selection, the templating base on the DNA stays in the pre-insertion site and will only move to the insertion site when the next correct nucleotide binds(*49*). A mechanism has been proposed that when a dNTP pool only contains incorrect nucleotides, the polymerase eventually tests the incorrect nucleotide by undergoing a conformational change in the fingers region to the closed complex, but the incorrect nucleotide cannot form a base pair with the templating base, causing a steric clash and leading the polymerase to dissociate(*85*). The slow dissociation rates for KF with incorrect nucleotides are similar to the slow dissociation rate for KF only, or the DNA-KF binary complex that only forms the open conformation. Without the next correct nucleotide available, this fingers

closing, or fluctuation in the fingers region could be the cause of the slow rate(*95, 96*). The amount of KF dissociating at this slow rate for dTTP is increased compared to the other incorrect nucleotides. This could be interpreted as dTTP being tested by the polymerase longer because, like the correct nucleotide, is a pyrimidine and does not create a large steric clash like purines do(*91*).

II. AAF Modified DNA

The results for SPR experiment monitoring Klenow fragment binding to DNA with an AAF modified templating base are in line with results from previous experiments(*33*). KF shows a higher binding affinity to DNA with an AAF modified templating base than to unmodified DNA (Table 1 and 5), and the fast and slow dissociation rates are both slower than those for the unmodified DNA construct (Table 2 and 6). This is true for KF alone as well as KF in the presence of nucleotide. The crystal structure of T7 DNA polymerase with DNA containing a dG-AAF templating base was grown in the presence of ddCTP, yet displayed no evidence of the incoming nucleotide in the active site(*68*). The crystal showed the AAF moiety displaced the O helix, moving it towards the active site and keeping the ddCTP from entering. Since the crystal is only a snapshot of the polymerase, it cannot confirm if a nucleotide is able to enter the active site enhancing KF affinity. The effect of nucleotides on unmodified DNA was obvious in the sensorgram data, especially the stabilizing effect of the next correct nucleotide (Figure 21). If a nucleotide were able to bind in the KF active site and increase KF binding affinity, the dissociation phase for the AAF results would resemble the dissociation phase of KF binding to unmodified DNA with dCTP, where the dissociation increases after dCTP is removed

from solution. The sensorgram showing KF binding and dissociation from DNA with an dG-AAF templating base shows polymerase dissociates at the same rate before and after the dNTP is removed from solution (Figure 24, black arrow), confirming that any dNTP, correct or incorrect, is unable to bind in the KF active site when DNA contains a dG-AAF modified template. The calculated dissociation rates confirm this as well, as the rates for KF dissociation in the presence and absence of dNTP do not show significant variations.

Unlike the results for the dG-AAF as a templating base, having dG-AAF correctly paired in the post insertion site did not lead to KF binding with high affinity (Figure 26a and Table 3). The addition of any nucleotide further decreased KF binding affinity, and the next correct nucleotide resulted in the largest KF destabilization, agreeing with previous reports that AAF is a strong block in the post-insertion site(*97*). One pattern that was present for both dG-AAF in the templating base and dG-AAF in the DNA primer template terminus; KF had higher affinity for modified DNA constructs with a terminal mismatch than for unmodified constructs with the same mismatch (Table 5 and 8). The KF binding affinity to DNA constructs with an AAF modified terminal mismatch is still decreased compared to the correctly paired construct with the same modification, but having the AAF modification on the templating G still increases KF binding affinity 3-5 fold over the DNA with an unmodified terminal mismatch. This implies there is an interaction between the AAF moiety and the protein, yet is not as significant as dG-AAF intercalating in the hydrophobic pocket. The increase could result from the AAF

moiety interacting with hydrophobic residues, Leu 361 and Phe 473, that normally interact with the base of the incoming nucleotide(*46*).

A. Slipping Mechanisms

The mismatched DNA constructs used in the SPR experiments shown here were designed to stimulate possible DNA slipping mechanisms. Frameshift mutations arising from modified DNA are influenced by not only the DNA sequence(*98, 99*), but also the editing role of the DNA polymerase(*100, 101*), and the possibility of a disproportionate dNTP pool(*102*). Previous studies have shown that the ability of KF to induce deletions of one or two bases on DNA modified with AAF depends on the sequence context near the adduct and the nature of the base incorporated opposite the adduct(*103, 104*). Repetitive sequences and, more specifically the recognition sequence of the restriction enzyme Nar I sequence (5'-GGCGCC-3') have been shown to induce frameshift mutations when modified with AAF through a slipping mechanism(*32, 104*). The SPR KF binding experiments performed here on AAF modified DNA tested how DNA sequence context and the type of base incorporated across from the modified template affect KF binding with correct and incorrect nucleotides (Figure 26). The slipping mechanisms tested depicted random DNA and were not part of a repetitive sequence. Mispairing dCMP at the 3'-primer terminus to the A one nucleotide before the dG-AAF templating base, tested the ability of DNA to realign one nucleotide with the modified dG-AAF (within the active site). The same process of ending the primer template terminus in a mispair was used across from the dG-AAF base, where the modified base could loop out of the duplex DNA. Unlike the NarI mechanism that is proposed to loop out

two bases, in the mechanism here only a single base would be displaced. Having an incorrect base pair just prior to the AAF modified base decreased KF binding with dCTP as well as dATP, the nucleotide that would suggest a slipping mechanism (Table 5). Instead of creating a slipped DNA structure, the mispaired primer-template terminus, in addition to the bulkiness of the AAF, did not allow for proper alignment of the polymerase at the primer template terminus, and the polymerase quickly dissociated.

For the DNA constructs used here, varying the base incorporated across from the dG-AAF to form mismatches lead to a decreased KF binding affinity for the DNA. The DNA constructs with an incorrectly paired G:A primer-template terminus that could result in a slipped mechanism did not increase KF binding (Figure 22 and Table 8). Mispairing and driving the DNA to loop out the dG-AAF base was not enough to increase KF binding. The movement of only one nucleotide may not be enough to clear the bulky adduct out of the polymerase active site. Having two nucleotides, like the NAR slipping mechanism, may be required to move the bulky adduct from the polymerase active site, allowing the movement of the fingers region to occur(*32*).

For dG-AAF as the templating base, the misalignment of the primer strand may be able to occur on fully paired DNA. The high affinity of KF for the AAF modified template keeps KF bound to the DNA in an open conformation for a long period of time. During this time, the template strand could undergo a rearrangement close to the polymerase active site. It is possible for the template

strand to loop out and misalign in such a way that AAF is no longer stabilized in the hydrophobic pocket, allowing for a nucleotide to enter the active site and for the polymerase to undergo a conformational change, resulting in the incorporation of an incorrect nucleotide(*68*).

III. AF modified DNA

The mutagenic outcomes of AF modified DNA tend to be single base substitutions, typically G to T transversions(*59, 105*). Based on the SPR binding results, G to T transversions caused by the dG-AF templating base on correctly paired DNA could occur in two possible ways. dATP was the only nucleotide that led to an increase in binding affinity for KF to the AF modified DNA (Table 5). The DNA used in these experiments has a T as the next templating base following dG-AF. If dG-AF causes a distorted DNA structure, the T at +1 may become the templating base, and allow for dATP to be incorporated. This mechanism can explain single base substitutions, but since not every dG-AF has a T downstream, this slipping mechanism cannot be the main mechanism by which G to T transversions occur. The more likely possibility would be when KF binds to dG-AF in the *syn* conformation. In the *syn* conformation guanine would be flipped out of the active site, mimicking an abasic site, where dATP tends to be incorporated(*106, 107*).

Previous studies have shown that the polymerase sits in an open conformation with an ordered O helix, and the templating dG-AF can adopt both *syn* and *anti* conformations(*37, 38, 108*). The T7 crystal structure obtained by Dutta *et al.* provided information about the protein structure, but the electron density of and

around the dG-AF base was of low quality. The inability to verify the modified base structure was attributed to the dynamic nature of dG-AF and the ability it has to rotate from *anti* to *syn* around the glycosidic bond(*69*). The *syn* or *anti* conformation of the dG-AF dictates how KF binds to the DNA, and I hypothesize the fast and slow dissociation rates correlate to KF dissociating from the two types of DNA. In the co-crystal structure of Bacillus fragment, a KF homolog from *Bacillus stearothermophilus*, with DNA containing an AF modified templating base, in the absence of nucleotide dG-AF is trapped in the *syn* conformation with a relatively unperturbed active site and the fingers region sit in an open conformation(*70*). This crystal structure suggests the slower KF dissociation rate would correspond to dG-AF binding in the *syn* conformation. Although the T7 crystal structure was unable to determine the exact location of dG-AF in the KF active site, the structure did confirm the AF moiety was not in the hydrophobic binding pocket like the AAF modified base, keeping the O helix unperturbed. This leaves the nucleotide binding site open, allowing for nucleotides to enter the active site. The similar binding affinities of KF with both correct and incorrect nucleotides suggest the polymerase was acting on nucleotides equally (Table 5). For the polymerase to test for correct Watson-Crick base paring with the incoming nucleotide, dG-AF must rotate from *syn* to *anti*. This rotation increases perturbations in the polymerase leading to an increase in the number of polymerases dissociating at the fast rate. Although KF binding with dTTP would create a mismatch, a higher percentage of polymerases are dissociating from KF at the fast rate when dTTP is in solution. This could suggest that under these conditions KF can incorporate dTTP over dCTP, leading to a base substitution.

The surface plasmon resonance results for KF binding to DNA containing an AF modified templating base (Table 5) matched well with previous biochemical results(*33*). When the base that is incorporated across from the dG-AF base was varied with a correct or incorrect nucleotide, the KF binding results resulted in a pattern not previously observed. A terminal mismatch on unmodified DNA decreased KF binding affinity 20-35 fold compared to a correctly paired duplex DNA. A terminal mismatch containing an AF modification actually increased KF binding over a correctly paired C:G-AF terminal base pair (Table 8). This implies incorrect geometry of a mismatch moves AF to either a location that simply interferes less with KF or the AF moiety is interacting positively with the polymerase, stabilizing the complex. The addition of nucleotides did decrease KF binding affinity for the AF modified DNA constructs, but the effect was small when AF was part of a terminal mismatch.

The PIFE experiments took advantage the fluorescent properties of AF to determine how AF was interacting within the DNA and within the polymerase. NMR structures of dG-AF modified terminal base paired with C or A resolved the AF moiety to be stacked within the DNA for both correctly paired and mismatched structure. The main difference between dG-AF correctly paired vs. mismatched was the location of the base positioned across from the dG-AF. The C across from dG-AF was looped out into the minor groove, making no interactions with dG-AF. The mispaired A in the A:G-AF mismatch had a defined orientation in the major groove, interacting with the Hoogsteen edge of dG-AF(*109*). This interaction is rather small

but can still explain the higher AF emission from the A:G-AF over the C:G-AF constructs in the absence of polymerase.

The crystal structure of *Bacillus* fragment with a correctly paired AF modified G in the post-insertion of the polymerase, revealed dG-AF to be in the *anti* conformation, G formed three hydrogen bonds with C, and AF placed in the major groove. The fluorene ring of the AF moiety stacks with the templating base, keeping the base from moving into the pre insertion site. The placement of the AF moiety also distorts the O1 helix, which then partially blocks the pre insertion site(*70*). The crystal was not grown in the presence of nucleotide, but the authors believe the correct base paring would allow for continued synthesis. The apparent dissociation constants (K_D) for the AF modified terminal base pair determined by SPR showed the presence of any nucleotide decreased KF binding affinity for both the correctly paired and the mismatched constructs (Table 8). Yet, KF binding affinity decreased more for the correctly paired construct over the A:G and G:G terminal mismatches. When KF binds to C:G-AF DNA, there is a large increase in AF fluorescence emission, but the addition of nucleotide led to a decrease in AF emission. It was initially postulated this decrease in PIFE was related to the decrease in binding affinity (that KF was not binding), but with the high concentration of polymerase used in the experiments, it is unlikely for KF to not be bound to the DNA. Therefore, the change was related to the position of AF within the polymerase. In the BF crystal structure mentioned above, when KF binds the correctly paired AF modified DNA, AF stacks with the templating base. This stacking interaction creates the large increase in AF emission seen when KF is added (Figure 28a, red line). When dNTP is added the

templating base must move from the stacked position to the polymerase active site to test for correct Watson Crick base pairing. By eliminating the stacking interaction, AF stability is decreased, producing a decrease in AF fluorescence. The K_D for KF binding to C:G-AF with nucleotide suggested the location of AF is disruptive to KF DNA interactions and the transition of the fingers region from open to closed. On the other hand, the single nucleotide incorporation assay shows incorporation of the next correct nucleotide, dATP (Figure 29a). The longer time frame of the experiment, 10 versus 2 minutes, might allow for the correct alignment and subsequent incorporation of dATP.

A. Slipping mechanism promoted by AF

There is no crystal structure of Klenow fragment or Bacillus fragment bound to AF modified DNA as part of a terminal mismatch. The PIFE experiment shows the addition of KF to an AF modified mismatch DNA did not increase AF emission to the same extent as it had for correctly paired (Figure 28b, red line). The presence of a mismatch in the terminal base pair must alter the position of AF within the active site keeping it from stacking with the templating base. The lower binding constants for the mismatched AF modified terminal base pair (90 and 89nM) suggest this movement of AF does not disrupt KF binding as much as it had for the C:G-AF construct (800 and 460nM). The single nucleotide incorporation study determined that KF can incorporate the next correct nucleotide, dATP, after a terminal A:G-AF mismatch, and is incorporated more than any other nucleotide. The G:A mismatch is the most common mismatch across from dG-AF, leading to G to T transversions(*110*). The incorporation assay also shows a small amount of

misincorporation of dCTP and dTTP. The apparent equilibrium binding constant for dCTP decreased binding affinity of KF the least of all the nucleotides.

For a misincorporation of dCTP to occur, the mismatched terminal base pair may be a positive factor. The NMR solution structure of A:G-AF in a terminal base pair shows dG-AF in the *syn* position and the paired dA rotated into the major groove. Theoretically, an active site rearrangement shown in Figure 30 could make dCTP the next correct nucleotide. After KF binds to the modified DNA, dG-AF rotates from *syn* to *anti*, but the bulky mismatch forces dA to stay in the major groove. The AF moiety of dG-AF could stack with the AT base pair at -2 to increase stability of the modified base with in the DNA. This rearrangement could cause a slipping mechanism where dG-AF is moved into the active site now serving as the templating base (Figure 30)

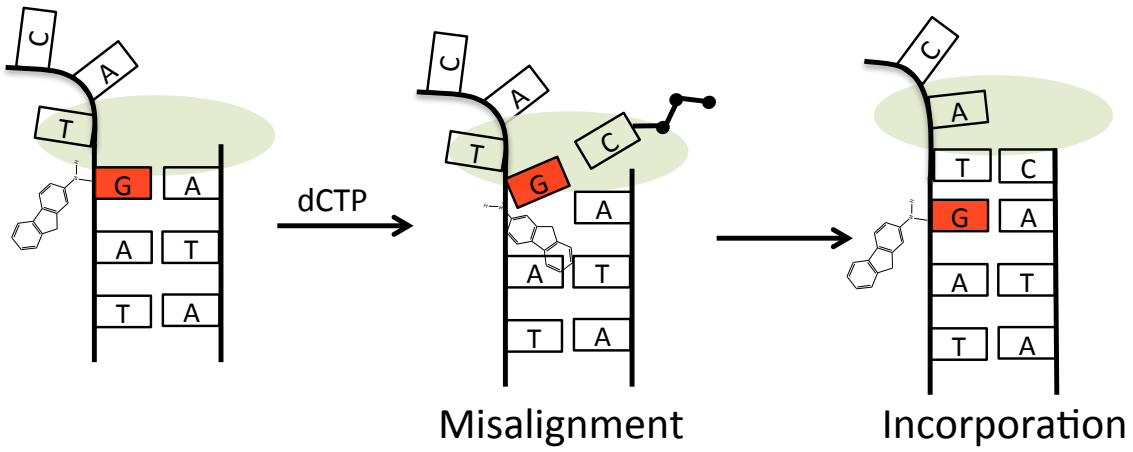

Figure 30. Proposed mechanism for the mis-incorporaton of dCTP across from dT after a A:G-AF base pair. When dCTP is introduced, dG-AF must flip from *anti* to *syn* conformation, causing AF to stack with the T:A base pair at +1 (# with respect to the adduct). This move the guanosine base to the insertion site, making it the templating base. After incorporation of dC, dG-AF returns to the *anti* conformation.

IV. Conclusion and Future Directions

We have shown the technique of surface plasmon resonance to be a useful tool for further understanding the basis of DNA polymerase binding and dissociation dynamics. The SPR experiments were optimized for use with Klenow fragment, but can be translated for use with many other DNA polymerases and countless DNA constructs. These experiments monitored the whole polymerase-DNA binding cycle, providing equilibrium and kinetic data from one experiment. The equilibrium dissociation constants determined from sensorgram data matched well with previous results, but it was the dissociation patterns of the sensorgrams that revealed something that had not seen before, or might have been overlooked in other techniques. The fitting of the dissociation phase revealed two kinetic off rates that are related to the conformation of the polymerase before it dissociates from the DNA. This is most obvious when comparing KF binding to unmodified DNA in the absence of dNTP and KF binding in the presence of the next correct nucleotide. The conformational change in the fingers region from an open to closed structure that is only induced by the next correct nucleotide keeps the KF bound to the DNA longer, and the dissociation rate does not increase until nucleotide is no longer present in the solution. In addition to expanding the details of polymerase conformational rearrangements under different conditions, the dissociation phase also shed some light on how dG-AF binds within KF when it is a templating base. It is known dG-AF can exist in both *syn* and *anti* conformation when KF is bound, and the KF dissociation phase for dG-AF DNA suggests more of the dG-AF rests in a *syn*

conformation when KF is bound. The rotation of the base from *anti* to *syn* removes the base from testing for Watson Crick base pairing with the incoming nucleotide. When this happens, the so-called A rule applies and an A is incorporated, which causes G to T transversions, the most common mutagenic outcome of AF.

The studies with the mismatches monitored the role that DNA context has on slipping mechanisms when the DNA contains an AAF modified templating base. The binding experiments for DNA containing a mismatched primer template prior to the AAF as the templating base showed KF had difficulty binding to and also determining a correct nucleotide for this DNA substrate. The results for having dG-AAF as part of a mismatched primer template terminus also showed poor KF binding. Both sets of results agree with previous statements of AAF being a strong block to replication unless part of a specific sequence. When dG-AF was placed as part of a terminal mismatch, KF binding levels increase over both DNA without the modification and DNA with the AF modification but correctly paired. Having an AF moiety and mismatched bases seem to improve KF binding. The single nucleotide incorporation study revealed that not only is KF only able to incorporate a base if a mismatch is modified with AF, but also after dA is incorporated across from a dG-AF templating base, possibly through the A-rule as noted above, there is a chance another misincorporation can occur. AF stacking interactions and base pairing of G with an incoming pyrimidine may allow for these misincorporations to occur. This type of template misalignment may occur easier in a polymerase with a more open active site, like the class of translesion synthesis polymerases. These types of polymerases are known to accommodate bulky adducts, and the large active site

may allow for an arrangement in the DNA as well. Experiments to test such a rearrangement in a translesion polymerase can be accomplished by using the same SPR system used in these experiments.

REFERENCES

1. Edwards, B. K., Noone, A.-M., Mariotto, A. B., Simard, E. P., Boscoe, F. P., Henley, S. J., Jemal, A., Cho, H., Anderson, R. N., Kohler, B. A., Eheman, C. R., and Ward, E. M. (2014) Annual Report to the Nation on the status of cancer, 1975-2010, featuring prevalence of comorbidity and impact on survival among persons with lung, colorectal, breast, or prostate cancer, *Cancer 120*, 1290-1314.
2. Berry, D. A., Cronin, K. A., Plevritis, S. K., Fryback, D. G., Clarke, L., Zelen, M., Mandelblatt, J. S., Yakovlev, A. Y., Habbema, J. D. F., and Feuer, E. J. (2005) Effect of Screening and Adjuvant Therapy on Mortality from Breast Cancer, *New England Journal of Medicine 353*, 1784-1792.
3. Etzioni, R., Tsodikov, A., Mariotto, A., Szabo, A., Falcon, S., Wegelin, J., diTommaso, D., Karnofski, K., Gulati, R., Penson, D., and Feuer, E. (2008) Quantifying the role of PSA screening in the US prostate cancer mortality decline, *Cancer Causes Control 19*, 175-181.
4. Jemal, A., Thun, M. J., Ries, L. A. G., Howe, H. L., Weir, H. K., Center, M. M., Ward, E., Wu, X.-C., Eheman, C., Anderson, R., Ajani, U. A., Kohler, B., and Edwards, B. K. (2008) Annual Report to the Nation on the Status of Cancer, 1975–2005, Featuring Trends in Lung Cancer, Tobacco Use, and Tobacco Control, *Journal of the National Cancer Institute 100*, 1672-1694.
5. Doll, R., and Hill, A. B. (1950) Smoking and Carcinoma of the Lung - Preliminary Report, *British Medical Journal 2*, 739-748.

6. Walboomers, J. M. M., Jacobs, M. V., Manos, M. M., Bosch, F. X., Kummer, J. A., Shah, K. V., Snijders, P. J. F., Peto, J., Meijer, C., and Munoz, N. (1999) Human papillomavirus is a necessary cause of invasive cervical cancer worldwide, *Journal of Pathology 189*, 12-19.

7. Burcham, P. C. (1999) Internal hazards: baseline DNA damage by endogenous products of normal metabolism, *Mutation Research/Genetic Toxicology and Environmental Mutagenesis 443*, 11-36.

8. Gupta, R. C., and Lutz, W. K. (1999) Background DNA damage from endogenous and unavoidable exogenous carcinogens: a basis for spontaneous cancer incidence?, *Mutation Research-Fundamental and Molecular Mechanisms of Mutagenesis 424*, 1-8.

9. Friedberg, E. C. (2003) DNA damage and repair, *Nature 421*, 436-440.

10. Lindahl, T. (1993) Instability and decay of the primary structure of DNA, *Nature 362*, 709-715.

11. Cheng, K. C., Cahill, D. S., Kasai, H., Nishimura, S., and Loeb, L. A. (1992) 8-Hydroxyguanine, an abundant form of oxidative DNA damage, causes G----T and A----C substitutions, *J. Biol. Chem. 267*, 166-172.

12. Brash, D. E., Rudolph, J. A., Simon, J. A., Lin, A., McKenna, G. J., Baden, H. P., Halperin, A. J., and Ponten, J. (1991) A role for sunlight in skin cancer - UV-induced P53 mutations in squamous-cell carcinoma, *Proceedings of the National Academy of Sciences of the United States of America 88*, 10124-10128.

13. Setlow, R. B. (1974) Wavelengths in sunlight effective in producing skin cancer - Theoretical analysis, *Proceedings of the National Academy of Sciences of the United States of America 71*, 3363-3366.

14. Setlow, R. B. (1966) Cyclobutane-Type Pyrimidine Dimers in Polynucleotides, *Science 153*, 379-386.

15. Ikehata, H., and Ono, T. (2011) The Mechanisms of UV Mutagenesis, *Journal of Radiation Research 52*, 115-125.

16. Hecht, S. S. (1999) DNA adduct formation from tobacco-specific N-nitrosamines, *Mutation Research-Fundamental and Molecular Mechanisms of Mutagenesis 424*, 127-142.

17. Ballschmiter, K. (2003) Pattern and sources of naturally produced organohalogens in the marine environment: biogenic formation of organohalogens, *Chemosphere 52*, 313-324.

18. Kondo, N., Takahashi, A., Ono, K., and Ohnishi, T. (2010) *DNA Damage Induced by Alkylating Agents and Repair Pathways*, Vol. 2010.

19. Basu, A. K., and Essigmann, J. M. (1990) Site-specificaly alklyated oligodeoxynucleotides - Probes for mutagenesis, DNA-repir and the structural effects of DNA damage, *Mutation Research 233*, 189-201.

20. Drabløs, F., Feyzi, E., Aas, P. A., Vaagbø, C. B., Kavli, B., Bratlie, M. S., Peña-Diaz, J., Otterlei, M., Slupphaug, G., and Krokan, H. E. (2004) Alkylation damage in DNA and RNA—repair mechanisms and medical significance, *DNA Repair 3*, 1389-1407.

21. Rosenber.B, Vancamp, L., Trosko, J. E., and Mansour, V. H. (1969) Platinum Compounds - A new class of potent antitumor agents, *Nature 222*, 385-&.

22. Baird, W. M., Hooven, L. A., and Mahadevan, B. (2005) Carcinogenic polycyclic aromatic hydrocarbon-DNA adducts and mechanism of action, *Environmental and Molecular Mutagenesis 45*, 106-114.

23. Alekseyev, Y. O., and Romano, L. J. (2000) In vitro replication of primer-templates containing benzo a pyrene adducts by exonuclease-deficient Escherichia coli DNA polymerase I (Klenow fragment): Effect of sequence context on lesion bypass, *Biochemistry 39*, 10431-10438.

24. Aguilar, F., Hussain, S. P., and Cerutti, P. (1993) Aflatoxin B1 induces the transversion of G-->T in codon 249 of the p53 tumor suppressor gene in human hepatocytes, *Proceedings of the National Academy of Sciences 90*, 8586-8590.

25. Dietrich, H., and Dietrich, B. (2001) Ludwig Rehn (1849–1930) – Pioneering findings on the aetiology of bladder tumours, *World J Urol 19*, 151-153.

26. Case, R. A. M., Hosker, M. E., McDonald, D. B., and Pearson, J. T. (1993) Tumors of the unrinary-bladder in workmen engaged in the manufacture and use of certain dyestuff intermediates in the British chemical-industry, *British Journal of Industrial Medicine 50*, 389-411.

27. Nagao, M., Honda, M., Seino, Y., Yahagi, T., and Sugimura, T. (1977) Mutagenicities of smoke condensates and charred surface of fish and meat, *Cancer Letters 2*, 221-226.

28. Tsuda, M., Negishi, C., Makino, R., Sato, S., Yamaizumi, Z., Hirayama, T., and Sugimura, T. (1985) Use of nitrate and hypocholrite treatments in determination of the contributions of IQ-type and non-IQ-type heterocyclic amines to the mugenicities in crude pyrolyic materials, *Mutation Research 147*, 335-341.

29. Sugimura, T. (2000) Nutrition and dietary carcinogens, *Carcinogenesis 21*, 387-395.

30. Weisburger, E. K., and Weisburger, J. H. (1958) Chemistry, Carcinogenicity, and Metabolism of 2-Fluorenamine and Related Compounds, In *Advances in Cancer Research* (Jesse, P. G., and Alexander, H., Eds.), pp 331-431, Academic Press.

31. Miller, J. A., and Miller, E. C. (1983) Some historical aspects of N-Aryl carcinogens and their metabolic-activation *Environmental Health Perspectives 49*, 3-12.

32. Gill, J. P., and Romano, L. J. (2005) Mechanism for N-Acetyl-2-aminofluorene-Induced Frameshift Mutagenesis by Escherichia coli DNA Polymerase I (Klenow Fragment), *Biochemistry 44*, 15387-15395.

33. Dzantiev, L., and Romano, L. J. (1999) Interaction of Escherichia coli DNA polymerase I (Klenow fragment) with primer-templates containing N-acetyl-2-aminofluorene or N-2-aminofluorene adducts in the adive site (vol 274, pg 3279, 1999), *J. Biol. Chem. 274*, 14514-14514.

34. Belguise-Valladier, P., and Fuchs, R. P. P. (1995) N-2-aminofluorene andN-2 acetylaminofluorene Adducts: The Local Sequence Context of an Adduct and

its Chemical Structure Determine its Replication Properties, *Journal of Molecular Biology 249*, 903-913.

35. Heflich, R. H., and Neft, R. E. (1994) Genetic Toxicity of 2-Acetylaminofluorene, 2-Aminofluorene and Some of Their Metabolies and Model Metabolites, *Mutation Research-Reviews in Genetic Toxicology 318*, 73-174.

36. Ohandley, S. F., Sanford, D. G., Xu, R., Lester, C. C., Hingerty, B. E., Broyde, S., and Krugh, T. R. (1993) Structural Chacaterization of an N-Acetyl-2-Aminofluorene (AAF) Modified DNA Oligomer by NMR, Energy Minimization, and Molecular Dynamics *Biochemistry 32*, 2481-2497.

37. Mao, B., Hingerty, B. E., Broyde, S., and Patel, D. J. (1998) Solution Structure of the Aminofluorene [AF]-External Conformer of the anti-[AF]-C8-dG Adduct Opposite dC in a DNA Duplex, *Biochemistry 37*, 95-106.

38. Mao, B., Hingerty, B. E., Broyde, S., and Patel, D. J. (1998) Solution Structure of the Aminofluorene [AF]-Intercalated Conformer of the syn-[AF]-C8-dG Adduct Opposite dC in a DNA Duplex, *Biochemistry 37*, 81-94.

39. Lone, S., and Romano, L. J. (2003) Mechanistic Insights into Replication Across from Bulky DNA Adducts: A Mutant Polymerase I Allows an N-Acetyl-2-aminofluorene Adduct To Be Accommodated during DNA Synthesis†, *Biochemistry 42*, 3826-3834.

40. Kunkel, T. A. (2004) DNA Replication Fidelity, *J. Biol. Chem. 279*, 16895-16898.

41. Bessman, M. J., Lehman, I. R., Simms, E. S., and Kornberg, A. (1957) Enzymatic Synthesis of Deoxyribonucleic Acid (DNA) *Federation Proceedings 16*, 153-154.

42. Bebenek, K., Joyce, C. M., Fitzgerald, M. P., and Kunkel, T. A. (1990) The fidelity of DNA synthesis catalyzed by derivatives of Escherichia coli DNA polymerase I, *J. Biol. Chem. 265*, 13878-13887.

43. Klenow, H., and Hennings.I. (1970) Selective Eliminaion of Exonuclese Activity of Deoxyribonucleic Acid Polymerase from Escherichia-coli B by Limited Proteolysis *Proceedings of the National Academy of Sciences of the United States of America 65*, 168-&.

44. Klenow, H., and Overgaar.K. (1970) Proteolytic Cleavage of DNA Polymerase from Escherichia-coli B into an Exonucelase Unit and a Polymerase Unit *Febs Letters 6*, 25-&.

45. Derbyshire, V., Grindley, N. D. F., and Joyce, C. M. (1991) The 3'-5' Exonuclease of DNA-Polymerase-I OF Escherichia-coli - Contribution of Each Amino-Acid at the Active-Site to the Reaction, *Embo Journal 10*, 17-24.

46. Ollis, D. L., Brick, P., Hamlin, R., Xuong, N. G., and Steitz, T. A. (1985) Structure of the Large Fragment of *Exchericha coli* DNA-Polymerase I Complexed with DTMP, *Nature 313*, 762-766.

47. Korolev, S., Nayal, M., Barnes, W. M., Di Cera, E., and Waksman, G. (1995) Crystal structure of the large fragment of Thermus aquaticus DNA polymerase I at 2.5-A resolution: structural basis for thermostability, *Proceedings of the National Academy of Sciences 92*, 9264-9268.

48. Beese, L. S., Derbyshire, V., and Steitz, T. A. (1993) Structure of DNA-Polymerase-I Klenow Fragment Bound to Duplex DNA, *Science 260*, 352-355.

49. Li, Y., Korolev, S., and Waksman, G. (1998) Crystal structures of open and closed forms of binary and ternary complexes of the large fragment of Thermus aquaticus DNA polymerase I: structural basis for nucleotide incorporation, *Embo Journal 17*, 7514-7525.

50. Doublie, S., Tabor, S., Long, A. M., Richardson, C. C., and Ellenberger, T. (1998) Crystal structure of a bacteriophage T7 DNA replication complex at 2.2 angstrom resolution, *Nature 391*, 251-258.

51. Kiefer, J. R., Mao, C., Braman, J. C., and Beese, L. S. (1998) Visualizing DNA replication in a catalytically active Bacillus DNA polymerase crystal, *Nature 391*, 304-307.

52. Dzantiev, L., and Romano, L. J. (2000) A conformational change in E-coli DNA polymerase I (Klenow fragment) is induced in the presence of a dNTP complementary to the template base in the active site, *Biochemistry 39*, 356-361.

53. Watson, J. D., and Crick, F. H. C. (1953) Genetial Implicaitons of the structure of deoxyribonucleic acid, *Nature 171*, 964-967.

54. Donlin, M. J., Patel, S. S., and Johnson, K. A. (1991) Kinetic Partitioning Between the Exonuclease and Polymerase Sites in DNA Error Correction, *Biochemistry 30*, 538-546.

55. Joyce, C. M., Potapova, O., DeLucia, A. M., Huang, X., Basu, V. P., and Grindley, N. D. F. (2008) Fingers-Closing and Other Rapid Conformational Changes in

DNA Polymerase I (Klenow Fragment) and Their Role in Nucleotide Selectivity, *Biochemistry 47*, 6103-6116.

56. Rothwell, P. J., and Waksman, G. (2007) A Pre-equilibrium before Nucleotide Binding Limits Fingers Subdomain Closure by Klentaq1, *J. Biol. Chem. 282*, 28884-28892.

57. Astatke, M., Ng, K., Grindley, N. D. F., and Joyce, C. M. (1998) A single side chain prevents Escherichia coli DNA polymerase I (Klenow fragment) from incorporating ribonucleotides, *Proceedings of the National Academy of Sciences 95*, 3402-3407.

58. Streisinger, G., and Owen, J. E. (1985) Mechanisms of spontaneous and Induced frameshift mutations in baceriophage-T4, *Genetics 109*, 633-659.

59. Bichara, M., and Fuchs, R. P. P. (1985) DNA binding and mutation spectra of the carcinogen N-2-aminofluorene in Escherichia coli: A correlation between the conformation of the premutagenic lesion and the mutation specificity, *Journal of Molecular Biology 183*, 341-351.

60. Gupta, P. K., Lee, M. S., and King, C. M. (1988) Comparison of Mutagenesis Induced in Single-Stranded and Double-Stranded M13 Viral-DNA by Treatment with N-hydorxy-2-aminofluorene *Carcinogenesis 9*, 1337-1345.

61. Hoffmann, G. R., and Fuchs, R. P. P. (1997) Mechanisms of Frameshift Mutations: Insight from Aromatic Amines, *Chemical Research in Toxicology 10*, 347-359.

62. Tan, X., Suzuki, N., Grollman, A. P., and Shibutani, S. (2002) Mutagenic Events in Escherichia coli and Mammalian Cells Generated in Response to

Acetylaminofluorene-Derived DNA Adducts Positioned in the Nar I Restriction Enzyme Site, *Biochemistry 41*, 14255-14262.

63. Chen, T., Mittelstaedt, R. A., Aidoo, A., Hamilton, L. P., Beland, F. A., Casciano, D. A., and Heflich, R. H. (2001) Comparison of hprt and lacI mutant frequency with DNA adduct formation in N-hydroxy-2-acetylaminofluorene–treated Big Blue® rats†, *Environmental and Molecular Mutagenesis 37*, 195-202.

64. Chen, T., Mittelstaedt, R. A., Shelton, S. D., Balachandra Dass, S., Manjanatha, M. G., Casciano, D. A., and Heflich, R. H. (2001) Gene- and tissue-specificity of mutation in Big Blue® rats treated with the hepatocarcinogen N-hydroxy-2-acetylaminofluorene†, *Environmental and Molecular Mutagenesis 37*, 203-214.

65. Strauss, B. S., and Wang, J. (1990) Role of DNA-polymerase E 3'- 5' exonuclease activity in the bypass of aminofluorene lesions in DNA, *Carcinogenesis 11*, 2103-2109.

66. Dzantiev, L., and Romano, L. J. (2000) Differential effects of N-acetyl-2-aminofluorene and N-2-aminofluorene adducts on the conformational change in the structure of DNA polymerase I (Klenow fragment), *Biochemistry 39*, 5139-5145.

67. Bell, J. B., Eckert, K. A., Joyce, C. M., and Kunkel, T. A. (1997) Base miscoding and strand misalignment errors by mutator klenow polymerases with amino acid substitutions at tyrosine 766 in the O helix of the fingers subdomain, *J. Biol. Chem. 272*, 7345-7351.

68. Dutta, S., Li, Y., Johnson, D., Dzantiev, L., Richardson, C. C., Romano, L. J., and Ellenberger, T. (2004) Crystal structures of 2-acetylaminofluorene and 2-

aminofluorene in complex with T7 DNA polymerase reveal mechanisms of mutagenesis, *Proceedings of the National Academy of Sciences of the United States of America 101*, 16186-16191.

69. Eckel, L. M., and Krugh, T. R. (1994) 2-aminofluorene Modified DNA Duplex Exists in 2 Interchangable Conformations, *Nature Structural Biology 1*, 89-94.

70. Hsu, G. W., Kiefer, J. R., Burnouf, D., Becherel, O. J., Fuchs, R. P. P., and Beese, L. S. (2004) Observing translesion synthesis of an aromatic amine DNA adduct by a high-fidelity DNA polymerase, *J. Biol. Chem. 279*, 50280-50285.

71. Lambert, I. B., Napolitano, R. L., and Fuchs, R. P. P. (1992) Carcinogen-Induced Frameshift Mutagenesis in Repetitive Sequence, *Proceedings of the National Academy of Sciences of the United States of America 89*, 1310-1314.

72. Napolitano, R. L., Lambert, I. B., and Fuchs, R. P. P. (1994) DNA-Sequence Determinatnts of Carcinogen-Induced Frameshift Mutagenesis, *Biochemistry 33*, 1311-1315.

73. Burnouf, D., Koehl, P., and Fuchs, R. P. P. (1989) Singel adduct mutagnesis - Strong effect of the position of a single acetylaminofluorene adduct within a mutaton hot spot *Proceedings of the National Academy of Sciences of the United States of America 86*, 4147-4151.

74. Tebbs, R. S., and Romano, L. J. (1994) Mutagenesis at a Site-specifically Modified NarI Sequence by Acetylated and Deacetylated Aminofluorene Adducts, *Biochemistry 33*, 8998-9006.

75. Strauss, B. S. (1992) The Origin of Point Mutatiions in Human Tumor-Cells, *Cancer Research 52*, 249-253.

76. Prakash, S., Johnson, R. E., and Prakash, L. (2005) Eukaryotic translesion synthesis DNA polymerases: Specificity of structure and function, In *Annu. Rev. Biochem.*, pp 317-353.

77. Vooradi, V., and Romano, L. J. (2009) Effect of N-2-Acetylaminofluorene and 2-Aminofluorene Adducts on DNA Binding and Synthesis by Yeast DNA Polymerase eta, *Biochemistry 48*, 4209-4216.

78. Rechkoblit, O., Kolbanovskiy, A., Malinina, L., Geacintov, N. E., Broyde, S., and Patel, D. J. (2010) Mechanism of error-free and semitargeted mutagenic bypass of an aromatic amine lesion by Y-family polymerase Dpo4, *Nature Structural & Molecular Biology 17*, 379-388.

79. Liedberg B, N. C., Lundsrtom I. (1995) Biosensing with Surface Plasmon Resonance- How it All Started, *Biosensors and Bioelectronics 10*, i-ix.

80. (2008) *Handbook of Surface Plasmon Resonance*, Illustrated ed., Royal Chemical Society.

81. Homola, J. (2003) Present and future of surface plasmon resonance biosensors, *Analytical and Bioanalytical Chemistry 377*, 528-539.

82. Šípová, H., and Homola, J. (2013) Surface plasmon resonance sensing of nucleic acids: A review, *Analytica Chimica Acta 773*, 9-23.

83. Albani, J. R. (2007) *Principles and Applications of Fluorescence Spectroscopy*.

84. Lakowicz, J. R. (1999) *Principles of Fluorescence Spectroscopy, Second Edition*, Kluwer Aceademic/Plenum Publishers, New York.

85. Markiewicz, R. P., Vrtis, K. B., Rueda, D., and Romano, L. J. (2012) Single-molecule microscopy reveals new insights into nucleotide selection by DNA polymerase I, *Nucleic Acids Research 40*, 7975-7984.

86. Vrtis, K. B., Markiewicz, R. P., Romano, L. J., and Rueda, D. (2013) Carcinogenic adducts induce distinct DNA polymerase binding orientations, *Nucleic Acids Research 41*, 7843-7853.

87. Joyce, C. M., and Derbyshire, V. (1995) Purification of Escherichia coli DNA polymerase I and Klenow fragment, In *Methods in Enzymology* (Judith, L. C., Ed.), pp 3-13, Academic Press.

88. Federley, R. (2010) New Insights into the Mechanism of DNA Replication on Unmodified and Benzo[a]pyrene-modified Tempaltes Using Surface Plasmon Resonance, In *Chemistry*, p 207, Wayne State University, Detroit, M'I.

89. Christian, T. D., Romano, L. J., and Rueda, D. (2009) Single-molecule measurements of synthesis by DNA polymerase with base-pair resolution, *Proceedings of the National Academy of Sciences 106*, 21109-21114.

90. Myszka, D. G. (1997) Kinetic analysis of macromolecular interactions using surface plasmon resonance biosensors, *Curr. Opin. Biotechnol. 8*, 50-57.

91. Dzantiev, L., Alekseyev, Y. O., Morales, J. C., Kool, E. T., and Romano, L. J. (2001) Significance of Nucleobase Shape Complementarity and Hydrogen Bonding in the Formation and Stability of the Closed Polymerase−DNA Complex†, *Biochemistry 40*, 3215-3221.

92. Garalde, D. R., Simon, C. A., Dahl, J. M., Wang, H., Akeson, M., and Lieberman, K. R. (2011) Distinct Complexes of DNA Polymerase I (Klenow Fragment) for

Base and Sugar Discrimination during Nucleotide Substrate Selection, *J. Biol. Chem. 286*, 14480-14492.

93. Freemont, P. S., Friedman, J. M., Beese, L. S., Sanderson, M. R., and Steitz, T. A. (1988) Cocrystal structure of an editing complex of Klenow fragment with DNA, *Proceedings of the National Academy of Sciences 85*, 8924-8928.

94. Tsoi, P. Y., Zhang, X. M., Sui, S. F., and Yang, M. S. (2003) Effects of DNA mismatches on binding affinity and kinetics of polymerase-DNA complexes as revealed by surface plasmon resonance biosensor, *Analyst 128*, 1169-1174.

95. Santoso, Y., Joyce, C. M., Potapova, O., Le Reste, L., Hohlbein, J., Torella, J. P., Grindley, N. D. F., and Kapanidis, A. N. (2010) Conformational transitions in DNA polymerase I revealed by single-molecule FRET, *Proceedings of the National Academy of Sciences 107*, 715-720.

96. Tsai, Y.-C., and Johnson, K. A. (2006) A New Paradigm for DNA Polymerase Specificity, *Biochemistry 45*, 9675-9687.

97. Mah, M. C., Boldt, J., Culp, S. J., Maher, V. M., and McCormick, J. J. (1991) Replication of acetylaminofluorene-adducted plasmids in human cells: spectrum of base substitutions and evidence of excision repair, *Proceedings of the National Academy of Sciences 88*, 10193-10197.

98. Clark, J. M., and Beardsley, G. P. (1989) Template length, sequence context, and 3'-5' exonuclease activity modulate replicative bypass of thymine glycol lesions in vitro, *Biochemistry 28*, 775-779.

99. Ripley, L. S., Clark, A., and deBoer, J. G. (1986) Spectrum of spontaneous frameshift mutations: Sequences of bacteriophage T4 rII gene frameshifts, *Journal of Molecular Biology 191*, 601-613.

100. Echols, H., and Goodman, M. F. (1991) Fidelity Mechanisms in DNA Replication, *Annu. Rev. Biochem. 60*, 477-511.

101. Kunkel, T. A. (1988) Exonucleolytic proofreading, *Cell 53*, 837-840.

102. Bebenek, K., Roberts, J. D., and Kunkel, T. A. (1992) The effects of dNTP pool imbalances on frameshift fidelity during DNA replication, *J. Biol. Chem. 267*, 3589-3596.

103. Shibutani, S., and Grollman, A. P. (1993) Nucleotide Misincorporation of DNA Templates Containing N-(deoxyguanosin-N-2-yl)-2-(acetylamino)fluorene, *Chemical Research in Toxicology 6*, 819-824.

104. Shibutani, S., Suzuki, N., and Grollman, A. P. (2004) Mechanism of Frameshift (Deletion) Generated by Acetylaminofluorene-Derived DNA Adducts in Vitro, *Biochemistry 43*, 15929-15935.

105. Gupta, P. K., Johnson, D. L., Reid, T. M., Lee, M. S., Romano, L. J., and King, C. M. (1989) Mutagenesis by Single Site-Specific Arylamine-DNA Adducts - Induction of Mutations at Multiple Sites, *J. Biol. Chem. 264*, 20120-20130.

106. Hogg, M., Wallace, S. S., and Doublie, S. (2004) Crystallographic snapshots of a replicative DNA polymerase encountering an abasic site, *Embo Journal 23*, 1483-1493.

107. Strauss, B. S. (1991) The A-rule of mutagen specificity - A consequence of DNA polymerase bypass of non-instructional lesions, *Bioessays 13*, 79-84.

108. Michales, M. L., Reid, T. M., King, C. M., and Romano, L. J. (1991) Accurate in vitro, translesion synthesis by Escherichia coli DNA polymerase I (large fragment) on a site-specific, aminofluorene modified oligonucleotide, *Carcinogenesis 12*, 1641-1646.

109. Gu, Z., Gorin, A., Hingerty, B. E., Broyde, S., and Patel, D. J. (1999) Solution Structures of Aminofluorene [AF]-Stacked Conformers of the syn [AF]−C8-dG Adduct Positioned Opposite dC or dA at a Template-Primer Junction, *Biochemistry 38*, 10855-10870.

110. Carothers, A. M., Urlaub, G., Mucha, J., Yuan, W., Chasin, L. A., and Grunberger, D. (1993) A mutational hot spot induced by N-hydroxy-aminofluorene in dihydrofolate reductase mutants of Chinese hamster ovary cells, *Carcinogenesis 14*, 2181-2184.

ABSTRACT

INVESTIGATION INTO THE BINDING INTERACTIONS OF KLENOW FRAGMENT TO DNA MODIFIED WITH CARCINOGENS AF AND AAF USING SURFACE PLASMON RESONANCE

by

ASHLEY M FLOYD

August 2014

Advisor: Dr. Louis J Romano

Major: Chemistry (Biochemistry)

Degree: Doctor of Philosophy

The two major forms of DNA adducts from the carcinogen N-acetoxyacetyl-2-aminofluorene, N-(deoxygunanonsin-8-yl)-2-acetylaminofluorene (dG-C8-AAF) and N-(deoxyguanosin-8-yl)-2-aminofluorene (dG-C8-AF), are both known to impede replication, though in different ways. AAF is a strong block to replication leading to frameshift mutations, while the AF adduct is more easily bypassed, causing base substitutions. Surface plasmon resonance (SPR) was used to study the binding of exonuclease deficient *E. coli* polymerase I, Klenow fragment (KF), to DNA modified with AF or AAF at two locations: as a templating base or in the last formed base pair. KF binding to the modified DNA bases was also monitored to DNA that contained a terminal mismatch. When the templating guanine is modified with either AF or AAF, KF binds tightly and the addition of the next correct nucleotide does not increase binding, nor does an incorrect nucleotide decrease binding. However when an AAF or AF modified guanine in the terminal base pair, bound KF is unable to form a stable structure. Interestingly, when the dG-AF was part of a terminal mismatch, KF

bound better to mismatched DNA than correctly base paired DNA, both in the presence and absence of nucleotide. Incorrect dNTP showed the least KF destabilization binding to the dG-AF mismatched DNA constructs. It is possible that the bulky, mismatched primer template terminus rearranges the active site allowing the modified dG to rotate and serve as a template for the incoming dCTP. SPR is a useful label free technique to determine both equilibrium binding constants (K_D), and dissociation rates (k_{off}) from the same set of data. The dissociation rates reveal that for most constructs, KF dissociates at two rates, a fast and a slow rate, relating to KF dissociating from different conformations.

AUTOBIOGRAPHICAL STATEMENT

Ashley M Floyd

EDUCATION

PhD in Chemistry (Biochemistry) 2007 - 2014
Wayne State University, Detroit MI
Thesis Title: Investigation into the Binding Interactions of Klenow Fragment to DAN Modified with Carcinogens AF and AAF using Surface Plasmon Resonance
Thesis Advisor: Dr Louis J Romano

BA in Chemistry

State University of New York at Buffalo, Buffalo NY 2003 – 2007

PUBLICATIONS

1. Silva, G. N.; Fatma, S.; **Floyd**, A. M.; Fischer, F.; Chuawong, P.; Cruz, A. N.; Simari, R. M.; Joshi, N.; Kern, D.; Hendrickson, T. L., A tRNA-independent Mechanism for Transamidosome Assembly Promotes Aminoacyl-tRNA Transamidation. *J. Biol. Chem.* **2013,** *288* (6), 3816-3822.
2. **Floyd**, A M, Romano, LJ, Interactions of Klenow Fragment with Carcinogenic Adducts N-2-Acetylaminofluorene and N-2-Aminofluorene in the Pre- and Post-insertion Site as Studied with Surface Plasmon Resonance (Manuscript in preparation to be submitted)

AWARDS

2007 Willard R Lenz, Jr Endowed Memorial Scholarship
2007 Thomas C Rumble University Graduate Fellowship
2007 A. Paul & Carol C. Schaap Distinguished Graduate Stipend